Electric Propulsion System for Exceptionally Short Takeoff and Landing Electric Air Vehicles

ELECTRIC PROPULSION SYSTEM FOR EXCEPTIONALLY SHORT TAKEOFF AND LANDING ELECTRIC AIR VEHICLES

By Parisa MAHVELATISHAMSABADI,

A Thesis Submitted to the School of Graduate Studies in the Partial Fulfillment of the Requirements for the Degree Master Of Science

McMaster University

Master Of Science (2019)

Hamilton, Ontario (Mechanical Department)

TITLE: Electric Propulsion System for Exceptionally Short Takeoff and Landing Electric Air Vehicles

AUTHOR: Parisa Mahvelatishamsabadi (McMaster University)

SUPERVISOR: Dr. Ali Emadi

NUMBER OF PAGES: xxiii, 157

Abstract

Over the past few years, electric propulsion systems have been widely used in automotive applications. The next decade is likely to see the electrification of aerial vehicles. In the past 20 years, the passengers demand in the aviation industry has increased by roughly 5% annually. Drastic increment in the passengers demand leads to many problems such as emission, noise pollution, airports capacity shortage and high fuel consumption. An electric airplane that can take off and land in extremely short runway can solve all the mentioned problems. Also, an airplane that is smaller and lighter with the ability to take off and land from an extremely short runway can be used as a new transportation system in congested cities and solve the urban road traffic and compensate for people's time wasted in traffic. With this in mind, in this thesis, the feasibility of converting a conventional fixed-wing direct-drive propeller airplane to an electric extremely short takeoff and landing airplane has been examined.

An overview of the history of electric aerial vehicles and flying cars is conducted where some of these vehicles are still under development phase. The main aim of this thesis is to address the effect of takeoff and landing runway length on the electric motor main specifications, including power, torque, and speed. Also, the effect of cruising speed on the motor specifications are investigated, and it is observed that there is a considerable difference between the amount of required power for the cruising mode and takeoff mode. In the end, the impact of the braking system and airplane weight on the landing distance are examined, and It is found that for an airplane with a cruise-efficient propeller, usage of thrust reverser is not practical and hence it is not recommended. Although if the propeller is designed to have

high efficiency at takeoff and landing, the thrust reverser can be a good solution to make the landing runway shorter.

Acknowledgements

I would like to express my gratitude to Dr. Ali Emadi, my supervisor at McMaster University, for his remarkable guidance, enthusiastic encouragements, great technical assistance, and excellent comments and suggestions he gave me during my research journey. I have learned a lot from his specialized knowledge and his great attitude, and that helps me in my professional career. Thanks are also due to Prof Hugh Liu from the University of Toronto who gave me so many valuable advice, useful critiques and helps in the early stage of this study.

I am also grateful to my family and friends, Dr. Masoumeh Omidzohour, Dr. Farhad Mahvelati Shamsabadi, Dr. Siavash Mahvelati Shamsabadi, Shiva Ghasemi, Negar Arabzadeh, and Paria Kargar Samani, for their motivation and support. Without their support, this study would never have been completed. Finally, I would like to dedicate my thesis to all these dear people.

Contents

List of Figures

List of Tables

Declaration of Authorship

I, Parisa Mahvelatishamsabadi, declare that this thesis titled, “Electric Propulsion System for Exceptionally Short Takeoff and Landing Electric Air Vehicles” and the work presented in it are my own. I confirm that all the following sections are done by me and other works and researches which are used in this thesis are clearly referenced.

- Chapter 1: Introduction
- Chapter 2: Electrified Aircraft
- Chapter 3: Extremely Short Takeoff and Landing Airplane
- Chapter 4: Aerodynamic Forces
- Chapter 5: Performance Modeling
- Chapter 6: Electric Aircraft Component Selection and Modeling
- Chapter 7: Airplane Modeling in Simulink Matlab and Results
- Chapter 8: Conclusion and Future Works
- and all the models built in Simulink Matlab

List of Abbreviations

CTOL	**C**onventional **T**ake-off and **L**anding
DEP	**D**istributed **E**lectric **P**ropulsion system
e-bike	**e**lectric bike
eVTOL	**e**lectric **V**ertical **T**ake-off and **L**anding
EM	**E**lectric **M**otor
EASA	**E**uropean **A**viation **S**afety **Agency**
ESTOL	**E**xtremely **S**hort **T**ake**O**ff and **L**anding
FAA	**F**ederal **A**viation **A**dministration
HWB	**H**ybrid **W**ing **B**ody
IATA	**I**nternational **A**ir **T**ransport **A**ssociation
LSALT	**L**owets **S**afe **Alt**itude
MTOW	**M**aximum **T**ake **O**ff **W**eight
NA	**N**ot **A**vailable
NASA	**N**ational **A**eronautics and **S**pace **A**dministration
OEM	**O**riginal **E**quipment **M**anufacturer
SEL	**S**ingle **E**vent noise equavalant **L**evel
STOL	**S**hort **T**ake-**O**ff and **L**anding
UAM	**U**rban **A**ir **M**obility
VTOL	**V**ertical **T**ake-off and **L**anding

List of Symbols

a	Lapse Rate for Gradient Layers in International Standard Atmosphere
a_0	Slope of $C_l - \alpha$ Curve
a_L	Landing deceleration
a_{Land}	Landing deceleration
a_{TO}	Takeoff Acceleration
a_TO	Takeoff Acceleration
AR	Wing's Aspect Ratio
b	Wing Span
b_{SP}	Spoiler Span
c	Local Sound of the Sound
$\bar{c}$	Wing's Chord
C_D	Total Airplane Drag Coefficient
C_{D0}	Airplane Parasite Drag Coefficient at zero lift
$C_{D0_{LG}}$	Landing Gear Drag Coefficient
$C_{D0_{HLD}}$	High Lift Devices Drag Coefficient
C_{De}	Airplane Parasite Drag Coefficient
C_{DG}	Total Airplane Drag Coefficient at Takeoff
$C_{D_{SP}}$	Spoiler Drag Coefficient
C_{Dtotal}	Total Airplane Drag Coefficient at Takeoff and Landing

C_{DW}	Total Wing Drag Coefficient
C_{DW0}	Wing Profile Drag Coefficient
C_{DWi}	Wing Drag due to Lift Coefficient- Wing Induced Drag Coefficient
C_l	Airfoil Lift Coefficient
C_L	Total Airplane Lift Coefficient
C_{LGmax}	Maximum Lift Coefficient at takeoff
C_{Lmax}	Maximum Airplane Lift Coefficient
C_{Ltotal}	Total Airplane Lift Coefficient at Takeoff and Landing
C_{LW}	Total Wing Lift Coefficient
C_P	Propeller Power Coefficient
C_T	Propeller Thrust Coefficient
d	Propeller Diameter
D	Drag
e	Span Factor Efficiency or Oswald Efficiency Factor
F_{Br}	Brake Force in Landing
g	Earth Gravity
g_0	Earth Gravity
h	Altitude
h_{HO}	Highest Obstacle Height
h_t	Terian Height from the Sea Level
J	Propeller Advance Ratio
k	Brake Coefficient
L	Lift
m	Aircraft Mass
M	Mach Number

n	Propeller Revolutionary Speed
P	Pressure
P	Power
P_A	Available Power
P_{EM}	Electric Motor Output Power
PD_L	Required Electric Motor Power Density for Landing
PD_TO	Required Electric Motor Power Density for Takeoff
P_{in}	Electric Motor Input Power
P_{in_EM}	Electric Motor Input Power
P_{in_prop}	Propeller Input Power
P_L	Required Power for Landing
P_{out}	Aircraft output Power
P_{out_EM}	Electric Motor output Power
P_{out_prop}	Propeller output Power
P_{prop}	Propeller Power
P_TO	Required Power for Takeoff
P_R	Required Power
P_s	Atmosphere Pressure at Sea Level
R	Universal Gas Constant
S	Wing Surface Area
S_{gLand}	Ground Roll Distance during Landing
S_{gTO}	Ground Roll Distance during Takeoff
S_{ref}	Wing Surface Area
S_{SP}	Spoiler Surface Area
t_{Land}	Landing (full braking) Time

t_{TO}	Takeoff Time
T	Temperature
T	Thrust
T_L	Required Power for Landing
T_{prop}	Propeller Thrust
T_TO	Required Power for Takeoff
T_R	Required Thrust
T_s	Atmosphere Temperature at Sea Level
V	Velocity
V_{avrg}	Average Velocity
V_{LO}	Lift-Off Velocity
V_{stall}	Stall Velocity
V_{Stall_G}	Stall Velocity at takeoff
V_{TD}	Touch Down Velocity
W	Weight
$W_{Battery}$	Battery Weight
W_{Empty}	Empty Aircraft frame Weight
$W_{FullPayload}$	Maximum Payload Weight
W_L	Required Motor Speed for Landing
W_{Max}	Maximum Aircraft Weight
$W_{Propulsion}$	Propulsion System Weight
W_TO	Required Motor Speed for Takeoff
δ_{SP}	Spoiler Deflection Angle
$\triangle C_{D_{HLD}}$	Change of Drag Coefficient by using High Lift Devices
$(\triangle C_{D_{SP}})_{@}Land$	Change of Drag Coefficient by using Spoiler in Landing

$\triangle C_{L_{HLD}}$	Change of Lift Coefficient by using High Lift Devices
$\triangle C_{L_{SP}}$	Change of Lift Coefficient by using Spoiler
$(\triangle C_{L_{SP}})_{@}Land$	Change of Lift Coefficient by using Spoiler in Landing
α	Angle of Attack
$\alpha_{L=0}$	Zero-Lift Angle of Attack
β	Propeller Pitch Angle
η_{EM}	Electric Motor Efficiency
η_{prop}	Propeller Efficiency
θ_c	Climb Angle
μ	Rolling Friction Coefficient
μ_{Br}	Rolling Friction Coefficient during Landing-Braking
ρ	Density
ρ_s	Atmosphere Density at Sea Level

Chapter 1

Introduction

The modes of transportation are changing. People are always thinking about a faster and more comfortable way to reach their destination. Cars are becoming more autonomous, and taxis are being equipped with ride-sharing applications such as Uber and Lyft. Even soft-mode transportations such as walking and biking, are being affected by some technologies like e-bike and bike-sharing [1]. Now it's time to use the sky for commuting passengers. The concept of "Air taxi" has been officially released in 2015 by some companies such as Airbus Vahana, Ehang, and Volocopter. They have made successful flight test of their prototypes in 2017 and 2018 [1]. Up to now, more than 70 projects are ongoing on this topic [2]. However, there are several obstacles that need to be overcome before industrializing this concept, including low battery's specific energy, society acceptance difficulty, noise pollution, safety concerns, and certifications issues. An airplane which can takeoff and land in an extremely short runway may be a possible solution.

1.1 Extremely Short TakeOff and Landing Air Vehicle Applications

1.1.1 Airport Shortage Capacity

In the past twenty years, the passengers demand in the aviation industry has grown about 4.8% per year [74] and based on Boeing prediction from the "Subsonic Ultra Aircraft Research", 4% growth is expected in the next twenty years [74]. The International Air Transport Association's report points that 2.8 billion passengers traveled all over the world in 2011. The report predicts that this amount will increase by 175 million passengers annually [62]. Fig. 1.1 depicts number of boarded passengers from 2004 to 2017 [81]. Based on statistics, total commuters around the world in 2017 was 4.09 billion. However, based on IATA's [1] report prediction, it should be 3.8 billion meaning rate of increase in air transport is even more than 175 million yearly. To summarize, it can be said that the rate of increase in air transport is roughly about 5% annually. Consequently, in the best case scenario, by 2025, the total worldwide travel passengers will be 5.4 billion.

[1]International Air Transport Association

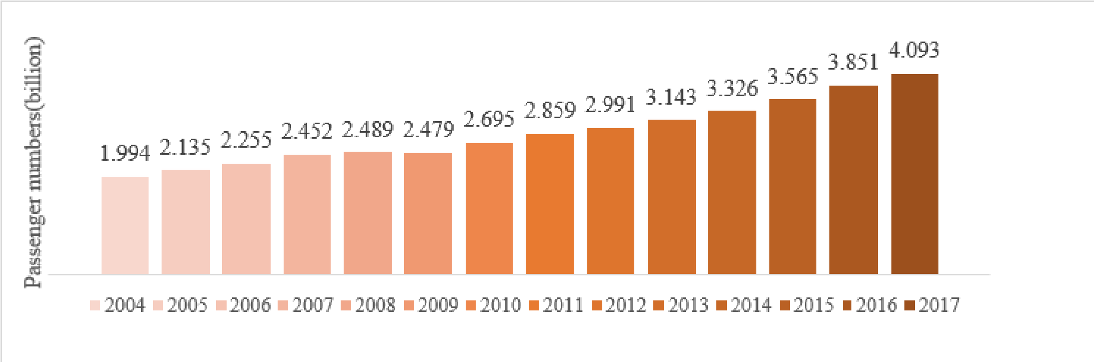

FIGURE 1.1: Total passengers boarded worldwide from 2004 to 2017 (in billion) [81]

Drastic increment in the passengers' demand can cause many problems, consisting of capacity shortage, noise pollution, emission, and high fuel consumption [74]. Nowadays, most of the airports all over the world are running at their maximum capacity while an increase is expected in the future. One of the main problems is the capacity shortage in central connection airports, and capacity shortage leads to flight delays, and even cancellations [101]. This problem is mainly due to the limited space for airplanes to take off and land. Fig. 1.2 shows the United States airport distribution with varying runway length [81].

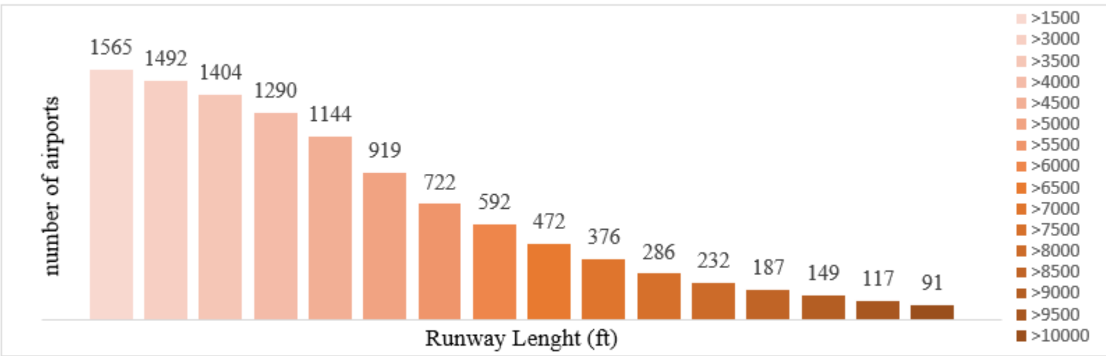

FIGURE 1.2: US airport distributions with different runway length [81]

Airport expansions or building new airports can be a solution to the passenger's demand increment. Nevertheless, it has some environmental consequences on the airport's neighborhood, such as noise pollutions and emissions.
Another possible solution to this problem can be an airplane that can take off and land in a shorter runway or smaller area than a regular plane. This concept first was introduced in 1970s [98]. By implementing this technology, the number of airplanes which take off and land in a specific time will increase. New take-off approaches such as Vertical Take-Off and Landing (VTOL), Short Take-Off and Landing (STOL) or Extremely Short Take-Off and Landing (ESTOL) can use the limited runway more effectively. Bauhaus Luftfahrt in one of their researches showed that by using ESTOL airplane and rearranging the take-off field, the airport capacity could be increased[101]. Another similar study has been conducted by the National Aeronautics and Space Administration (NASA). Results explicated a significant increase in the airport capacity and huge decrements in travel's delay by using ESTOL planes [111].

1.1.2 Urban Road Traffic

People from all over the world are always thinking about a solution just like a flying car to save their time when they are stuck in high congested road traffic. Every day many people are traveling through cities, which creates long traffic jams and consequently wasting hours of people's time. Drivers can be stuck in traffic in big populated cities for about 50 to 100 hours per year [83]. In more detail, Los Angles, Moscow, New York, and São Paulo inhabitants lose about 102, 91, 91, and 89 hours annually in traffic jams respectively [1]. In some cities, there is no other area left for building new transportation infrastructure. However, the aviation industry has a great potential to use three-dimensional airspace to avoid ground traffic and help people saving their time. As an example, based on Uber's white paper, a round trip between downtown Sao Paulo and San Francisco's Marina can take more than four hours. However, by applying an aerial vehicle, it can only take about thirty minutes [80]. Based on my experience a single trip from downtown of Hamilton to Richmond hill center in Canada takes about 60 minutes by a road vehicle such as car and the travel time can be raised to 100 minutes in rush hours. On the other hand, by using an aerial vehicle with the cruise speed of roughly 150 mph, the whole trip would only takes around 16 minutes. It worth mentioning that a capable aerial vehicle should have an adequate range and speed and its "stop stations" in the town for boarding passengers should be readily accessible [3]. Then the whole trip can be a combination of air and ground travel. [1] reported that for trips of more than 20 km, the air taxi could save costumers time if the person is using air and ground mobility. The passenger boarding and de-boarding time and time for getting to "takeoff stations" are taken into account. In conclusion, not only a suitable areal transportation system can help intracity travels, but also it can be beneficial for city-to-city trips, which are usually more than 100km.

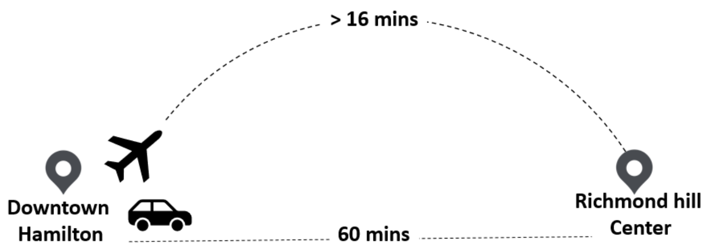

FIGURE 1.3: Example of comparison between road and air trip

1.2 Challenges in Developing Urban Air Vehicle

1.2.1 Costs

Nowadays, Due to the low production volume of aerial vehicles, flying trips are high-priced and infrequent. Current global civil rotorcraft production is only about 1000 units annually. Previous studies declare that if the production becomes double, then the cost will decrease by 15% for aerospace and automotive products [80]. Based on Uber's assumption if the VTOL aircraft costs about $1.2M at first prototype, by mass production of roughly 5,000 units per year, the price will decrease to $200,000, which is affordable [80]. Another factor besides the vehicle's price is building new infrastructures for boarding passengers and charging vehicles which need huge money investment; however, the "air road" is almost cost-free [1]. Constructing a 35 kilometers highway or subway line may cost something between hundreds of million to billions of dollar. However, the urban aerial transportation system only needs a few stop stations and charging sites [1]. Approximately four million dollars is needed for building a small stop station and around $100,000 for installing one high-speed battery charger [1].

1.2.2 Lack of sufficient stop stations and ports

"Ports" are generally hubs with multiple take-off and landing spots/runways with charging or fueling infrastructures. "Stop stations" are stations suitable only for one aerial vehicle with minimal infrastructure. Top of parking garages and towers, helipads, outdated airports, and unused lands surrounding highways can be used as stop stations and ports. Another novel suggestion which was proposed by NASA is the idea of using highway cloverleaf as stop stations. Standard highway cloverleaf's diameter is approximately about 255'. NASA proposed an elevated flat as a vertical stop station as shown in Fig 1.4 to grant the highest safety for passengers and minimize distraction to road traffic [80]. By some adjustments, this proposition can be used as a runway for ESTOL vehicles.

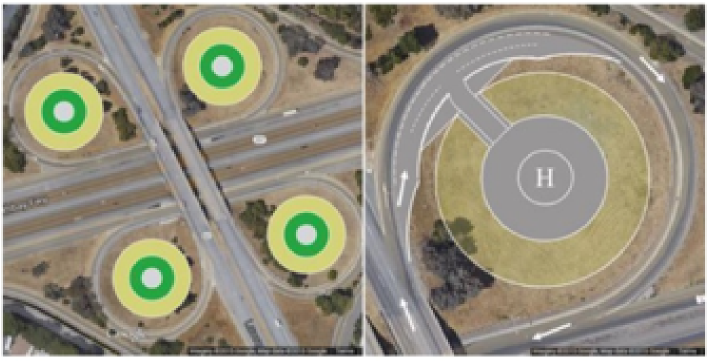

FIGURE 1.4: Proposed stop stations by NASA for VTOL aircraft [80]

Lack of sufficient stop stations and ports is one of the most challenging barriers in developing urban aerial transportation systems.

1.2.3 Safety

An aerial vehicle should be safer than a driving car on fatalities per passenger miles. Since the highest cause for flight accidents is due to human situational awareness and control loss, pilot aid should evolve to a fully automated system over time to decrease human flaws and increase safety. Engine failure and fuel management errors are the next highest cause of aerial accidents, which contained

18% of general aviation accidents [80]. Problems relating to engine failure can be fully solved by using electric redundant propulsion systems.

1.2.4 Noise level

One of the essential aspects that should be considered for an urban aerial vehicle to be acceptable to communities is the vehicle noise production as these vehicles are going to operate directly overhead and close to urban regions. To be acceptable for society, the vehicle's noise should blend into the existing background noise [80]. A medium-sized truck moving at a speed of 35 to 55 mph can make the sound level of 75-80 dB at 50 feet. In the long-term goal, numbers of urban aircraft are going to be more than the numbers of trucks, so their noise level should be less than trucks [80]. Based on Uber's report, a reasonable noise level goal for these vehicles should be half of the medium-sized trucks. This is almost like sensing noise from 25 feet distance of a Prius driving by 35 mph. Moreover, this is approximately one-fourth as loud as the smallest four-seats current helicopter [80].
Other features such as the duration and the repetition of the noise are important ones. As an example, if a 70dB(A) sound remains for 2 seconds, it would produce 73 dB SEL, and if it lasts for 4 seconds, it will increase to 76 dB SEL. Single event noise equivalent level or SEL is a metric for measuring short-term annoyance [80]. Repetition of the noise depends on the number of aircraft operating at the same place and at the same time, which extremely depends on take-off and landing strategies. Furthermore, the duration of the sound made by the vehicle depends on the vehicle's take-off and landing method. Besides, it should be mentioned that inside cabin noise should be less enough inherently as adding a large amount of

noise-reduction insulation leads to a significant weight penalty, which is undesirable [84].

1.3 Thesis Contribution

A lightweight two-seat airplane is modeled in Simulink MATLAB, and the feasibility of ESTOL electric lightweight airplane is investigated even when the airplane body, wing, and propeller structure are not optimized. The developed mode is flexible to changes of several variables meaning that any lightweight fixed-wing electric airplane can be tested and modeled by this model.
The main purpose of this study is to analyze the electric motor specifications based on takeoff and landing distances. In addition, the effect of cruising speed on the electric motor's power-speed and torque-speed profile is studied. In the end, the impact of two other parameters on the landing distance are investigated, which are the braking system of the airplane and the maximum airplane weight.

1.4 Thesis Outline

The necessity of using electric propulsion system for the future air transportation is described in the Chapter 2. Moreover, any aerial transportation system intended to be used in cities should take off and land from the smallest area as possible. The reasons why an ESTOL vehicle is a appropriate choice as an urban air vehicle are given in Chapter 3. In the following, the aerodynamic forces acting on a moving fixed-wing airplane are explained in Chapter 4. The first section presents a method to calculate the air density based on flying height, and then the procedure to calculate lift and drag for the airplane are given. The mechanics of flight and the aircraft motion equations in takeoff, cruise, and landing are described in Chapter 5. Based on these equations and relations the required power and thrust at each flight segment can be calculated. This study is conducted on a specified airplane. Therefore, the selected components are elaborated and defined in the Chapter 6. Chapter 7 is about how we modeled the airplane in MATLAB Simulink. Two models are built in Matlab Simulink. The first model can find the required thrust and power for takeoff, cruising, and landing. Then the airplane's requirements are fed to a numerical calculation model and subsequently results from the numerical model are used in the second Simulink model for validation.

Chapter 2

Electrified Aircraft

Electric aircraft is one of the most promising solutions to the global environmental issues associated with transportation. However, the low battery energy density, temperature-sensitive performance, and electric motor power density are the main significant challenges [97].

In this chapter, first, the common electrified power architectures are presented. In the following, an overview of full-electric aerial vehicles are given, and at the end, the necessity of using electric propulsion system for the future air transport is explained.

2.1 Electric Propulsion Architectures

There are mainly two electrified architectures which rely on the battery as energy storage: All electric and hybrid electric. The all-electric, which is the case study of this thesis, uses batteries as the only energy source to power the aircraft. On the other hand, the hybrid configuration utilizes the gas engine and batteries for powering the vehicle. Hybrid-Electric configuration divides into three subcategories. Gas turbine engine and battery-powered electric motors are both mounted on the shaft in the parallel hybrid architecture. It means both of them can provide propulsion at any time. In a series hybrid configuration, only the electric motor is connected to the shaft, and the gas turbine drives an electrical generator which is charging the batteries [88]. The first serial hybrid airplane is made by Simens and EADS named Diamond [71]. Using hybrid electric architecture can be a desirable solution as gas turbines are very efficient, and they can charge batteries during the flight. One of the problems associated with gas turbines is their noise which is undesirable for flying at low altitude. However, when the airplane is flying at cruising altitude, the gas turbine can charge the batteries. Today's batteries' specific energy is low, which leads to a short trip range. By using a hybrid configuration instead of fully electric configuration, the airplane's trip range becomes longer. However, in this thesis, a full electric architecture is chosen.

Turboelectrics architectures do not rely on the batteries for providing energy. They use a gas turbine connected to electric generators which produce electricity. Then the energy from the generators can be used to run the electric motors connected to propellers or fans [88].

2.2 Overview of Electric Flight in the Past and the Future

In this chapter, an overview of electric aircraft in the past and in the future is presented. The first successful flight powered by batteries was in summer 1884 where Krebs and Charles Renard made the first fully-controlled airship [103]. Years later, the first battery-powered airplane which is done by Militky and Brditschka, completed its first flight in 1973 [107]. It was flying for about 9 minutes [107]. Since then, many attempts were made for making electric aircraft. Some of them are presented in the section 2.2.1. Based on [103]'s database, 46% of electric aircraft concepts are developed by the start-up companies, and only 20% are being lunched by aerospace OEMs such as Boeing and Airbus[103]. The rest are from motor and other aerospace companies [103].

Commercial aircraft can classified as: General aviation (fewer than 6 passengers), Commuter (fewer than 20 passengers), Regional (30-100 passengers), Single-aisle (100-200 passengers) ,and Twin-aisle (more than 200 passengers) [88]. The main focus of this thesis is on the first category. Currently, all-electric aircraft are operating as research purposes and for technology demonstration. In the following sections, a summary and overview of electrified aircraft in general aviation and commuter aircraft are presented. Electrification of regional, single-aisle, and twin-aisle airplanes are out of the scope of this thesis.

2.2.1 General Aviation and Motor Gliders

General aviation and small sport airplanes are a great platform for testing new propulsion system concepts. Because, currently most of them are propeller-based and changing only the power plant is manageable. Mostly small electric motors on the order of 60 to 80 kW are being used for general aviation which is not a big deal for motor industry. Therefore, manufacturing electric small airplanes is not challenging from the motor side. The challenge would be the batteries energy density

,which determines the airplane's weight and consequently the range capability of the plane. Ultralight aircraft can be divided into two categories: General aviation, and Motor gliders. Aircraft in general aviation section can use the runway for taking off or they can vertically take off. Some of the electric airplanes in general aviation which utilize takeoff runway are demonstrated in Table 2.1. eVTOLs which stands for electric Vertically Takeoff and Landing aircraft are presented in Table 2.3. Table 2.2 summarized state of art's electric motor gliders specification. Most of the information and all the pictures are taken from the manufacturer website and product's catalog. The "Pax" is the total number of seats and the "MTOW" stands for Maximum Takeoff Weight which includes the aircraft body frame, batteries, motors and payload weights.

2.2.2 Commuter Aircraft

Mostly a commuter aircraft carries more than 10 and less than 20 passengers. In 2015, Siemens introduced the development of a 260 kW electric motor which weighs around 100 lbs. In the other words, it has 5kW/kg power density, which is sufficient for developing a commuter aircraft. It means that it is possible to electrify a twin-engine commuter by current motor technology. However, the battery energy density challenge remains. For bigger airplanes such as single-aisle or twin-aisle, the motor specific power should be improved by the factor of 5-10 from the motor's state of art [88], which is above the scope of this thesis.

TABLE 2.1: Electric Light Aircraft Specifications

Name	Image	Pax	MTOW kg	Wing AR	Motor	Battery	Endurance /Range	Max Speed
E-fan1		2 [4]	550 [4]	NA	2 motors each 30kW [107]	Li-Po 207 Wh/kg [5] 250V	1 hr /NA	270 km/h
Sonex E-Flight		1 [89]	600 [89]	9.8 [89]	1 motor 60 kW [6] 22.6 kg[89, 6]	Li-ion 17kWh [6]	50 mins /140 km [6]	208 km/h [89]
Green Cri		1 [89]	175 [7]	NA	4 motors each 11kW each 10 kg [8]	Li-po 20 kWh 28.6 kg [7]	NA /463 km [89]	226 km/h [89]
E-Cristaline Cri-Cri		1 [89]	170 [89]	NA	2 motors each 25.6 kW each 10 kg [89]	Li-po 3kWh 125 Wh/kg 24 kg [89]	1.7 hr /462 km [89]	260 km/h [89]
E-Cessna 172		2 [89]	169 [89]	7.5 [89]	1 motor 125 kW 19 kg [89]	Li-po 47 kg[89]	2h /177 km [89]	302 km/h [89]
Electraflyer-C		1	284 [89]	18 [89]	1 motor 13.4kW[89, 107] 1.03kW/kg[107] 2800 rpm[89]	Li-po 5.6kWh [107] 160 Wh/kg 35.3 kg [89]	1.5 hr /169 km [89]	144 km/h [89]
PC Aero Electra 1		1 [108]	300 [107]	11.65 [89]	1 motor max:31 kW 16kW 4.7 kg [89, 107]	Li-ion 5.8kWh [89] 64kg [9]	3 h /400km[89, 107]	160 km/h [89]
YUNeec e430		2	455 [89]	16.8 [89]	1 motor 40 kW 2450rpm 19 kg[106]	Li-po 160 Wh/kg[89] 13.3kWh 83.5 kg[107]	2-2.5 h /225 km [89]	150 km/h [89]

Name	Image	Pax	MTOW kg	Wing AR	Motor	Battery	Endurance /Range	Max Speed
Sun-Flyer 2		2	862 [10]	12 [10]	1 motor max:86 kW 70kW [11]	Li-ion 260Wh/kg [10]	3.5 hr[10] NA	250 km/h [10]
Pipistrel WATTsUP		2 [12]	550 [89]	11.3 [89]	1 motor 85 kW 2200rpm [89]	Li-po 17kWh 126 kg[89]	1.5 h /200 km [89]	248 km/h [89]
Pipistrel Alpha Electro		2	550 [13]	11.3 [64]	1 motor max: 60kw 50 kW[13] 2100-2400rpm	Li-po 21kWh 126 kg[13]	1 hr /120 km [13]	130 km/h [13]
Pipistrel Panthera Electro		2	1315 [14]	10.5 [14]	1 motor max: 200 kW 145 kW[14]	NA	NA /400 km [15]	324 km/h [14]
Siemens Extra 330LE		2	1000 [16]	6 [16]	1 motor max:260 kW 5.2kW/kg 50kg,2500rpm[16]	Li-ion 18.6 kWh[17] 150 kg[18]	20 mins [16] /NA	337 km/h
Magnus eFuesion		2	600 [19]	6.5 [19]	1 motor max:85 kW 45 kW 324 Nm 2500rpm[19]	10.1 kWh[19]	1 hr [20] /NA	180 km/h [19]
MC30 Firefly		1	183 [89]	10.35 [89]	1 motor 19 kW 5.4 kg [89]	4.7kWh 54kg[89]	4.5 h /800 km [89]	162 km/h [89]

TABLE 2.2: Electric Motor Gliders Specifications

Name	Image	Pax	MTOW kg	Wing AR	Motor	Battery	Endurance /Range	Max Speed
E-Genius		2 [89]	938 [89]	19 [21]	1 motor 60kW [22, 108] 2,000 rpm [22] 45 kg [89]	Li-ion 56 kWh [3] 205Wh/kg [89]	2.5 hrs[89] /322 km	270 km/h [89]
Pipistrel G2 Taurus		2	472 [23]	18.6 [89]	1 motor max: 40 kW 30 kW, 11kg 2200rpm[89, 105]	3 battery configs Li-po 20Ah, 4.75kWh 30Ah,7.1 kWh 40Ah,9.7kWh[24]	NA /200 km [89, 105]	130 km/h [24]
Pipistrel G4 Taurus		4 [108]	680 [89]	NA	1 motor 145 kW, 90 kg 5500rpm [89]	Li-po 90kWh 500 kg[89]	2.75 h /400 km [89]	216 km/h [89]
Electra Flywer ULS		1	235 [25]	NA	1 motor 15 kW 2500 rpm[25]	Li-po 3.3 kWh 20.5 kg[25]	1 hr[25] /NA	65 km/h [25]
Yuneec Eviva		2	455 [89]	20.3 [89]	1 motor 40 kW,23kg[89]	Li-po 62 Ah,67 kg[89]	1.3 hr 206 km[89]	230 km/h [89]
Silent 2 electro		1	300 [89]	20 [89]	1 motor 25 kW, 9.5kg 5.46 Nm/kg 2.63kW/kg 4600rpm[107]	Li-po 4.2kWh 270Wh/kg[89] 31.4 kg [75]	40 mins[26] /NA	220 km/h [89, 26]
Arcus E		2	812 [89]	25.7 [27]	1 motor 42 kW,1500rpm [89] max T:216N.m 29 kg[27]	Li-ion Saft VL41M [89]	NA	280 km/h [89]
Antares 20E		1	660 [28]	31.7 [89]	1 motor 42 kW,1500rpm[89] 1.44kW/kg 8.1Nm/kg,29 kg[107]	Li-ion 136 Wh/kg 80kg[89]	NA	280 km/h [107]

TABLE 2.3: eVTOLs Specificaion

Name	Image	Pax	MTOW kg	Motor	Battery	Endurance /Range	Max Speed
City Airbus		4 [29]	2200 [30]	4 motors each 204kW Each 49 kg,20Nm/kg max T:1500 Nm 1300 rpm[31]	110kWh[32] 500kg	15 mins[29] /96km [30]	120 km/h [29]
Vahana	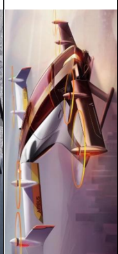	1	835 [33]	8 motors each 45 kW [109]	NA	30 mins 100 km [109]	175 km/h [109]
Ehang 184		1	360 [109]	8 motors each 152 kW [34]	Li-Po [109] 14.4 kWh [35]	25 mins[36] 16 km [37]	100 km/h [36]
Joby Aviation S2		2	900 [100]	NA	Li-ion 200 Wh/kg [87]	NA 320 km [100]	322 km/h [100]
Lilium Jet		2	600 [109]	36 electric fans total 320 kW [38]	NA	1 hr /300km	300 km/h [36]
VC 200	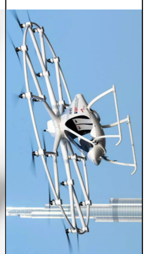	2	450 [109, 39]	18 DC motors each 3.9 kW [109]	Li-ion [39]	27 mins 27 km [39]	100 km/h [39, 109]

2.3 Why electric propulsion systems?

To meet the set goals for reducing global emission, it is crucial to eliminate petrol, gas and gasoline usage in transportation. However, this is not the only reason to advocate for electrified air transport. In the following, other reasons to support this idea are presented.

2.3.1 Safety

As mentioned in the previous section, there are mainly two important factors which lead to aircraft accidents. The first one is due to the human error, and the second one is the engine and fuel management system failure. The latter one can completely be solved by using a fully electric propulsion system. Additionally, compared to the conventional combustion engine propulsion system, an electric propulsion system has less complexity. This will help with simplifying the control section as electric motors do not need extra mechanical facilities such as gearboxes for controlling speed and torque. They can directly be attached to the propeller for small size aircraft, and they can provide demand torque in any speed range. Moreover, they can react really fast to the changes; it takes about milliseconds for an electric motor to respond to the digital control signal. For preventing human errors, the whole system should be fully automatic in the long-term goal. To accomplish such a goal, the system complexity level should be as low as feasible, and the control strategy should be as simple as possible. Due to the reasons which have explained earlier, electric systems are appropriate candidates for automated systems.

2.3.2 Global Emission

Transportation is the largest source of greenhouse gas emissions. Hence, all the emerging transportation systems should be environmentally friendly [80]. The aviation industry produces about 628,000,000 tons of CO2 annually, which means it contributes %2-2.5 of total global CO2 emissions. In the US, the aviation industry contributes about %11 of the greenhouse gases produced by the transportation site [88]. In 2016, US aviation industry consumed 17 billion gallons of fuel which produced 781,000,000 tons of CO_2 [89].
At 2009 the aviation industry agreed to a set of commitments for reducing the global emission. The object is including a %50 reduction in CO2 emission by 2050 compared to 2005 and %1.5 improvement in annual fuel efficiency by 2020 compared to 2009 [97]. To achieve the long-term goal, which is 50% reduction in CO2 emission, the upgraded technologies are not sufficient, and some revolutionary new technologies such as new aircraft concepts and new energy sources are required [97]. Potential availability timeline of these upcoming technologies and aircraft configurations are given in the Fig. 2.1.

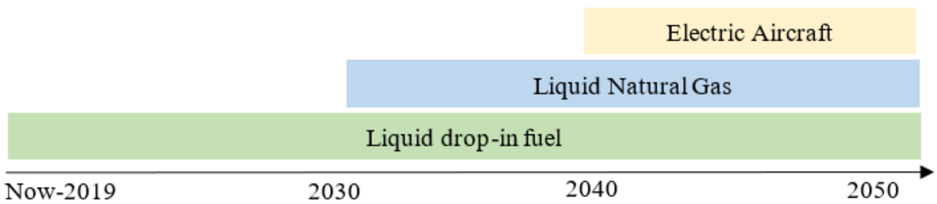

FIGURE 2.1: Potential timeline of future aircraft configurations [97]

An electric vehicle is one of the promising solutions for emission reduction in the future. In the case of an electric vehicle, the operational emission is zero, but the indirect emission which is from the power source for producing electricity must be considered. If fossil fuels are used for generating electricity, it will produce CO2 emissions, but these emissions can be filtered easier near the ground level compared to higher altitude [88]. In the best case, if the electricity source is powered by renewable energy sources such as wind, solar, and nuclear, the indirect emissions will be approximately zero.

2.3.3 Fuel Depletion

Using alternative energy sources is mandatory for the aviation industry, not only because of emissions but also because of the limited fuel resources. The Fig. 2.2 shows the fuel price in the past 30 years [40]. It is apparent from the Fig. 2.2 that the fuel price tends to rise due to higher demand, and it will become worse in the coming years. The fuel expense is the main operational costs (about 40%) in the transportation industry based on [93]. This is the reason why increasing the efficiency and decreasing the fuel consumption are essential for the aviation and automobile industry.

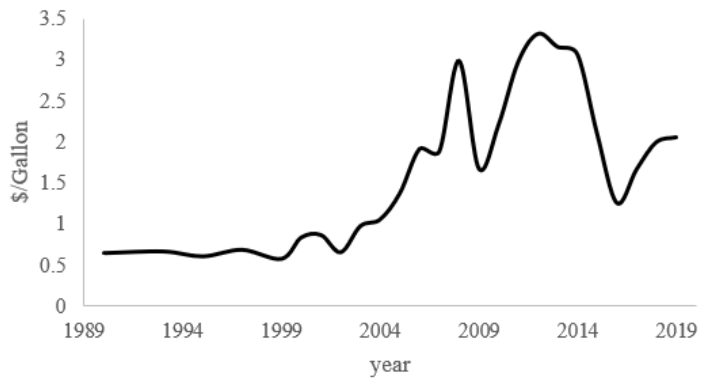

FIGURE 2.2: Fuel price in last 30 years [40]

A possible solution for reducing fuel consumption is a hybrid wing body configuration, which is almost an enormous flying wing. This concept was introduced for the first time in the late 1980s. The main goal of designing a Hybrid Wing Body (HWB) aircraft is achieving high aerodynamic efficiency. Hence, it is designed based on the optimized aerodynamic performances. An example of the blended wing aircraft is the 500-seats aircraft developing at the German Aerospace Center and it is expected to be on service by 2040 [97]. However, in this thesis, only the electric concept is being considered.

2.3.4 Power/Energy

Flying at higher effective altitude may sequences in a reduction in internal combustion engine's power because at higher altitude the air density is lower, and the air density is one of the factors which determines the engine's power. Based on the engine's design, this reduction can be more than even 30% of the engine's full power. This situation would not have any effect on electric motors. However, this is not the case in urban air vehicles because they are usually flying in low altitude. But the most important advantage of using electric motors is their ability to use significantly higher power than their continuous power for short bursts(even over 2X continuous power) [95]. Fig 2.3 is an example of electric motor continuous and maximum power. During takeoff, the vehicle requires more power [88] and electric motors can provide this amount of high power without any need for increasing the propulsion system size. Accordingly, the weight penalty can be minimized [72].

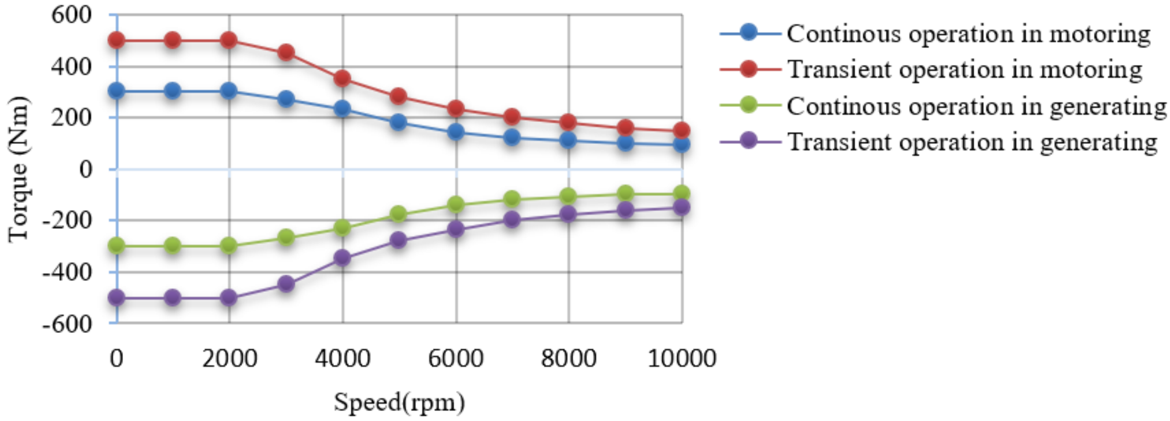

FIGURE 2.3: Comparison of continuous and transient operations for electric machines

2.3.5 Reverse Operation

The other benefit of Electric Motor (EM) is that their rotation direction can be easily controlled and reversed without any mechanical changes. This ability is useful for providing reverse thrust during landing and braking [72]. Reverse thrust is one of the major factors which make the required runway for landing shorter. In conventional STOLs, thrust reversal system is used for changing the engine's rotation direction, but it adds additional weight to the aircraft, which is undesirable.

2.3.6 Efficiency and Energy Consumption

Nowadays the most common advanced engines which are using in the aviation industry, are turbofan engines with bypass duct [62]. Light aircraft may use spark-ignition or diesel engines due to their lower price [88]. The combustion engines generate more heat compared to the produced power that's why their efficiency is mainly between 45 to 55% from fuel to propulsor [88] while the electric propulsion system's efficiency is up to 90%. The electric propulsion system technology has shown that the vehicle efficiency can improve up to 10 times more than existing helicopters and 5 times more than existing CTOL aircraft. Many companies such as Siemens already achieved an electric propulsion system with a turbo-like specific power that is more than 3 times efficient than a small helicopter turboshaft engine. NASA Maxwell X-57 showed in its final report that by utilizing distributed electric propulsion (DEP) system, the efficiency of a CTOL aircraft during take-off and landing can be improved around 4 times [69].

As electric motors have higher efficiency, the total energy consumption by the electric aircraft is lower than the conventional one for the same trip mission. A great comparison of energy consumption is reported in [2]. The comparison is between Dash 8-100 and Zunum hybrid-electric aircraft. These two airplanes are almost the same size except that the Zunum plane has 13 more seats. Based on calculation for a single flight of 190km, the Dash 8-100 consumes 2,640 kW while the Zunum only needs 950 kW [2]. The energy consumption of a pure electric aircraft can be assumed one-third of the conventional one [2].

2.3.7 Costs

As said in the first chapter, one of the barriers for wide uses of aircraft as urban transportation is their high maintenance and production costs. The operational costs for electric vehicles are less than conventional ones due to their high efficiency and low energy use, as discussed in section 2.3.6. A good example of operational cost comparison between conventional and electric aircraft is presented in [67]. Based on its results, it is shown that the compound helicopter costs roughly about $55 per passenger by using electric motors. However, New York Helicopter costs about $875 per passenger for a 2-passenger trip [67]. Cost analysis in [67] shows that operational cost can be decreased from $3.5 per mile initially to $0.6 per mile in the long term, which is even less than UberX and UberPool ride costs ($2.34 and $1.38 per mile respectively in 2016- United States). Another cost comparison between two VTOL aircraft is given by reference [100]. Energy cost per mile for Joby S2 which is a VTOL Tilt-thrust aircraft is $0.05. In comparison, it costs $0.53 for the Robinson R22, which is a conventional helicopter [100]. Furthermore, the operating cost is decreased by the factor of about 6 by utilizing an electric propulsion system. The operating costs per mile for Joby S2 is $0.2, which on the other side, for the Robinson R22 is $0.53 per mile [100]. Based on Porsche Consulting analysis, the total cost for an eVTOL aircraft will be $1.8 per kilometer in long term goal [1]. Additionally, maintenance of an electric propulsion system is easier than a conventional one due to its less complexity and fewer components, and this is a huge advantage for the aircraft as it can operate more frequent and for a longer time in transportation service.

Having said that, electric aircraft will need a lot of new initial infrastructures such as charging stations, and it will be necessary for the electricity grid and transmission systems to upgrade.

2.3.8 Noise Production

As said before, for wide approval of urban aerial mobility system, the aircraft noise should be merged into the background noise. Compared to piston or turbine engines, the electric motor produces less noise. The propulsion systems with conventional engines are mechanically more complicated, containing gearboxes and cross shafts, which are other sources of noise. Besides, electric motors do not need to ingest and expel a large amount of air for the combustion process, which make extra noise[80]. A comparison from a study conducted by Porsche consulting shows that an electric passenger drone is 4 times more quite than a conventional helicopter [1]. Thus, the next generation of urban aircraft should be fully electric at least at taking off and landing when they are flying at low altitude and near the ground.

2.3.9 Design Diversity

The ease of installing electric motor as the power system without significant structural complexity provides an excellent opportunity to the aircraft designers. The airplane's designer can place electric motors wherever is desirable. Because of that, three configurations are now feasible:

1. **Distributed Propulsion System** A higher number of smaller electric motors can be used all over the aircraft instead of using one or two main engines. This configuration is called a Distributed Propulsion System or DPs. A great example of this configuration is NASA X-57, which is a fixed-Wing airplane with a distributed electric propulsion system. Practically, this was almost impossible by using combustion engines, as they add high complexity to the system by using drive shafts and gearboxes [100]. In addition, electric motors are scalable, which means they can achieve the same efficiency, whether they are small o big. By applying this technology, electric motors can be installed everywhere along with the aircraft. It means they can be places where the drag is high and help to reclaim drag losses [95]. An excellent advantage of using a distributed propulsion system is the power drop in motor size as more number of EM are using [88]. Manufacturing smaller motors are more straightforward; consequently, instead of using one or two high power motors, several smaller ones can be utilized. Plus, a distributed propulsion system can increase redundancy and safety in the vehicle's operation.

2. **Wing-tip Mounted Propulsion** Another advantage of placing electric motor anyplace which is wanted is "wingtip mounted propulsion" concept. There are significant drags and vortex formations behind the wing due to the pressure difference between the top and down of the wing. Various kinds of devices, such as winglets are made to decrease this effect. A possible solution to reduce the drag would be mounting the propulsion system at the wingtips [2] and electric motors give the opportunity of placing them where

ever is beneficial.

3. **Boundary Layer Ingestion** Many companies are proposing the idea of installing the propulsion system at the aft for large aircraft. The air ingested by aft-mounted propulsion is slower and more turbulent, which leads to lower fan loss [103] and consequently lower total drag [77].

However, in this thesis, none of these advantages are considered, and only a simple airplane with one electric motor is considered.

2.3.10 Preparation time

By using electric motors, there is no delay due to the time waiting for rotors to spin up or down and less delay means less takeoff and landing time. Besides, electric motors do not need warm-up time which combustion engines need [107][77].

Chapter 3

Extremely Short Takeoff and Landing Airplane

There are mainly two ways for an aircraft to take off and land. First is using the runway to increase the aircraft velocity to the lift off velocity and to become airborne by using wings. The second approach is to take off and land vertically similar to a helicopter. In this section, first, various types of takeoff and landing approaches will be explained, and then, the reasons explaining why an ESTOL vehicle is a fitting choice for the urban air vehicle will be presented.

3.1 Takeoff and Landing approaches

1. **Conventional Take-Off and Landing (CTOL):** Presence of a sufficient runway is necessary for CTOL aircraft taking off and landing. During the take-off, the flaps and slats are extended downward so more lift force can be provided. In the meantime, the aircraft accelerates to reach a specific speed

called lift-off speed. At this point, the aircraft starts to fly off the ground. This category of aircraft including the majority of fixed-wing aircraft have some advantages and disadvantages. The most important advantages of them are high efficiency, high speed, and high range but their main drawback is the need for long runways. Currently, the lack of such runways is indeed one of the main problems of overpopulated cities and congested airports.

2. **Vertical Take-Off and Landing (VTOL):** These aircraft can take off and land vertically. The first person who sketched of an aerial vehicle was Leonardo da Vinci [1]. The drawing was a vehicle with an aerial screw on the top [1]. Later in 1901, the first helicopter flew above Berlin [1]. But Helicopters in general are too noisy, polluting, inefficient, and expensive [80]. They are mainly inefficient because of the rotor tip speeds, which is required to achieve a sufficient cruise speed. Furthermore, they have approximately 3 to 4 times lower lift-to-drag (L/D) ratio compared to fixed-wing airplanes in the cruising mode [100]. This cause a shorter range and higher operational costs. Moreover, their noise production makes them an unacceptable candidate for operating in high population areas. There are many companies working on VTOL vehicles such as eVolo VC200 Volocopter and eHang 184, which use a multi-copter concept. This approach is significantly slow (maximum airspeed of about 100 km/h), and they have short-range capability and low efficiency in cruising mode.

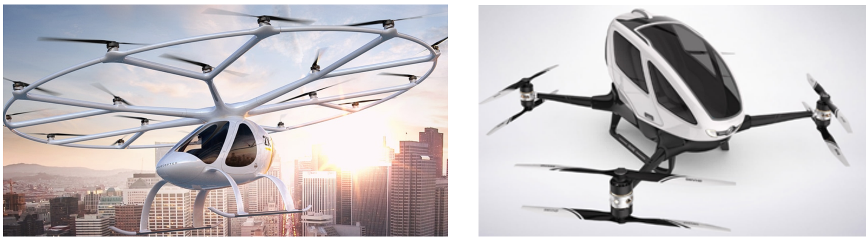

(A) eVolvo VC200 (B) eHang 184

FIGURE 3.1: Example of Multi-Copter aircraft [41][42]

The best types of VTOL aircraft are those that posses the advantages of vertical takeoff and land with high-speed cruising ability. Many companies are now investing to combine the vertical takeoff and landing ability with the high-speed cruise. They can be categorized into three groups.

(a) **Separated Configuration Systems** In this category, two separated propulsion systems are used: one for taking off and landing and the other for forward flying. For instance, the vehicle concept announced by Zee uses two separated systems, one for vertical lift and the other for cruise mode [43]. Although the implementation of this configuration is straightforward, it adds additional and unnecessary weight to the system and extra weight leads to a shorter range [80]. This is why the gyrodynes need extra power compared to conventional helicopters. This configuration is highly recommended for applications requiring a high duration of hovering mode with brief high-speed travels [68], which is not suitable for urban air transport applications.

FIGURE 3.2: The Fairey Rotodyne Y with two separated system for taking off and cruising [102]

(b) **Tilt-Thrust** Two of the most outstanding types of VTOL vehicles trying to combine vertical takeoff with high speed forward ability are tilt-rotor aircraft and tilt-wing aircraft. They can combine the advantages of vertical lifting and landing (e.g., a helicopter) with the high forward speed and range (e.g., a fixed-wing airplane) by changing their rotor or wing position [84]. For the forward flight, rotors or the entire wing tilt forward, and for takeoff and land, they tilt vertically. Joby Aviation uses a distributed set of tilting prop-rotors which are six to twelve depending on the size, capacity, and the requirements of the vehicle [100]. The angle of these prop-rotors changes during the different flight conditions. Therefore, the required thrust for vertical lift and cruise can be provided by only one system. Nevertheless, this model has a higher complexity due to its rotating parts, and it needs a complicated control strategy [80].

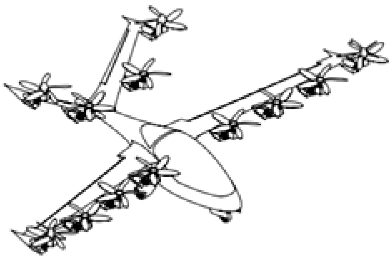

(A) Takeoff Mode

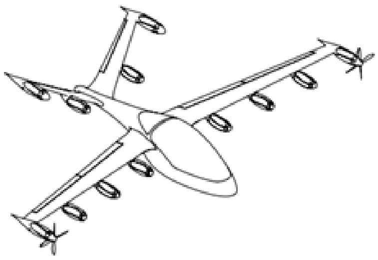

(B) Cruising Mode

FIGURE 3.3: Tilted-rotor aircraft: Joby S2 configuration during takeoff and cruising modes [100]

A3/Airbus's concept, named Vahana utilizes the tilt-wing approach, which can rotate the wings to the forward and the aft. It has two wings with four prop-rotors on each [44]. Reducing complexity is the key benefit of this approach comparing to tilted-rotor models, as the whole wing is rotated and it can be done by only two actuators [80]. However, it needs more power and energy for taking off as it does not benefit from the wing during the take-off. Also, the redundancy is reduced as it only depends on tilting the whole wing and not the individual rotor's links [100].

(A) Takeoff Mode

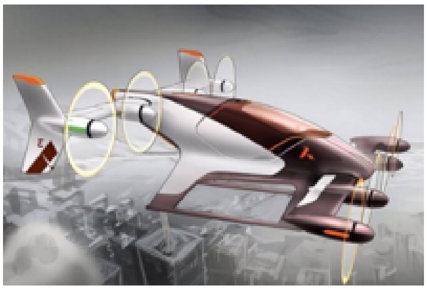

(B) Cruising Mode

FIGURE 3.4: Tilted-Wing aircraft: Airbus Vahana configuration during takeoff and cruising modes [44]

(c) **Tail-Sitter** A tail-sitter aircraft is an aircraft with a sizable tail that can support the entire weight of aircraft [82]. In the standing position, the force is applied upwards, and when it is adequate, it accelerates the aircraft against gravity and make it to takeoff [68]. After taking off vertically, it transients to the forward flight similar to a typical airplane without any changes in the mechanical arrangement. The main advantage of this configuration is its simple implementation.

FIGURE 3.5: Tail-sitter aircraft: AeroVironment SkyTote [4]

Table 3.1 provides a summary of specifications of VTOL vehicles and concepts that have the potential to be used in Urban Air Mobility network.

TABLE 3.1: Summary of VTOL vehicles characteristics that can be used in Urban Air Mobility (UAM) network

Vehicle's Name	**Joby S2**	**Lilium Jet V1**	**Vahana**	**TF-X**	**M400 Skycar**	**Volocopter 2X**	**Ehang 184**
Manufacturer	Joby Aviation	Lilium Aviation	Airbus	Terrafugia	Moller	Volocopter	Ehang
Country	USA	Germany	USA	USA	USA	Germany	China
Capacity	2[100]	2[109]	1[45]	4[46]	4[92]	2[73]	1[109]
MTOW(kg)	1084[100]	600[109]	815[45]	NA	1089[92]	450[73]	360[109]
Range in the air (km)	320[100]	300[47]	60[45]	800[46]	1209[92]	27[73]	NA
Top Speed (km/h)	320[100]	300[47]	200[45]	320[46]	530[48]	100[73]	100[42]
Approximate Price	$200,000[100]	NA	NA	$280,000 [49]	$500,000[50]	$338,000	200, 000– 300, 000[51]
Power Plant	Full Electric	Full Electric	Full Electric	Hybrid Electric	Hybrid Electric	Full Electric	Full Electric
Category	Tilted-Rotor	Tilted-Ductedfan	Tilted_Wing	Tilted-Rotor	Tilted-Rotor	Multicopter	Multicopter

3. **Short Take-Off and Landing (STOL):** Short Take-Off and Landing (STOL) is one of the potential solutions to increase airports capacity and solve the road traffic problem. Vehicles in this category need a short runway to takeoff and land. Compared to CTOLs, STOLs vehicles mostly have a higher power-to-weight ratio with complicated high lift systems and strong brakes.

   Runway length is a function of the square of stall speed, which is the minimum required speed for flying. There are two possible solutions to make the takeoff distance shorter: to reach the lift-off speed faster by increasing the thrust, and to Lower the lift-off speed by increasing the lift coefficient or decreasing the wing loading [72]. In this thesis, the analysis for the first solution is presented.

The runway length for the landing can be minimized by strong brakes and low landing speed. Increasing lift coefficient and decreasing the wing loading can help to reduce the touch-down speed. Drag can be increased by using flaps and slips on the airplane's wing. Furthermore, thrust reversers can be beneficial as they can temporarily reverse the applying thrust. Consequently, instead of applying forward thrust, it applies the thrust to the back and this force can make the airplane stop faster.

In general, the STOL performance is defined by the longest required runway to the takeoff or to land. There are several definitions on what makes and aircraft an STOL type. Two of the most common definitions are as following: According to the Department of Defense Dictionary of Military and Associated Terms and Dictionary of Aeronautical Terms definition for STOL, a STOL military vehicle should take off and reach the attitude of 15 meters (or 50-foot) within 450 meters (or1500-ft) or land from the attitude of 15 meters (or 50-ft) to the ground within 450 meters (or 1500-foot) [78]. Columbia Encyclopedia uses almost the same definition as Department of Defense Dictionary of Military and Associated Terms and Dictionary of Aeronautical except for a small difference in runway length. Columbia Encyclopedia states that the aircraft should be able to clear a 15-m (50-ft) obstacle within 305-m (1000-ft) of the runway [66].These definitions are a somewhat unclear in the terms of the vehicle size and configuration. A better definition is given by the McGraw-Hill Dictionary of Scientific and Technical Terms.

According to this dictionary, a STOL aircraft is a heavier-than-air aircraft than cannot take off and land vertically, but it can take off and land from a more confined area than normally required by the same size aircraft [61]. STOL aircraft can use the airport's capacity more effectively as with the equivalent runway length, a larger number of STOL aircraft can take off and land compared to CTOL ones. This makes them a great candidate for solving the high congested airport's problem. It also make it feasible to use the abandoned airports located in the middle of cities. Nevertheless, it might not be the best solution for an urban aerial vehicle, because the vehicle should take off and land from a minimal area such as the top of buildings and existing helipads in cities. In Table 3.2 a summary of STOL vehicles' specifications that can be used in Urban Air Mobility network is presented. Most of the information is adopted from the manufacturer website and vehicles data-sheets.

4. **Extreme Short Take-Off and Landing (ESTOL):** Extreme Short Take-Off and Landing (ESTOL) vehicle can be a practical solution for the airport congestion, and travel delay problem. With a higher thrust-to-weight ratio, the airplane climbs faster, and finishes the takeoff phase in a shorter time and distance. Consequently, a high lift system is demanded. The main strategies implemented in ESTOLs are almost the same as STOLs but with a subtle improvement in aircraft propulsion system, power plant or aerodynamics. In the years following the world war 2, NASA heavily funded researches on the ESTOL aircraft. The NASA ESTOL aircraft goal is a 100-passenger airplane with the ability to take off and land in less than 2,000 feet with a cruise Mach

TABLE 3.2: Summary of STOL vehicles characteristics that can be used in Urban Air Mobility (UAM) network

Vehicle's Name	**Aero mobile 4**	**Sky Runner**	**Maverick LSA**	**PAL-V1**	**Transition**
Manufacturer	Aeromobile	Sky Runner	I-TEC	PAL-V International	Terrafugia
Country	Slovakia	USA	USA	Netherlands	USA
Capacity	2[52]	2[53]	2[54]	2[55]	2[56]
Runway(m) over (0ft/50ft) obstacle	397/595[52]	182/NA[53]	92/NA[54]	180/330[55]	NA/427[56]
MTOW(kg)	960[52]	816[53]	650[54]	910[55]	665[57]
Range in the air (km)	750[52]	222[53]	NA	400[55]	640[56]
Cruise Speed (km/h)	360[52]	65[53]	65[54]	160[55]	160[56]
Approximate Price	$1.5 million	139, 000–154, 000[53]	$94,000[54]	400, 000–600, 000[55]	194, 000–279, 000[55]
Power Plant	Hybrid Electric	Gasoline	Gasoline	Gasoline	Hybrid Electric

number greater than 0.8 and with a minimum range capability of 1,400 miles [86]. All these abilities are achieved separately in other vehicles. However, there is no vehicle that has all these features together. It has been shown that a short runway between 130 to 300 ft is possible for ultralight airplanes with state of the art's technology [70]. Additionally, placement of runways up to 500ft is feasible in the urban areas such as congested cities [72]. Taking off in an extremely short runway can be achieved by incorporating two improvements: an aerodynamics improvement, which is to increase the lift coefficient and decrease the drag. The other is power plant improvement. Lately, after the inception of the Upper Surface Blowing (USB) technology in aerospace, it has been shown that the lift coefficient can be increased to 10 [106]. In this thesis, the lift coefficient is assumed as a normal one for a wing (without any complicated high lift systems), and the power plant improvement is considered.

3.2 Why ESTOL?

The desired vehicle is spending more time in cruise mode than hovering mode. Hence, it should be efficient in moving forward while it should take off and land from the smallest possible area. An airplane uses wing and propellers for having an efficient cruising mode while helicopter utilizes a rotor lift method for the best performance in hovering mode. Therefore, it seems that an airplane which can take off and land in an extremely short runway is a better solution for this application. Another possible solution is an aircraft that can tilt its rotors or wings so it can offer satisfying efficiency in both the hovering and cruising modes. Based on the requirements described previously, the vehicle should take off and land from a small area, and it should be fully electric. In this section, reasons will be presented as to why an electric ESTOL aircraft is the better selection.

3.2.1 Certification process and Air traffic control

The challenges for developing new aircraft is not only technical barriers, but also the certification peocess enforced in many aviation agencies. Any proposed aerial vehicle should be qualified by aviation authorities that mainly includes the US Federal Aviation Administration (FAA) and the European Aviation Safety Agency (EASA) [80]. Unsurprisingly, the certification process is a time-consuming and complicated procedure. An excellent example of a long delay for approval is a tilt-rotor craft named AugustaWestland AW609, which took about 12 years to qualify [72]. It has been shown that a fixed-wing STOL aircraft can reduce the flight risk compared to VTOLs; hence, the certification process can be completed faster [72]. Based on the Porsche Consulting study, along with VTOL aircraft, the multicopters are the first ones that will be commercially available; however, their range and speed capabilities are insufficient as urban mobility applications. In the other side, The Tilt-x aircraft need the longest time to get certified by the FAA and enter the market[1]. The difference of "time to market" between fixed-wing airplane and rotorcraft are mainly because of the potential failures rooted in three primary sources. First one is the flight stabilization system that controls the vehicle stability during the takeoff and the transition [72]. This system is mainly a complex fly-by-wire system that is not necessary for an electric fixed-winged STOL vehicle. The second source is the power system that should deliver power from the batteries to the motors, and the last one is the energy source, which is a battery [72]. Loss of power in VTOL aircraft means loss of control, which is one of the most hazardous circumstances. Unlike a VTOL aircraft, a fixed-wing ESTOL aircraft can maintain attitude control in the case of power loss [72].

3.2.2 Safety-in term of control

It has mentioned before that for the widespread use of these vehicles in the future, it is essential that flight control become fully automotive. Therefore, the vehicle's control strategies should be as easy as possible to minimize potential failures.

VTOL crafts suitable for this application are tilted-rotor and tilted-wing ones. They combine the flight characteristics of the helicopter and the fixed-wing airplane; accordingly, their control system should blend the flight control part of both vehicles. Because of the transition from vertical to horizontal flight in VTOL vehicles, the aircraft model changes significantly [82]. This is one of the primary reasons that controlling a VTOL aircraft is more sophisticated than ESTOL. [95] presented the main challenges of controlling "NASA GL-10", which is a tilt-wing aircraft.

Another major reason for failure is associated with the number of parts in a system. The possibility of a system breakdown increases with the number of parts. The propulsion system of tilt-x aircraft has more moving part compared to the ESTOL propulsion system, and all these parts need an accurate control strategy. Failure in each part can fail all the system and cause a fatal accident.

3.2.3 Stop stations and ports

Nowadays, cities do not have adequate infrastructure for landing and taking off an aircraft, and the infrastructures that do exist are often reserved for emergency uses. There are just a few helipads in major cities that can be used as stop stations. So, as a starting point, it is essential to develop a vehicle that can take off and land as fast as possible so the maximum capacity of each existing stop station can be used. The fastest approach for taking off is the approach used in airplanes with an extremely short runway.

The "possible building" is a building with a roof long enough to serve as the runway. Fig 3.6 presents possible building numbers based on the required runway length in large congested cities such as New York City [72]. It can be observed that the number of possible buildings exponentially increases if the runway length becomes shorter.

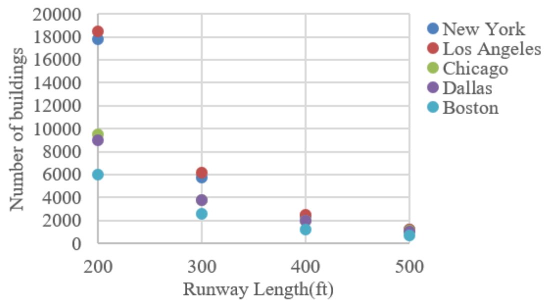

(A) Number of Possible Buildings when Runway length is less than 500ft

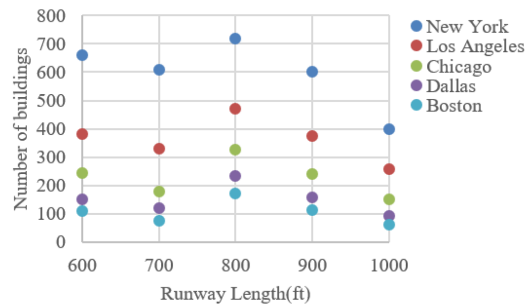

(B) Number of Possible Buildings when Runway length is more than 600ft

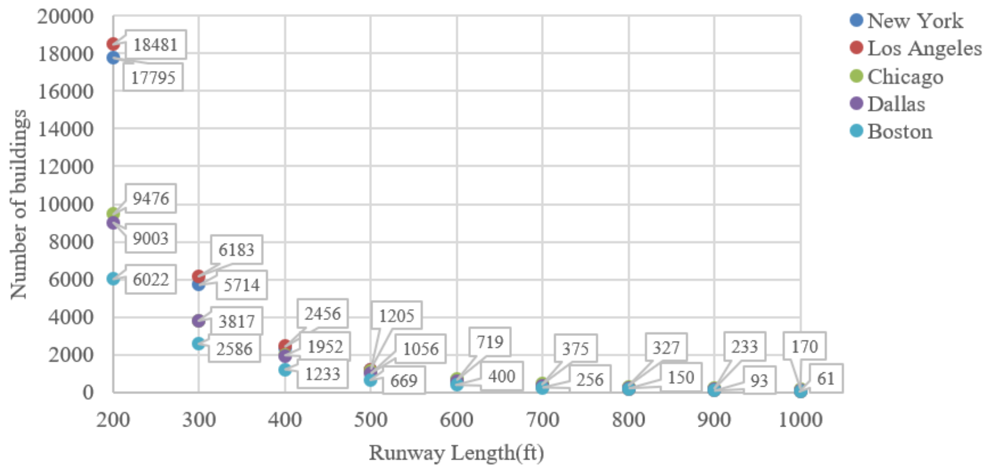

(C) Total Number of Possible Buildings

FIGURE 3.6: Number of possible building that can be used as stop stations for takeoff and landing [72]

Based on [1], at starting phase, only 5 landing ports with 120 aircraft are sufficient for a large city. A city with only 5 stations can give 10 possible connections. Later, in the second phase, 40 stop stations should be located in each city, and the ultimate goal is to have approximately 100 stop stations and ports with around 1000 vehicles for megacities with a population of 5 to 10 million people [1]. As a starting point, developing an ESTOL aircraft which can take off and land in less than 500 ft (or 150m) can solve the problem of ground traffic in populated cities. Based on Fig 3.6, the number of possible buildings for an airplane which can take off and land in 900 ft is 93 to 233. It means even building an ESTOL aircraft that can take off and land within 900 ft can solve the problem.
Accordingly, the best candidate based on limited stop stations is ESTOL vehicle with a lifting system as an airplane. However, the only problem with ESTOL vehicles is that they may need different runways in different directions due to wind and weather condition changes. Hence, in some specific cities, the STOL and ESTOL vehicles may need more than a single runway.

3.2.4 Noise

It has been proven that a fixed-winged aircraft produces less noise than a rotorcraft vehicles including helicopters and tilted-x aircraft [72]. Furthermore, it has been concluded that the repetition and duration of the sound are essential factors for sensing noise. If a vehicle can take off and land in a shorter time, more vehicles can take off and land at the same station and at the same time. It also means the repetition of the noise is more frequent. Moreover, noise duration is depends on the takeoff and landing approach. The duration of noise becomes shorter with faster takeoffs and lands. In conclusion, there is a trade-off between takeoff and landing speed and the produced noise by the vehicle. By choosing ESTOL as the strategy for taking off and landing instead of VTOL, the noise duration can be reduced, the system efficiency can be increased, and noise repetition can be managed by an external management system.

3.2.5 Battery Technology

Energy storage of mobility sector, including cars and aircraft, are constrained by two factors: weight and size. For aerospace applications, weight constraint plays an important role. It means that the energy should be stored in the lightest and smallest volume as possible.

The two most important factors for using a suitable battery in an electric aerial vehicle are the specific energy of batteries and their charging rate.

The specific energy of a battery, which determines the vehicle's range, is the amount of energy provided by the battery per unit weight [80]. Today's batteries' specific energy is inadequate for a long-range trip, but by introducing new batteries chemistry, this problem can be addressed. All-electric commercial aircraft will need a battery specific energy of at least 1,800 Wh/kg [88], which is unreachable with the current battery technology. Current Lithium-ion battery cells have the specific power of 150 to 250 Wh/kg and Lithium-sulfur cells achieve to 350 Wh/kg while the theoretical specific energies for lithium-sulfur cells is 2,680 Wh/kg. Progress in the cathode and anode materials have a great potential to increase the lithium-ion battery specific power.

Current airplanes utilize liquid hydrocarbon fuel to produce energy. An advantage of this type of energy source is that the weight of fuel decreases during the flight as it burns, and because of that, the trip range can be extended as the vehicle becomes lighter (the vehicle weight can decrease to 75% of its initial weight) and therefore, less power is needed for the remaining trip [88]. This will not happen by using a battery as energy storage because the battery's weight remains constant during the whole flight. Consequently, a battery-powered aircraft with the same initial weight as a conventional one will use 12-13 percent more energy at the propeller to have the same range trip [88]. However, it does not mean that the electric aircraft should storage more energy to have the same range capability because the efficiency of the electric propulsion system is much more than the conventional one. The revised equations for electric vehicle range and endurance are given in [71].

Due to all limitations mentioned here, it is crucial to design a vehicle which can take off and land by consuming as minimum energy as possible and fixed-wing airplanes that use the wing's advantages require less power for lifting compared to rotorcraft [72]. According to a white paper published by Uber, a 4-passenger VTOL aircraft with the gross weight of 1,800 kg needs 500 kW for a short time takeoff (about 1 minute) and 71 kW for cruising with the speed of 240 km/h which is a significant difference between takeoff power and cruising power [80].

The second important factor, which determines the vehicle total operational time, is the battery's charging rate. Current batteries charge at slow rates, and cannot support high-frequency operations. Having this in mind, it is necessary to use a vehicle that consume less energy per mission. In this case, the vehicle can complete more flights before recharging. The ESTOL airplanes consume less energy to complete the whole mission compared to VTOL ones [80]; hence, using them for this application are more reasonable.

3.2.6 Weight

The last reason for using ESTOL airplane is about the weight of aircraft. A lighter aircraft can achieve a longer range and higher payload capacity, which means a higher passenger number per vehicle. It is already mentioned that STOL aircraft need less energy for their flight modes, including takeoff and landing compared to VTOLs. Consequently, their power system can be lighter. Additionally, there is no need for an extra system to tilt the wing or the props, which adds extra weight to the aircraft [72], and adding extra weight to the aircraft means more power for the whole trip would be required.

Chapter 4

Aerodynamic Forces

To analyze an airplane's performance, it is required to simplify the methods for determining the forces acting on the airplane. This chapter provides simplified equations to obtain two main forces acting on a moving airplane, which are lift and drag. The lift is perpendicular to the flight's direction, and the drag is parallel to it. These forces depend on the flying altitude or in other words on the air density. The first section presents a method to calculate the air density in each flying height, and then the procedure to calculate lift and drag for the airplane are given.

4.1 The International Standard Atmosphere

The aircraft's performance depends on the properties of the atmosphere which the aircraft is operating in. The most important characteristic is the air density. The atmosphere is consisting of approximately %78 nitrogen, %21 oxygen, and %1 other gases. In most aerospace applications, the atmosphere can be assumed as homogeneous gas of uniform composition [94]. For a perfect gas, the relation between the pressure, the air density, and the temperature can be written from ideal gas law which is presented at Eq 4.1. The R in this equation is universal gas constant and it is equal to 287 J/kg.K.

$$P = \rho RT \tag{4.1}$$

The pressure and the temperature of the atmosphere depend on on many factors such as altitude, location, time of the day, and season. Taking all these factors into account is almost impossible; therefore, an "International Standard Atmosphere model" is defined [65]. This model can present atmosphere properties to a reasonable degree. Based on experimental observations, the temperature change with respect to altitude is given at the Fig 4.1. It can be seen that it consists of two different regions: the first region, which is constant temperature and it's called isothermal region and the second region, which is the gradient region.

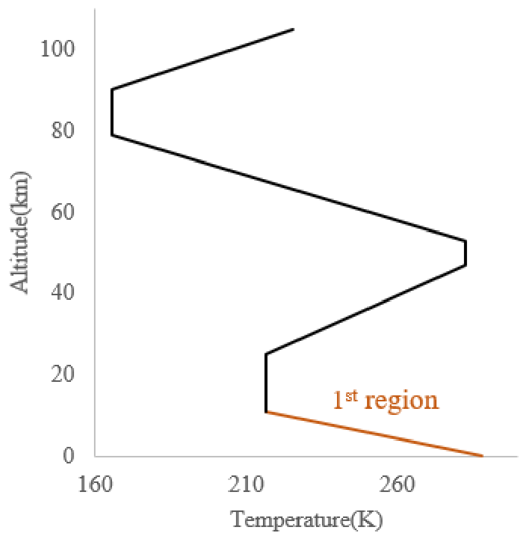

FIGURE 4.1: Temperature distribution in the standard atmosphere

Operating area of general aviation and urban aviation application is only in the first region or in the other word troposphere region. Eq 4.2 presents the relation between temperature variation to the altitude changes in this region. Then the relation between T , P, and T, ρ are given by Eq 4.3, and Eq 4.4 respectively.

$$T_2 = T_1 + a_1(h_2 - h_1) \tag{4.2}$$

$$\frac{P_2}{P_1} = \frac{T_2}{T_1}^{(-g_0/(a_1R))} \tag{4.3}$$

$$\frac{\rho_2}{\rho_1} = \frac{T_2}{T_1}^{-(g_0/(a_1R)+1)} \tag{4.4}$$

Where a_1 is the $\frac{dT}{dh}$ in the first region, g_0 is the gravity of the earth and it's equal to $9.8m/s^2$, and $R = 287J/kgK$. Air pressure, density ,and temperature at sea level are given as: $P_s = 1.013 \times 10^5\ N/m^2$, $\rho_s = 1.225kg/m^3$, and $T_s = 288.16K$. Fig 4.2 shows the air temperature, density ,and pressure variation in the first region calculated based on Eq 4.2 to Eq 4.4.

4.2 Aerodynamic Forces on Airfoil

An airfoil is a streamlined body which can produce more lift than drag when it is placed in a suitable angle of attack. The forces acting on an airfoil in a moving stream of air depend on seven variables: 1. Air velocity 2. Air density 3. Airfoil area 4. Viscosity coefficient 5. Speed of local sound 6. Compressibility of the airflow, and 7. The angle of attack. In the following sections, all of the above factors will be discussed separately.

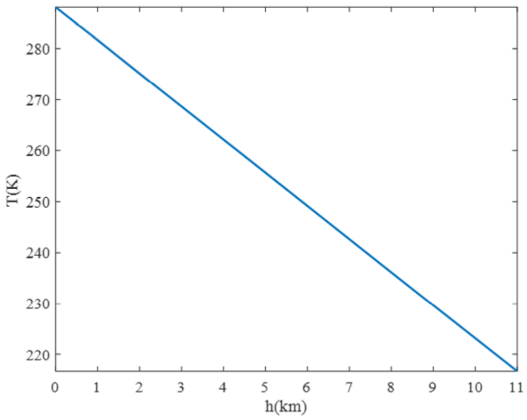

(A) Air Temperature

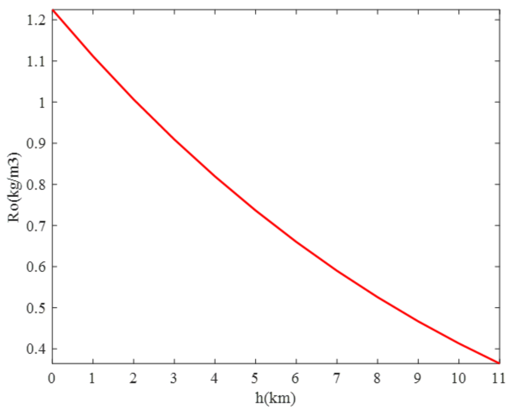

(B) Air Density

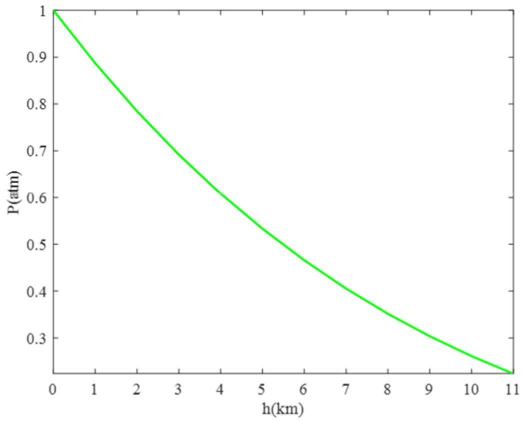

(C) Air Pressure

FIGURE 4.2: Atmosphere properties variations from 0 to 11 km from the sea level

4.2.1 Angle of Attack

In the previous section, a complete approach for calculating the local air density is presented. One of the most important factors for calculating airfoil's lift and drag forces is airfoil's angle of attack. In the following figure, the V is the velocity of the center of gravity of the airplane. The angle of climb,θ_c, is defined as the angle between the airplane's flight direction and the horizontal line. The angle between the horizontal line and the airplane's thrust is called θ. The angle of attack is measured with respect to the thrust line, and it is the angle between the velocity and the thrust line, that is to say $\alpha = \theta - \theta_c$. These angles are illustrated in the Fig 4.3.

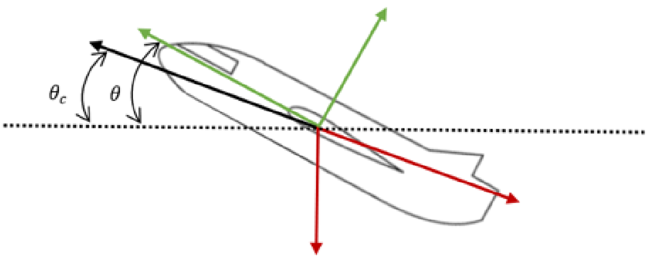

FIGURE 4.3: Airplane's angle of attack

4.2.2 Lift Coefficient for an Airfoil

As a starting point, the lift coefficient is estimated by a two-dimensional wing or in essence by an airfoil. A typical airfoil lift coefficient versus angle of attack curve is given at the Fig 4.4. The value of α when the lift is zero is defined as the "zero-lift angle of attack $\alpha_{L=0}$. C_l reaches a maximum value and then drops as the α increases. In this circumstance, the airfoil is stalled, the lift rapidly decreases, and the drag increases. This phenomenon is caused by airflow separation on the top of the airfoil [93].

The relationship between the lift coef. and the angle of attack before onset of stalling can be written as Eq 4.5.Which a_0 is the slope of $C_l - \alpha$ curve.

$$C_l = a_0 \times \alpha \tag{4.5}$$

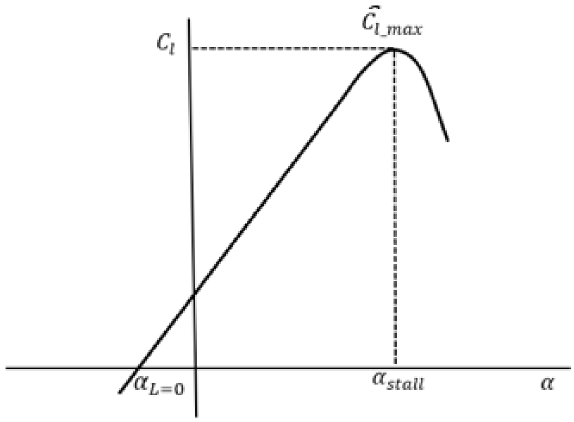

Figure 4.4: Airfoil lift coefficient versus angle of attack

4.3 Aerodynamic Forces on a Wing

Several wing configurations are demonstrated in Fig 4.5.

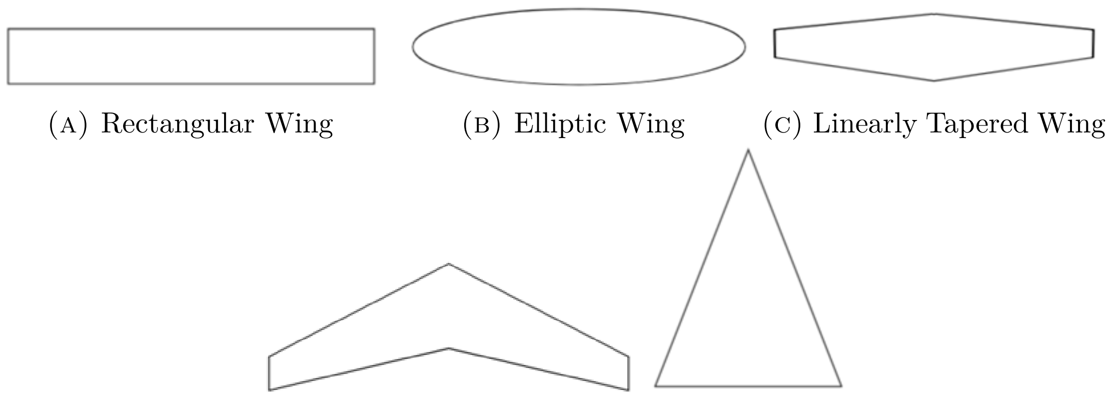

(a) Rectangular Wing (b) Elliptic Wing (c) Linearly Tapered Wing

(d) Swept Linearly Tapered (e) Delta Wing

Figure 4.5: Wing Configurations

One of the essential parameters in characterizing a wing is its aspect ratio. The aspect ratio of a wing is the ratio between the wing length and the chord for a rectangular wing where the wing chord is constant all over the wing. Rectangular wings are mostly used in low-cost airplanes due to the inexpensive manufacturing process. The b in the Eq 4.6 is the wingspan, and the $\bar{c}$ is the airfoil chord.

$$AR = \frac{b}{\bar{c}} \tag{4.6}$$

However, if the chord is not constant all over the wing, the aspect ratio can be written as follows:

$$AR = \frac{b^2}{S} \tag{4.7}$$

Where S is the wing's surface area. For the most modern airplanes, the "linearly tapered wings" is being used. The other types of wings such as "Swept linearly tapered" or "Delta wings" are suitable for high-speed airplanes and supersonic ones where the airplane should fly faster than the sound speed [85].

4.3.1 Lift coefficient for a wing

The flow field around a finite wing is a three-dimensional flow which is different from an infinite wing. This difference is mainly because of the wing-tip vortices. The air around the wing-tip tends to flow from high-pressure to the low-pressure surface. This phenomenon creates a circular motion around the wing, which is called *downwash*. It has two primary influences: first, it reduces the effective angle of attack, and second, it adds a drag which is defined as *induced drag*. Therefore, the lift and drag coefficients of a finite wing should be different from the infinite one.

When the aspect ratio is more than 4, the wing is considered as high aspect ratio wing. Two approximations should be considerate based on the Prandtl's lifting line theory — one for the compressible and the other one for the incompressible airflow. For incompressible airflow the $C_l - \alpha$ curve's slope changes to:

$$a = \frac{a_0}{1 + \frac{a_0}{\pi e AR}} \qquad : AR > 4 \tag{4.8}$$

$$a = \frac{a_0}{\sqrt{1 + \frac{a_0}{\pi e AR} + (\frac{a_0}{\pi e AR})^2}} \qquad : AR < 4 \tag{4.9}$$

e in these equations is the span factor efficiency which is always between zero and one. For elliptical planform, the e is equal to one, but for the other platforms, it is always less than one. For a typical subsonic aircraft, the e value is between 0.85 and 0.95 [65].

For compressible airflow, the following modifications should be made.

$$a = \frac{\frac{a_0}{\sqrt{1-M^2}}}{1 + \left(\frac{a_0}{\pi e AR \sqrt{1-M^2}}\right)} \qquad : AR > 4 \tag{4.10}$$

$$a = \frac{a_0}{\sqrt{1 - M^2 + \frac{a_0}{\pi e AR} + (\frac{a_0}{\pi e AR})^2}} \qquad : AR < 4 \tag{4.11}$$

M is Mach number which is the ratio between the velocity and the local sound speed. The c in the Eq 4.12 is the local speed of sound.

$$M = \frac{V}{c} \tag{4.12}$$

There are four possible definitions based on the Mach number's value. If the Mach number is less than one, then the aircraft is a "subsonic" aircraft. If it is equal to one, then it is called "sonic", and if it is higher than one, the plane is a "supersonic" plane [93]. The last definition is" hypersonic" aircraft, which is when the Mach number is more than five [93]. The relation between the air density variations and the Mach number can be presented as Eq 4.13 [65].

$$\frac{\rho_0}{\rho} = (1 + \frac{\gamma - 1}{2} M^2)^{\frac{1}{\gamma - 1}} \tag{4.13}$$

If the Mach number is less than 0.3, then the airflow can be considered as an incompressible flow. This is mainly because the change in the air density is less than 5% in this condition [65]. The Fig 4.6 shows the changes of the air density to Mach number by using Eq 4.13. In this equation, γ is equal to 1.4 [65].

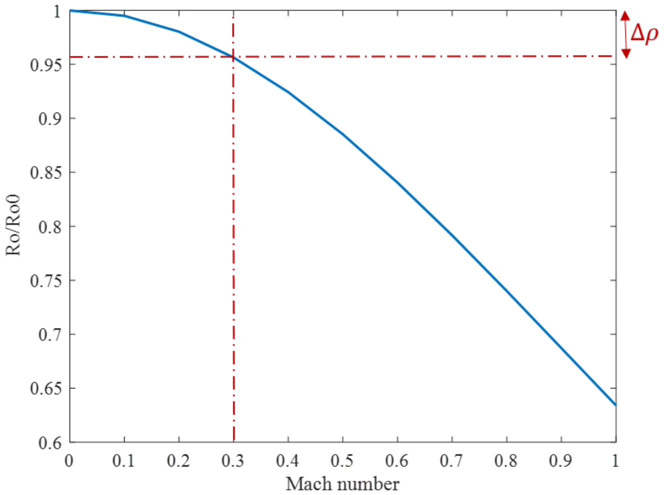

FIGURE 4.6: Air density change vs Mach number

In this thesis, the maximum speed of the aircraft is limited to 270 km/h. Accordingly, the Mach number is always less than 0.3, so the airflow is being considered as an incompressible flow at all times.

4.3.2 Drag coefficient

A *clean airplane* is an airplane in the cruising mode which means all the gears are up and no flap and high lift systems are being used [94]. Whenever flaps or landing gears are expanded, the drag rapidly increases. The total drag coefficient for the wing is coming from two sources: the profile drag and the drag due to the lift or the Induced drag. Hence, the total drag can be written as Eq 4.14 [65].

$$C_{DW} = C_{DW0} + C_{DWi} \tag{4.14}$$

where:

$$C_{DWi} = \frac{{C_{LW}}^2}{\pi e AR} \tag{4.15}$$

Note that the profile drag is also including two parts: the skin friction drag, and the pressure drag due to the separation. C_{Dw0} can be obtained from experimental data.

Eq 4.14 can be expanded for the whole airplane such as it's shown in Eq 4.16 [65].

$$C_D = C_{De} + \frac{C_L^2}{\pi e AR} \tag{4.16}$$

Here C_D is the total airplane drag coefficient, and C_L is the total airplane lift coefficient (including the wing, tail, and fuselage). C_{De} is the parasite drag coefficient which includes the profile drag of the wing and the friction and pressure drag of the other components of the airplane such as tail surface, fuselage, landing gear. C_{De} is a function of lift coefficient [65]. Hence it can be written as Eq 4.17 which r is a constant.

$$C_{De} = C_{D0} + rC_L^2 \tag{4.17}$$

By substituting Eq 4.17 into Eq 4.16 and redefining e which is called Oswald efficiency factor, the new equation can be written in the form of Eq 4.18 [65]. Based on McCormick, for high wing airplanes, the e is around 0.8 as the upper boundary layer is not distributed by the fuselage. On the other hand, for a low wing airplane, the Oswald efficiency factor can be assumed around 0.6 [85]. For gliders, a value of 0.9 can be chosen due to their high aspect ratio and long wingspan [71].

$$C_D = C_{D0} + \frac{C_L^2}{\pi e AR} \tag{4.18}$$

4.3.3 Effect of High Lift Devices on the Lift and Drag Coefficients

Between all the conventional airfoils, The NACA 23012 airfoil achieves the maximum value of the lift coefficient, C_{Lmax}, and it is around 1.8 in high Reynolds number. The second highest one is NACA 2412, which has a lift coefficient of about 1.7. If we want to increase the lift coefficient during the takeoff, we should use some mechanical devices known as flaps and slats. These mechanical devices can temporarily change the airfoil configuration without any change in cruising mode. Deflecting the flaps usually shifts the lift curve upward without changing the slope as it is comparable to adding camber to the airfoil [85]. It should be noted that it decreases the stall angle, which is not helpful. A visual comparison between a wing without flap and a wing with flap is illustrated in Fig 4.7. Using flaps and slats may change the curve's slope and the lift at zero angle of attack.

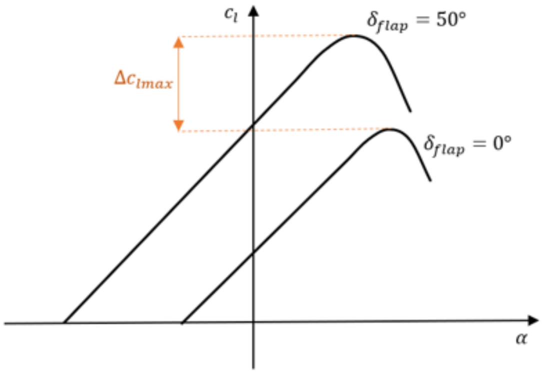

FIGURE 4.7: Comparison of lift coefficient of a wing with and without plain flap

Table 4.1 shows different possible high lift device configurations that can be employed and the associated lift coefficient increment. A complete table for slotted flaps is given by [85]. Each set has its advantages and disadvantages. Most small aircraft use plain flaps as it is easy to implement, and it does not add noticeable drag. The increment of lift coefficient by using split-flap is more than plain flap, although the drag associated with this flap is much higher than a plain one [94]. Slotted flaps can increase the lift coefficient more than the plain and split flaps, and the drag associated with this kind of flaps is less than the other two. However, the pitching moment associated with slotted flaps is too high [94]. A comparison between all the trailing edge devices is presented in the Fig 4.8. In this thesis, a plain flap is used as a high lift device to increase the lift coefficient at takeoff and landing.

TABLE 4.1: High Lift Devices

Name	Type	Image	C_L increment
Plain Flap	Trailing Edge	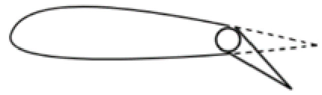	0.7-1.0 [91, 85, 99]
Split Flap	Trailing Edge	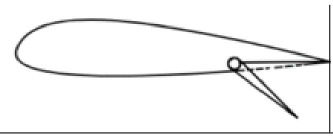	0.9-0.95 [91, 99]
Single Slotted Flap	Trailing Edge	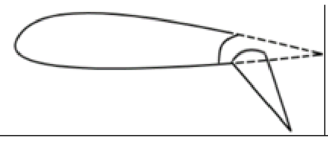	1.15-1.5 [91, 85, 99]
Double Slotted Flap	Trailing Edge	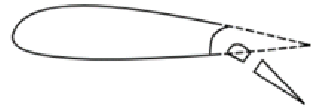	1.35-1.6 [91, 85]
Triple Slotted Flap	Trailing Edge	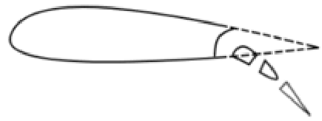	
Fowler Flap	Trailing Edge	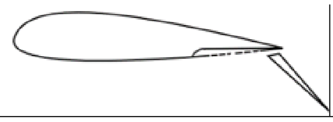	1.35 [99]
Leading Edge Flap	Leading Edge	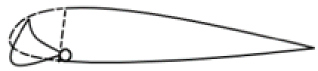	0.2-0.3 [91]
Leading Edge Slat	Leading Edge	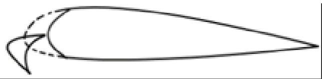	0.3-0.55 [91, 99]
Kruger Flap	Leading Edge	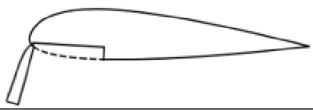	0.3-0.4 [91]

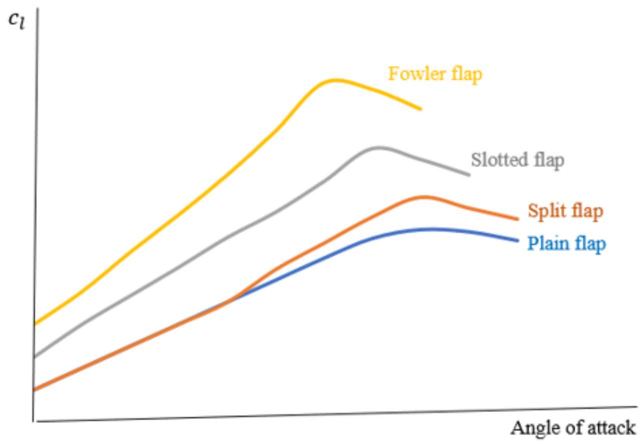

FIGURE 4.8: Comparison of lift coefficient of a wing with plain, split, slotted , and fowler flaps

By using a high lift device, the drag force acting on the airplane changes as well. Changes of the C_L and C_D by applying commonly used high lift trailing edge systems are given by Torenbeek [104]. Based on [104], the trend in performance by using plain flap is presented in Fig 4.9. The typical reflection plain angle for takeoff is 20°, and on landing, it is about 40° [104]. Therefore, in this thesis, the points shown in the red circles are employed. It's worth mentioning that for each thrust to weight ratio, an optimum deflection angle can be obtained, but for the sake of simplification a constant value is chosen.

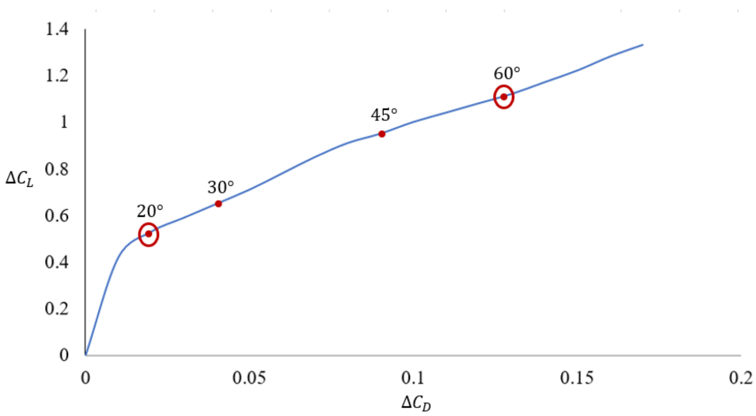

FIGURE 4.9: Lift and drag changes with respect to deflection angle for plain flap

A combination of trailing and leading-edge high lift systems can be used. Some of these combinations are given in Table 4.2.

TABLE 4.2: Combination of Leading and Trailing High Lift Devices

Name	Image	C_L increment
Plain Flap + Leading Edge Slat		1.1 [99]
Single Slotted Flap + Leading Edge Slat	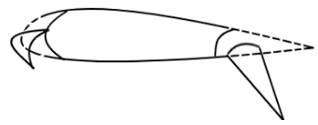	1.25 [99]
Double Slotted Flap + Leading Edge Slat	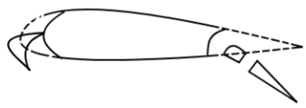	1.45[99]
Fowler Flap + Leading Edge Slat	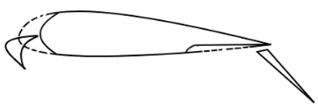	1.55 [99]

4.3.4 Effect of Spoilers On Lift and Drag Coefficients

Spoilers are devices that help the airplane to slow down faster. They are usually long, narrow, and plate-like surfaces which are mounted on the wings and can decrease the lift and increase the drag dramatically. STOL aircraft should have spoilers to kill the lift after touchdown [94]. The effect of spoilers on the airplane aerodynamic is mostly the opposite of the high lift devices meaning that spoilers cause flow separation, which leads to decrement in lift and increment in drag [96]. The disadvantage of using spoilers for an urban aerial vehicle in landing is the noise and vibration created due to the turbulent flow behind the spoiler which can be bothering for passengers [96]. An estimation method to calculate the changes of lift and drag coefficient by using spoiler is given by [96]. The drag coefficient of the spoiler with the area of S_{SP} and deflection of δ_{SP} is determined by the following equation [96].

$$C_{D_{SP}} = 1.9sin(\delta_{SP})\frac{S_{SP}}{S_{ref}} \tag{4.19}$$

Additionally, the contribution of spoiler with a span of b_{SP} to the airplane's lift coefficient can be approximately modeled as Eq 4.20 [96]. For more accurate results, a wind tunnel test or using a CFD model is suggested.

$$\triangle C_{L_{SP}} = -C_L\frac{b_{SP}}{b} \tag{4.20}$$

As starting point, a typical value of $\frac{b_{SP}}{b} = 0.3 - 0.7$, $\frac{S_{SP}}{S_{ref}} = 0.03 - 0.1$, and $\delta_{SP} = 30° - 90°$ can be considered [96].

4.4 Total Lift and Drag Coefficients for an Aircraft In Takeoff and Landing

The total lift coefficient is presented by the Eq 4.21, where $\triangle C_{L_{HLD}}$ and $\triangle C_{L_{SP}}$ are the changes in C_L by using high lift devices and spoiler respectively.

$$C_{L_{total}} = C_{L_{max}} + \triangle C_{L_{HLD}} + \triangle C_{L_{SP}} \tag{4.21}$$

The drag coefficient in the landing by considering landing gears, high lift devices and spoilers can be written as Eq 4.22. The only difference between landing and takeoff is the extra drag added by the spoiler in landing.

$$C_{D_{total}} = C_{DW0} + C_{D0_{LG}} + C_{D0_{HLD}} + kC_L^2 + \triangle C_{D_{SP}} \tag{4.22}$$

Where $C_{D0_{LG}}$ and $C_{D0_{HLD}}$ stand for landing gear drag and high lift devices drag coefficients. The $\triangle C_{D_{SP}}$ is the changes in the drag by using spoiler and for takeoff it is equal to zero. A reasonable estimations for $C_{D0_{LG}}$ and $C_{D0_{HLD}}$ are given by [96]. The $C_{D0_{LG}}$ varies from 0.006 to 0.0012 and $C_{D0_{HLD}}$ is in the range of 0.007 to 0.014 based on the airplane's configuration [96].

4.5 Thrust Reverser

The decelerating forces applied to an aircraft during landing are mainly from wheel brakes, aerodynamics brakes (such as spoiler) and thrust reversers [110]. Thrust reversers play a significantly important role, especially on a wet runway when the wheel brakes are not operating well. Conventional propeller thrust reverser works by changing the propeller's blade pitch angle. For conventional airplanes which are using combustion engines, it is recommended that thrust reversers only be used at higher speeds (higher than 60 knots) and that is mainly because of reignition concerns [110]. However, by using an electric motor as the power plant, the thrust reverser can be used even at very low speeds. Thrust reversers commonly are being used in big aircraft, and it is not common to be used in small piston airplanes because the energy of the aircraft after the touchdown is usually small enough which is manageable only by brakes (especially in the propeller aircraft where the aircraft's speed is usually not high). The conventional thrust reversers only are being used in a small fraction of the airplane's operating time, but they have a considerable impact on the airplane's weight, its noise production, and performance [110]. The Boeing Commercial Airplane Company has estimated that the total cost of using thrust reverser on B-767 is around $125,000 per year, which is way more than the savings associated with reduced brake wear [110]. In conclusion, thrust reversers are costly, and they add additional maintenance expenses while they are only being used in a small fraction of the entire airplane's operating time. Reversing the propeller rotation is another solution in a propeller-driven airplane. However, reversing the engine's rotation would be an extremely troublesome task. Although they are some engines that can rotate in both directions, they need to be stopped and then restarted to change their direction. This process is time-consuming, which cannot be used in the landing phase because it takes only a few seconds. By having an electric motor as the propulsion system, we can easily and instantaneously change the motor rotation. The only problem associated with the latter approach is that propeller is just like an airplane wing meaning that they are designed for one direction of travel. Therefore, changing the rotation direction of the propellers is not an efficient way of thrust reversing.

Chapter 5

Performance Modeling

The previous chapter discussed aerodynamic forces acting on a moving airplane and methods to find the lift and drag coefficients for the entire airplane, including the wing, spoiler, and high lift devices. This chapter focuses on the mechanics of flight and the aircraft motion equations in takeoff, cruise, and landing. For each airplane, it is necessary to address a number of specifications including the required runway length, cruising speed, flying altitude, and range. This chapter presents the essential information to evaluate an airplane's performance.

5.1 Equations of Motion

There are mainly four physical forces acting on a moving airplane as shown on the Fig 5.1. These forces are: the lift which is perpendicular to the flight direction, the drag which is parallel to the flight direction, the weight caused by gravity, and the last one is the thrust which is produced by the propulsion system.

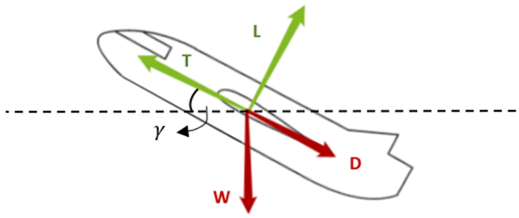

FIGURE 5.1: Forces acting on a moving airplane

The lift and drag forces can be calculated from the lift and drag coefficient as shown in Eq 5.1 and Eq 5.2 respectively.

$$L = \frac{1}{2}\rho V^2 S C_L \tag{5.1}$$

$$D = \frac{1}{2}\rho V^2 S C_D \tag{5.2}$$

The equations of motion of an airplane can be written as:

$$T - D - W \sin\gamma = m\frac{dv}{dt} \tag{5.3}$$

$$W \cos\gamma = L \tag{5.4}$$

5.2 Steady Level Flight Analysis

Level steady flight means that the airplane is flying at a fixed altitude with a constant speed. By applying these conditions to the flight scenario, the $\gamma =$

$0, \dot{V} = 0$. Therefore, the Eq 5.3 and Eq 5.4 becomes:

$$T = D = \frac{1}{2}\rho V^2 S C_D \tag{5.5}$$

$$W = L = \frac{1}{2}\rho V^2 S C_L \tag{5.6}$$

By having a specific cruising speed (V) and flying altitude (which dictates the respective air density- ρ), we can calculate the required thrust to maintain a given altitude and speed by the following steps:

1. Calculate required C_L from Eq 5.6
2. Calculate C_D from Eq 4.18
3. Calculate thrust from Eq 5.5

As an example, for a given airplane, the required thrust for remaining on a given altitude based on the airplane's velocity is calculated. Consider an aircraft flying at the sea level with the following given specifications.

TABLE 5.1: Exampled airplane specifications

Wing Chord(m)	Wing Span(m)	Wing Airfoil	MTOW(kg)
1.82	16.25	1412	8988

The required thrust based on different airplane speed is given in Fig 5.2. We can observe that maintaining at sea level by using the minimum thrust is possible if the airplane moves forward at a speed of 112.4 m/s.

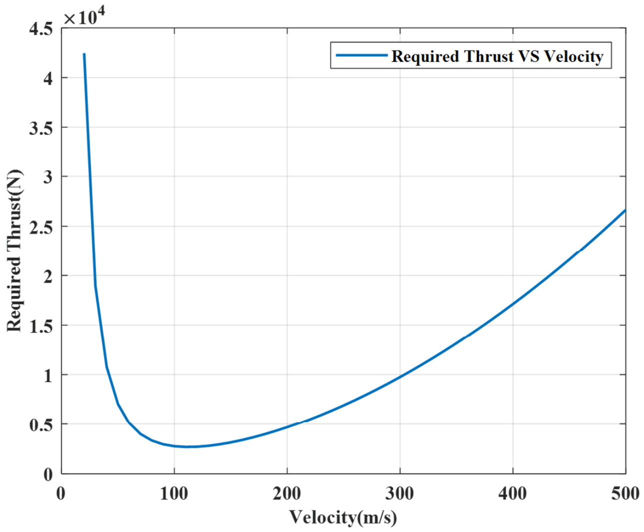

FIGURE 5.2: Required thrust based on airplane's velocity for remaining at sea level altitude

The best speed, the speed at which the airplane requires minimum thrust to remain at a given altitude, can be determined. To find the minimum required thrust, we rewrite the Eq 5.5 as following:

$$T_R = D = \frac{W}{L/D} = \frac{W}{C_L/C_D} \tag{5.7}$$

In this equation, the weight is constant. Therefore, to have the minimum thrust, the C_L/C_D should be maximum. To find the maximum point, we take a derivative from C_L/C_D and find the condition where the derivative is equal to zero.

$$\frac{C_L}{C_D} = \frac{C_L}{C_{D0} + K{C_L}^2} \tag{5.8}$$

$$\frac{d}{dC_L}(\frac{C_L}{C_D}) = \frac{d}{dC_L}(\frac{C_L}{C_{D0} + K{C_L}^2}) = \frac{C_{D0} - K{C_L}^2}{(C_{D0} + K{C_L}^2)^2} = 0$$
$$\Longrightarrow C_{D0} = K{C_L}^2 \Longrightarrow {C_L}^* = \sqrt{\frac{C_{D0}}{K}} \tag{5.9}$$

In which K is equal to $\frac{1}{\pi eAR}$. Based on the calculated C_L from Eq 5.9, the proper speed can be obtained from Eq 5.10.

$$W = 1/2\rho V^2 S C_L \Longrightarrow V_{(\frac{C_L}{C_D})_{max}} = \sqrt{\frac{2W}{\rho S {C_L}^*}} \tag{5.10}$$

The speed obtained from the Eq 5.10 is the speed that the airplane can maintain at a given altitude with the minimum required thrust. It should be mentioned that the proper speed for remaining on a specific altitude with the minimum thrust is different from proper speed by using the minimum power. By definition, power is thrust multiplied by the speed.

$$P_R = T_R V \tag{5.11}$$

Therefore, to find the proper speed that the airplane can remain at the given altitude by using the minimum power, we should take the derivative of required power with respect to the speed. The wing loading is the ratio between the aircraft weight and the wing area.

$$WingLoading = \frac{W}{S} \tag{5.12}$$

Based on this definition, the required power can be rewritten as the following equation.

$$P_R = 0.5\rho V^3 S C_{D0} + \frac{2KS(W/S)^2}{\rho V} \tag{5.13}$$

If we take derivative of the Eq 5.13 with respect to the velocity and solve the equation, we can obtain the condition for the minimum required power which is:

$$C_{D0} = 1/3 K {C_L}^2 \Longrightarrow (C_L)_{Min\,Power} = \sqrt{\frac{3C_{D0}}{K}} \Longrightarrow V_{Min\,Power} = \sqrt{\frac{2(W/S)}{\rho (C_L)_{Min\,Power}}} \tag{5.14}$$

For a given airplane, we can calculate the required power based on different cruising speeds and find the speed that gives the minimum required power to remain at the sea level. The required power-speed curve is shown in Fig 5.3. As it can be seen from the figure, the minimum power occurs at a velocity of 85.4 m/s. However, previously, it was observed that the minimum thrust happens at 112.4 m/s. It means that the speeds for minimum thrust and minimum power are not the same as expected.

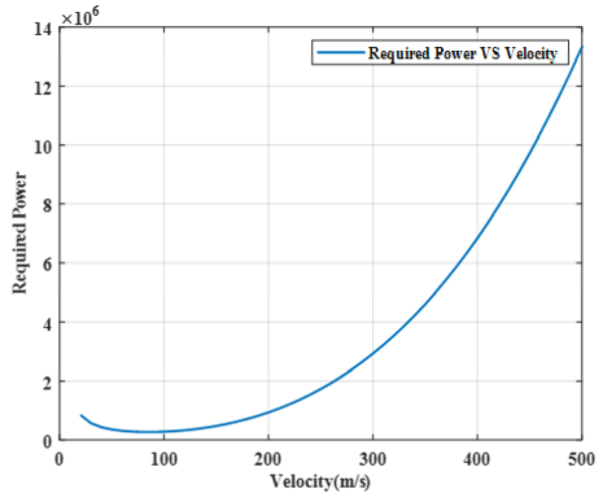

FIGURE 5.3: Required power based on airplane's velocity for remaining at sea level altitude

5.3 Takeoff Analysis

The total takeoff distance includes two stages. The first stage is to start from rest to a point where the nose of the aircraft starts lifting from the ground. The second stage is then climbing until 35 ft height clearance based on the FAA regulation. The Fig 5.4 shows the detailed portions of takeoff runway.The aim of this thesis is to analyze the electric motor specifications for the ground roll distance.

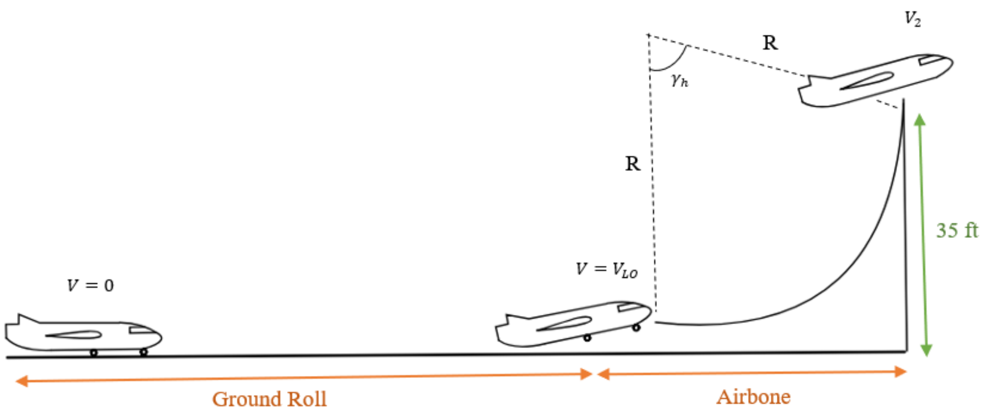

FIGURE 5.4: Takeoff distance

5.3.1 Takeoff Ground Roll Distance Analysis

At the beginning, the airplane starts from a velocity of zero. When it exceeds the "Lift-Off Velocity", the airplane is capable of flying. The lift-off velocity is described by Eq 5.15 .

$$V_{LO} = 1.1 V_{Stall_G} = 1.1 \sqrt{\frac{2W}{\rho S C_{LGmax}}} \tag{5.15}$$

Where the C_{LGmax} is the maximum lift coefficient at the ground. Estimating C_{LGmax} can be very challenging, and for better results, it should be measured from experimental tests. In the absence of such measurements, it can be considered as 0.7 to 0.85 of the C_{Lmax}. As mentioned in Section 4.3.3, C_{Lmax} can increases from 0.7 to 1.0 by using a plain flap on the wings, and it can increase to 5 for wings with complicated high lift systems. The maximum lift coefficient for a STOL aircraft is about 3 and that of a regular transport aircraft with high lift systems such as flaps and slats is about 2.4 [93]. The C_{Lmax} is usually obtained by wind tunnel tests; however, in practice, it may be up to 13% higher [104].

The force diagram for an airplane on the ground as shown in Fig 5.5 is the same as the cruising mode with one difference. An extra force is applied to the aircraft because of the friction between the tires and the ground.

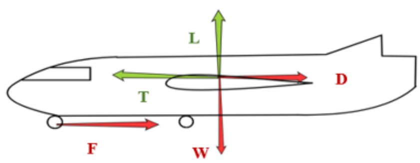

FIGURE 5.5: Forces acting on the airplane in takeoff-ground roll stage

Therefore, for the takeoff phase, we have the following dynamic equation where μ varies from 0.02 for a smooth paved surface such as concrete to 0.1 for long grass field [104]. The specified value of the rolling friction coefficient is given in Table 5.2.

$$T - D - F = T - D - \mu(W - L) = m\frac{dv}{dt} \tag{5.16}$$

TABLE 5.2: Rolling friction coefficient on different runways [104]

Type of Runway	Dry Asphalt	Dry Concrete	Short Grass	Long Grass
μ	0.04-0.05	0.02-0.04	0.05-0.07	0.07-0.1

Constant acceleration is assumed during the takeoff. Accordingly, the average speed of the airplane is equal to $V_{LO}/2$ and the aircraft travells the takeoff ground roll distance in t_{TO} seconds, which is presented in the Eq 5.17.

$$t_{TO} = \frac{S_{gTO}}{0.5V_{LO}} \tag{5.17}$$

By having the total takeoff time, the constant acceleration is equal to:

$$a_{TO} = \frac{V_{LO}}{T_{tO}} \tag{5.18}$$

Now airplane velocity can be calculated at each time from $V = time.a_{TO}$. By having the velocity at each time, the lift and drag can be determined from Eq 5.19 and Eq 5.20.

$$L = \frac{1}{2}\rho V^2 S C_{LGmax} \tag{5.19}$$

$$D = \frac{1}{2}\rho V^2 S C_{DG} \tag{5.20}$$

When an aircraft is flying close to the ground, the wingtip vortices decreased because of the interaction with the ground [65]. Hence, the induced drag is reduced when the airplane is flying near the ground. This phenomenon is called the *ground effect* [65]. The ϕ is the associated parameter that takes this effect into account.

Consequently, instead of using Eq 4.18, the following equation has been used to calculate C_{DG} [65].

$$C_{DG} = C_{D0} + \frac{\phi}{\pi e AR} {C_{LGmax}}^2 \tag{5.21}$$

A good approximation of ϕ is given by McCormick based on wingspan(b) and the height of the wing from the ground(h) [85].

$$\phi = \frac{(16h/b)^2}{1 + (16h/b)^2} \tag{5.22}$$

Now we can calculate required thrust and power at each velocity based on Eq 5.16 as shown in Eq 5.23 and Eq 5.24.

$$T = D + \mu(W - L) + ma_{TO} = D + \mu(W - L) + m\frac{V_{LO}}{t_{TO}} \tag{5.23}$$

$$P = (D + \mu(W - L) + m\frac{V_{LO}}{t_{TO}}).V = (D + \mu(W - L) + m\frac{V_{LO}}{t_{TO}}).(time.a_{LO}) \tag{5.24}$$

5.4 Landing analysis

The landing phase of an aircraft includes three stages: 1. The *approach*, in this phase the aircraft's speed is 1.3 V_{stall} at the altitude of 50ft and it decreases to 1.15 V_{stall} at the end of this stage [93]. 2. The *flare* and 3. The *ground roll*, which starts as the aircraft wheels touch down the ground until it fully stops. The detailed diagram of landing stages is illustrated in the Fig 5.6. In this thesis, only ground roll distance for landing is studied.

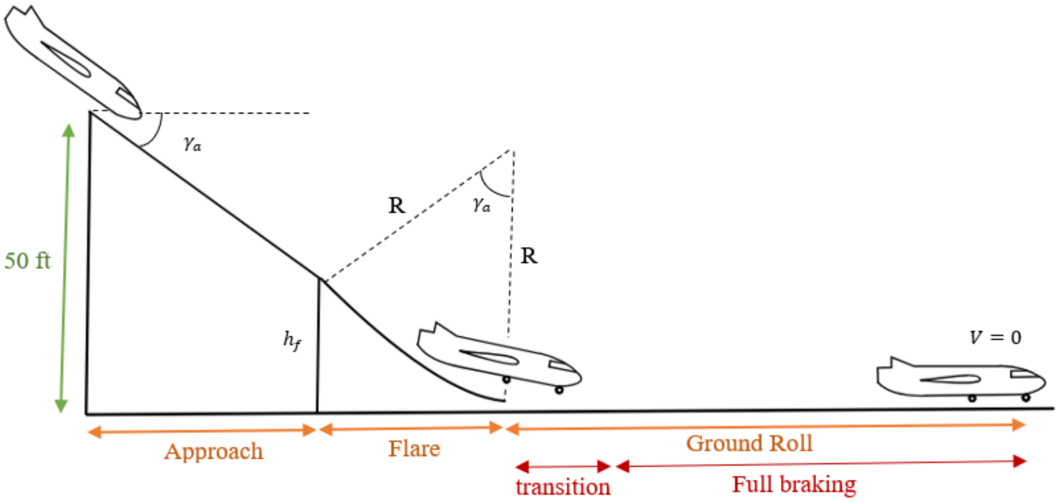

FIGURE 5.6: Landing distance

5.4.1 Landing Grand Roll Analysis

The ground roll distance includes two stages: the transition distance or free roll and the full braking distance. The transition distance is the traveled-distance from airplane touchdown until the point where all braking systems such as spoilers, thrust reverser, and wheel brakes are applied[93]. The minimum time that a pilot can act or activate all the braking devices should not be less than one second [93]. As this airplane is an ESTOL aircraft, the minimum time (1sec) is considered. The dynamic motion equations of the aircraft from the touch down to fully stop are as following:

$$-T - D - F_{Br} = ma \tag{5.25}$$

Where F_{Br} is the brake force. The rolling friction force which is equal to $\mu(W - L)$ now is replaced with brake force. The brake force comes from wheel brake by utilizing disk or drum brake [96], and it can be presented by $F_{Br} = k\mu_{Br}(W - L)$. By substitution F_{Br} into Eq 5.25, we have:

$$-T - D - k\mu_{Br}(W - L) = ma \tag{5.26}$$

k is a number between 0 and 1, which shows how much of the maximum brake power is using by the pilot [96].

In a conventional airplane without the thrust reverser, the thrust is equal to zero, which leads to the landing ground roll distances shown in Eq 5.27. Based on this equation, the ground roll is dictated by the aircraft configuration.

$$S_{gLand} = \frac{{V_{TD}}^2}{(2(D + \mu_{Br}(W - L)))_{@0.7V_{TD}}} \tag{5.27}$$

As there are not much data available of the propeller operation in the reverse direction, It was assumed that the airplane is equipped with a thrust reverse that functions by changing the propeller pitch. Reversible propeller produces a reverse thrust of about 40% of the forward thrust 15. The rolling resistance will be greatly increased by applying brakes. A typical value of 0.4-0.5 can be considered for μ_{Br} on a hard runway [65]. Additional drag term is added by using spoilers, and the parasite drag increases about 10% by using spoilers [65].

Similar to the assumption made during the takeoff, it was assumed that the deceleration during the landing is constant (Eq 5.29). The deceleration value should be in a reasonable range for passengers convenience. The a/g factor for different types of aircraft is given by Torenbeek [104] in Table 5.3.

TABLE 5.3: a/g value for different types of aircraft [104]

Aircraft Type	a/g
Light aircraft with simple brakes	0.3-0.35
Turboprop aircraft with propeller thrust reverser	0.35-0.4
Jet with ground spoiler and speed brakes	0.4-0.5
aircraft with nosewheel braking	0.5-0.6

The total time during full braking phase is presented in Eq 5.28. Constant velocity is assumed in the transition phase, which is equal to the touchdown velocity or $1.15V_{stall}$.

$$t_{Land} = \frac{S_{gLand} - V_{stall}}{V_{avrg}} = \frac{S_{gLand} - 1.15V_{stall}}{0.5 \times 1.15V_{stall}} \tag{5.28}$$

$$a_{Land} = \frac{0 - 1.15V_{stall}}{t_{Land}} \tag{5.29}$$

In Eq 5.28, $1.15V_{stall}$ is subtracted from the landing ground roll distance due to the transition phase. If the transition time is more than 1 sec, then V_{TD} should be multiplied by the transition time. The airplane velocity is required for calculating the lift and the drag, and it is given in Eq 5.30.

$$V = 1.15V_{stall} + a_{Land} \times (time - 1) \tag{5.30}$$

Now the required thrust that should be provided by the thrust reverser can be calculated from the Eq 5.26.

Chapter 6

Electric Aircraft Components Selection and Modeling

An airplane is modeled in Simulink Matlab for three phases of taking off, cruising, and landing. The model is flexible to changes of:

- Mission profile such as flying altitude, and desired cruise velocity.
- Wing specifications such as wing chord, wing span, wing height ,and airfoil type.
- Spoiler specifications such as spoiler chord, spoiler span,and spoiler deflection angle.
- Component weights and payloads such as battery weight, propulsion system weight, number of passengers, and empty frame weight.
- Number of electric motors and propellers
- The propeller diameter.
- Takeoff and landing distances.

In other words, the model can be used for any direct drive propeller fixed-wing airplane. However, analysis is conducted on a specified airplane. First of all, the airplanes components' features should be defined. The Selected components are more elaborated in the following sections. In the following, the total weight estimation and the total drag and lift coefficients are described. In the end, the airplane mission profile will be outlined.

6.1 Electric Aircraft Components

Components of an electric aircraft are divided into three main categories: propulsion system, energy storage and wing and airfoil. The main focus of this study is on the propulsion system.

6.1.1 Propulsion System

The required power for each mission is based on the aircraft design and the mission profile, but the available power is a characteristic of the using power plant. If we are using propeller attached to the electric motor, not all the power from the electric motor is available to drive the airplane. Some parts of it are dissipated by the propeller. Eq 6.1 reveals the available power to the aircraft.

$$P_A = \eta_{prop} \times P_{EM} = \eta_{prop} \times \eta_{EM} \times P_{in} \tag{6.1}$$

Electric Motor Model

The responsibility of the electric motor is to convert energy from the battery to the shaft. In this thesis, It is assumed that the electric motor can provide any range of power and torque in the total mass of 30 kg. It may result in enormously high power density, which is not practical with today's electric motor technology. However, this thesis aims to see the effect of runway length on the required power and torque.In conclusion, It is assumed that any power density is achievable. It should be mentioned that only one electric motor attached to a propeller without any gears is considered.

Propeller Model

The propeller is used to convert the electric motor shaft power to propulsive power for moving the aircraft. Working principle of airplane wing and propeller are comparable as both are made of airfoil sections to generate aerodynamic forces. The force produces by the wing is the lift that can make the aircraft airborne, and the force generated by the propeller is the thrust which moves the airplane horizontally. The only difference between a propeller and a wing is that the chord lines of wing airfoil sections are almost the same along the wing while for a propeller the chord lines are twisted [65]. The *Pitch Angle*, which is usually shown by β is the angle between the chord line and the propeller plane. Propellers can have two or more blades. Increasing the number of blades decreases noise production, but it increases the structural weight. On the other hand, lowering the blade numbers make the propeller noisier, and a longer propeller diameter is required [91]. An ordinary 3-blades propeller is utilized for the modeled aircraft.

The propeller efficiency depends on many factors such as aircraft speed, propeller revolutionary speed, and the propeller diameter. In summary, the propeller efficiency depends on the *Advance Ratio* of the propeller, which is characterized by the Eq 6.2 [93].

$$J = \frac{V}{nd} \tag{6.2}$$

Where the V is the free stream airspeed, d is the propeller diameter, and the n is the propeller speed in revolutions per second. The efficiency of the propeller at zero airspeed is zero. The propeller efficiency data,η_{prop}, can be driven from experimental data, or it can be approximately estimated by using the Eq 6.3 where C_T and C_P are propeller thrust and power coefficients, respectively. These coefficients are available from the experimental results [90].

$$\eta_{prop} = J(\frac{C_T}{C_P}) \tag{6.3}$$

Fig 6.1 depicts a typical propeller efficiency based on the advance ratio. For a particular value of propeller pitch angle (β), the propeller efficiency increases as J increases, and it reaches to a maximum value and then reduces. The maximum efficiency value of a common propeller is around 80 to 85%.

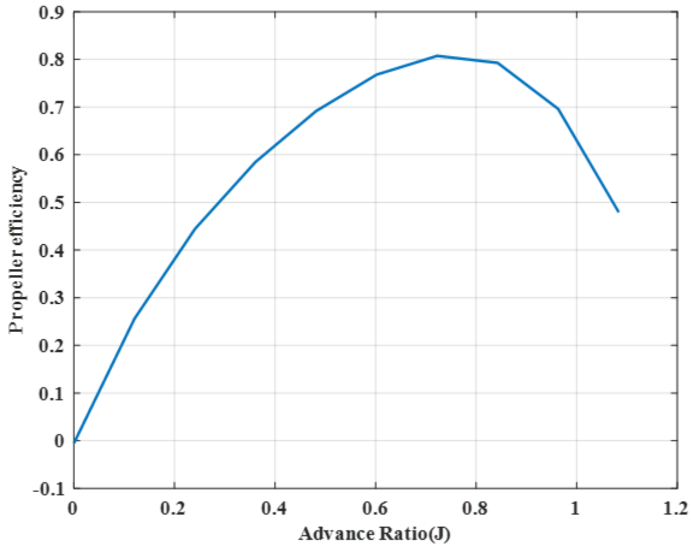

FIGURE 6.1: Typical propeller efficiency based on advance ratio

The propeller power and thrust are defined as Eq 6.4 and Eq 6.5 [90].

$$T_{prop} = C_T(n, V, D)\rho n^2 d^4 \tag{6.4}$$

$$P_{prop} = C_p(n, V, D)\rho n^3 d^5 \tag{6.5}$$

A propeller with a diameter of 1.65m is selected as the airplane's propeller. The propeller C_T and C_P are obtained from McCormick book [85].

6.1.2 Energy Storage: Battery

In conventional airplanes, the energy is stored in the form of liquid hydrocarbon fuel. The best choice in terms of energy density based on state-of-the-art battery technology for the mobility industry is Lithium ions battery because they are lightweight and have long life span [89]. Nevertheless, they have very low specific energy compared to conventional airplane fuel. The main challenge needs to overcome before electrification in the aviation industry is increasing battery specific energy. Up to now, Lithium-ion batteries have the energy density of 150-270 Wh/kg while Lithium-sulfur cells reach over 350 Wh/kg [88]. We expect an increment to 300 Wh/kg for Li-ion batteries in 2025 with the charge capability of 80% full charge in 15 to 30 minutes [1]. The goal for 2035 is to achieve a battery with the specific energy of 400-500 Wh/kg [1]. Fig 6.2 show the trajectory of battery technology development in the next 20 years based on prediction made in [2]. According to historical data, an improvement of %8 is expected for battery specific energy yearly[2].

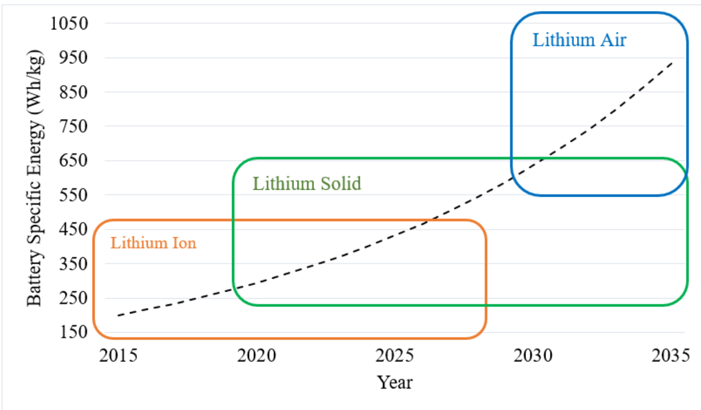

FIGURE 6.2: Battery technology improvement from 2015 to 2040 [2]

The theoretical specific energy for various battery cells are listed in Table 6.1. In practice, batteries specific energy are remarkably lower than values presented in the Table 6.1 because of additional weight added to the battery, including battery case, controller, separators, etc. [88].

Table 6.1: Theoretical batteries specific energy

Lithium-Sulfur	Alminium-Air	Lithium-Air
2,680 Wh/kg	8,140 Wh/kg	In charge state: 11,000 Wh/kg In discharge state: 3,500 Wh/kg

The battery total energy should be calculated for the whole mission. The mission is defined on different characters, including the minimum range (endurance), the takeoff and landing runway length, the climb and descent rate, and the wanted cruising speed. Once the total required energy for the whole mission is calculated, we can use the state-of-the-art's battery specific energy to calculate battery weight. However, for this thesis, Just like the electric motor, it is assumed any battery specific energy is accomplishable, and the only thing that matters is the battery weight. Again this assumption may lead to an unbelievable high energy density according to the airplane mission profile, but it is not a concern for this research. In conclusion, a battery weight of 150 kg is considered, and this assumption is gained from electric aircraft records provided in section 2.2.1.

6.1.3 Wing and Airfoil

Airfoil Selection

A typical airfoil from the off-the-shelf airfoils is chosen. NASA 1412 is the airfoil that is employed for the simulated airplane, and its lift coefficient with respect to the different angle of attack and its polar drag are depicted at Fig 6.3 (a) and (b) respectively. The data are extracted from the [58].

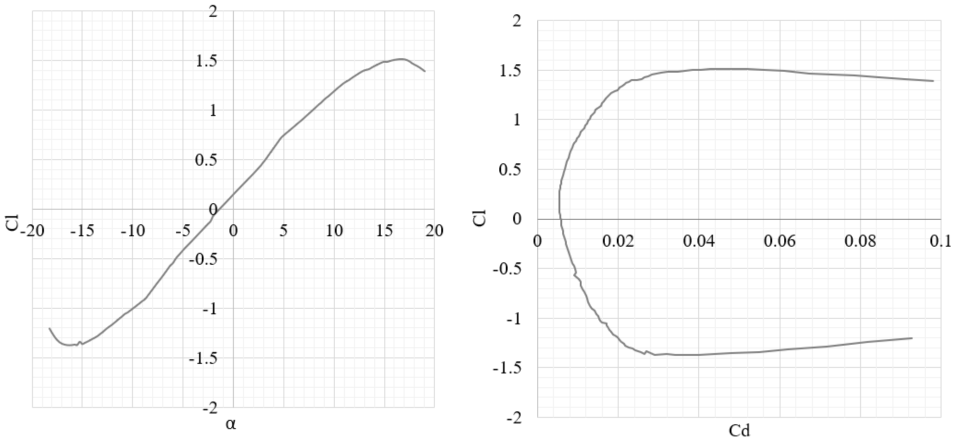

(A) Lift coefficient versus angle of attack

(B) Drag polar

Figure 6.3: Lift and Drag coefficients for NACA 1412 airfoil [58]

Wing Location Selection

Several wing shapes are briefly reviewed in section 4.3 but another factor which is playing an influential role in the wing lift production is the vertical wing location. There are three different arrangements which are depicted in Fig 6.4: Low wing, Mid wing, and high wing configuration.

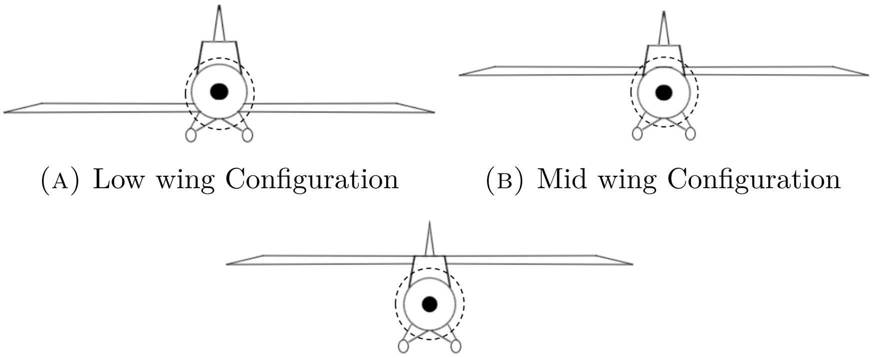

(A) Low wing Configuration (B) Mid wing Configuration

(C) High wing Configuration

FIGURE 6.4: Wing Location Configurations

If the wing is close to the ground, it may cause an undesirable ground effect. The ground effect usually leads to a reduction in vortex-induced drag, which may shorten the takeoff distance and increased the landing distance. The detailed model is given in section 5.3.1. However, sometimes it may cause early breakaway of the airflow and even makes the flow below the wing reverse and consequently increase the takeoff distance [104]. Generally speaking, low wing airplane produces less lift and suffers less from induced drag. That leads to a longer runway for both takeoff and landing. In the case of STOL or ESTOL aircraft, any tiny improvement is considerable. Hence, for these applications, usually a high wing configuration is advised. Also, propeller STOL airplanes usually need maximum allowable propeller diameter. If the low wing layout is taken for this case and the propellers are mounted on the wing, then a very tall and heavy landing gear should be utilized to provide propeller clearance over the ground [104]. Because of mentioned arguments, a high wing structure is applied for the thesis case study. Another reason for choosing a high wing layout is that it is easier for passengers to embark and disembark.

Wing Geometry

A simple rectangular wing with the wingspan of 10m and wing chord of 1.4m is selected. The aspect ratio of this wing is around 7. These values are picked according to STOL airplanes specifications given in [70].

High Lift Device Selection

The high lift system which is used for this airplane is a simple combination of a slot and a plain flap. Based on the deflection angle of the plain flap which mentioned in section 4.3.3, an increment of 0.5 and 1.0 is achieved for takeoff and landing respectively. Moreover, as mentioned previously in section 4.4, by applying high lift devices, the zero-drag coefficient varies as well. Table 6.2 presents the assumed values for the changes in the lift and drag coefficients by employing high lift devices in the modeled aircraft.

TABLE 6.2: Changes in the lift and drag coefficient due to the high lift devices

Flight Phase	$\triangle C_{L_{HLD}}$	$\triangle C_{D_{HLD}}$
Takeoff	0.5	0.007
Cruise	0	0
Land	1.0	0.009

Spoiler Selection

Spoilers are only using at the landing period; consequently, they only have effects on lift and drag coefficients on the landing phase. Because the modeled airplane is a lightweight aircraft, a small spoiler with a moderate deflection angle is appropriated. Table 6.3 shows the specifications of the related spoiler. Then $(\triangle C_{D_{SP}})_{@Land}$ and $(\triangle C_{L_{SP}})_{@Land}$ are calculated based on Eq 4.19 and Eq 4.20. It should be mentioned that this spoiler is not the best feasible spoiler for this airplane, and further researches and analysis are needed to find the best spoiler configuration which is beyond the scope of this study.

TABLE 6.3: Changes in the lift and drag coefficient due to the spoiler usage

b_{SP}	S_{SP}	$\frac{b_{SP}}{b}$	$\frac{S_{SP}}{S}$	δ_{SP}	$(\triangle C_{D_{SP}})_{@Land}$	$(\triangle C_{L_{SP}})_{@Land}$
4 m	0.1 m	0.071	0.028	70°	0.048	-0.198

6.2 Total Aircraft Weight

The airplane weight is consisted of several groups such as: airplane empty frame weight, propulsion system weight, battery weight, and payload weight. The propulsion system weight is including the electric motor, and the controller.

$$W_{Max} = W_{Empty} + W_{FullPayload} + W_{Propulsion} + W_{Battery} \tag{6.6}$$

In the section 6.1.1 and 6.1.2, it is mentioned that the battery weight is 150 kg and the electric motor weighs 30kg. The propulsion system, including the motor and the controller, can be considered to weight around 40-50kg. The payload includes passengers and their luggage. For each passenger, the average weight of 75 kg is assumed. Plus, for each the baggage, the average weight of 8 kg is considered. Consequently, the maximum payload is equal to 166kg. The only unknown value in Eq 6.6 is the aircraft empty frame's weight. Table 6.4 summarizes the data on existing electric aircraft's empty frame weight. It is apparent from the Table 6.4 that for a single-person aircraft the empty weight is less than 150kg and for a two-seat aircraft the empty weight is in the range of 150kg to 500kg.

The frame structure of modeled airplane is comparable to the Pipistrel Alpha Electro, but with spoilers and high lift devices implemented on it, Hence, it is slightly heavier. 280 kg is assumed as the empty frame weight. Using Eq 6.6, the maximum takeoff weight of aircraft comes to 646kg. The ratio between airplane MTOW and empty frame should be in a reasonable range.Table 6.4 highlights that the chosen empty frame weight and payload are in a reasonable range in comparison to other existing airplanes.

TABLE 6.4: Existing electric airplanes weight (empty frame, battery, electric motor, and payload)

Airplane Name	Seat	Empty Frame	Frame+Motor+Battery	Payload	MTOW	MTOW/Empty Frame
PC Aero-Electra 1	1	100		100	300	3
E-Cristaline Cri-Cri [89]	1	76	100	70	170	2.23
Electra Flyer ULS [25]	1		111		238	>2.14
Electraflyer-C	1		172		283	>1.64
MC30E Firefly	1	44	113[89]	70[89]	183[89]	4.15
Cassna 172 [89]	2		543	140	679	>1.25
Goshawk [59]	2		326		544	>1.66
Sun Flyer [60]	2		662	200	862	>1.3
Pipistrel Alpha Electro [64]	2	251	350	200	550	2.2
Taurus Electro G2	2	253	With 20Ah battery: 306 With 30Ah battery: 332 With 40Ah battery: 358	166.5 140.5 114.5	472.5	1.86
Pipistrel Watts Up[89]	2		314		550	>1.75
Magnus eFuession	2		410		600	>1.46
Sonex E-Flight [89]	2	418	530	70	600	1.43
YUNeec inc.e430[89]	2	160	250	220	470	2.93
Modeled Airplane	2	280	480	166	646	2.3

6.3 Total Lift and Zero Drag Coefficients

Now based on the Eq 4.21and 4.22, the total lift and drag coefficient for takeoff and landing phase are calculated. Table 6.5 and Table 6.6 present the effect of each device on the lift and drag coefficients and the final values which are used for the modeling in the next chapter. As stated in the Chapter 5, the required lift coefficient for the cruising phase should be determined according to the cruising mission requirement and no devices have effects on the lift and drag coefficients in the cruising period.

TABLE 6.5: The effect of each device on the lift coefficient for the modeled airplane

Flight Phase	Spoiler	Landing Gear	High Lift Device	Wing	Total
Takeoff	0	0	+0.5	+1.6	2.1
Landing	-0.198	0	+1	+1.6	2.4

TABLE 6.6: The effect of each device on the drag coefficient for the modeled airplane

Flight Phase	Spoiler	Landing Gear	High Lift Device	Wing	Total
Takeoff	0	0.006	0.007	0.036	$0.049{+}k{C_{LTO}}^2$
Landing	0.048	0.006	0.009	0.036	$0.058{+}k{C_{LTO}}^2$

In the primary analysis, these assumptions are valid compared to the maximum lift coefficient for STOL airplane, which is provided by [70].

6.4 Mission Profile

the Lowest Safe Altitude (LSALT) refers to an altitude that is at least 500 feet above the highest obstacle. According to the FAA, no person may operate an aircraft in congested areas bellow an altitude of 1,000 feet above the highest obstacle [63]. As an example of a city with a high number of skyscrapers, New York City has more than 6.486 high-rise buildings of at least 35 meters, and the tallest building is about 541m (1,776 feet). The average building's height is around 600 feet. Flying altitude is calculated by Eq 6.7 where h_t is the city height from the sea level and h_{HO} is the highest obstacle height.

$$h = 1000 + h_{HO} + h_t \tag{6.7}$$

In the case of New York City, the $h_t = 32.8$ feet and the $h_{HO} = 1,776$ feet. Consequently, the safe flying altitude is at least 2810 feet. For other cities, this value can be less or more. The tallest building in Toronto, which is our case study is the CN Tower with a height of 1,815 feet. Therefore, the safe flying ALT for the Toronto city is around 3100 feet. In conclusion, a flying altitude of 3500 feet (1066 m) is decided. Fig 6.5 displays the total mission profile. It should be noted that the duration of the mission depends on the total battery energy.

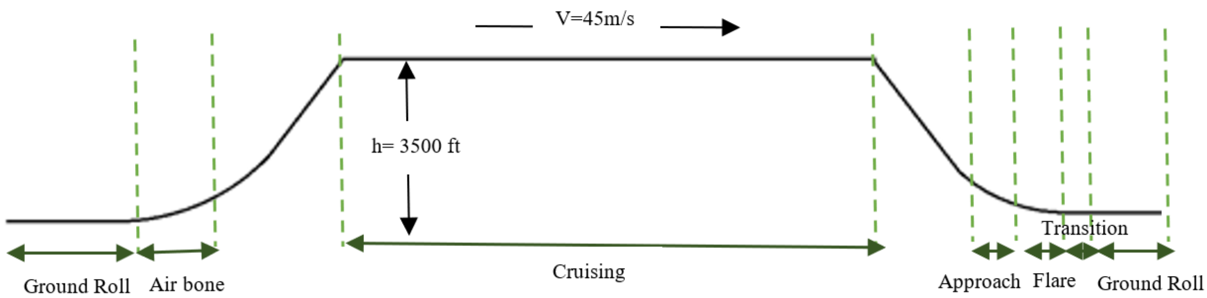

FIGURE 6.5: Airplane's Mission Profile

The main focus of this thesis is analyzing of the required power and torque on three flight stages: The ground rolls on take-off and landing, and cruising stage.

A moderate cruising speed of 45m/s or 162 km/h is chosen as base speed. The effect of cruise speed on the required power is analyzed in the following chapter.

Chapter 7

Airplane Modelling in Matlab Simulink and Results

7.1 Airplane Modelling and Validation

Two models are built in Matlab Simulink. The first model is for finding the thrust and power requirements. Then the airplane's requirements are fed to a numerical calculation model and subsequently results from the numerical model are used in the second Simulink model for validation. As mentioned in chapter 6, the first model is flexible to several changes, hence any simple propeller fixed-wing airplane can be studied.

7.1.1 Airplane Model for Finding Thrust and Power Requirements

The first model, which is shown in the Fig 7.1 is built to determine the necessary thrust and power for each phase of the flight, including takeoff, cruise, and landing. The power, torque ,and speed requirements are computed according to the airplane specification. As illustrated in Fig 7.1, the model has seven main portions. The detail function of each block is as follows:

1. **Airplane's Properties:** The properties of the desired airplane are set into this block, including: Number of passengers, air-frame weight, propulsion system weight, battery weight, wing chord, wingspan, wing height,spoiler chord, spoiler span, deflection angle of the spoiler, cruise velocity, number of motors and propellers, propeller diameter, and takeoff and landing distances. This section allows the model to be applicable to any small fixed-wing aircraft.

   The takeoff and landing distances vary because this thesis aims to observe the effect of takeoff and landing distances on the electric motor power and torque. However, in the following sections, to understand the results from the numerical model, a 50m runway is chosen as the takeoff and landing distance.

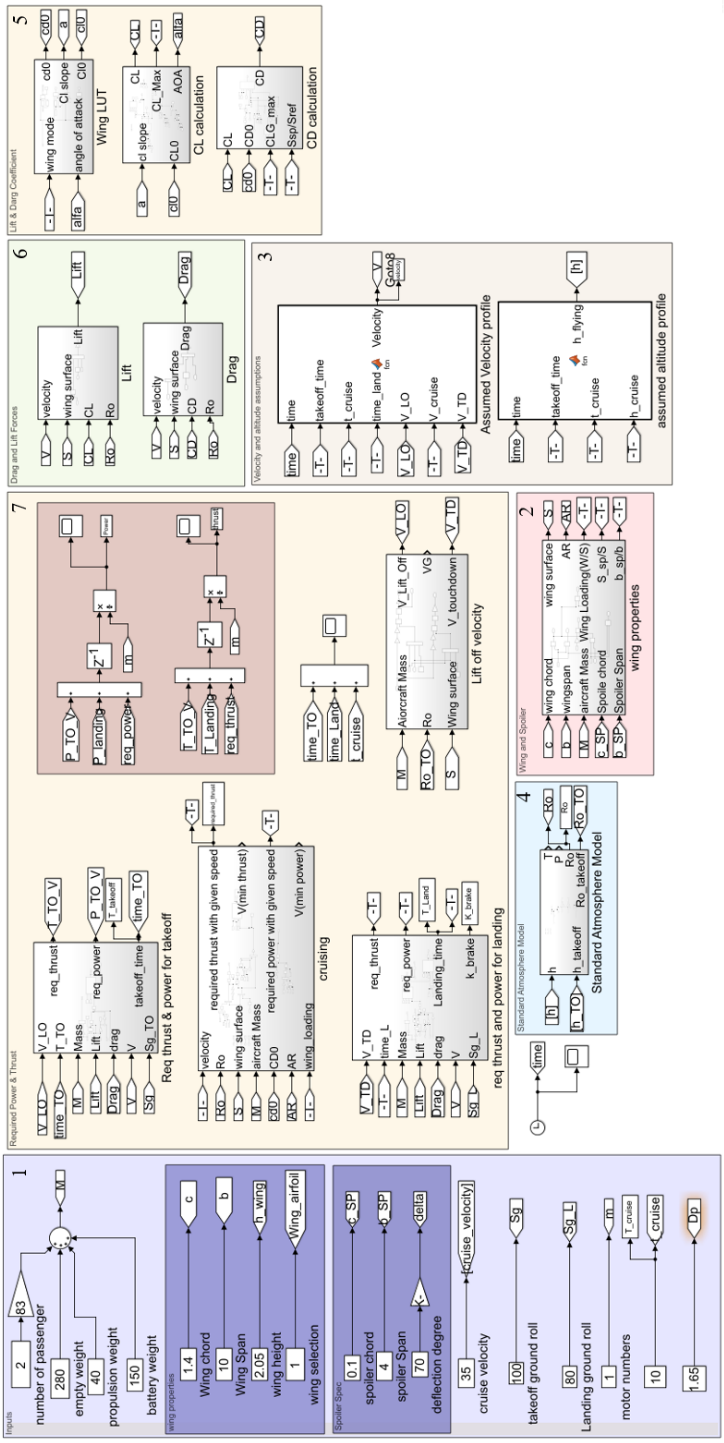

FIGURE 7.1: Airplane Simulink model (first model) for finding thrust and power requirements

TABLE 7.1: Chosen Airplane Specifications

Number of Seats	2	Wing Chord	1.4 m
Air-frame Weight	280 kg	Wingspan	10 m
Propulsion Weight	40 kg	Wing Height	2.05 m
Battery Weight	150 kg	Spoiler Chord	0.1 m
Number of Motors	1	Spoiler Span	4 m
Propeller Diameter	1.65 m	Spoiler Deflection Angle	70°
Flying Altitude	3500 ft	Takeoff Distance	Variable
Cruise Velocity	45 m/s	Landing Distance	Variable

2. **Wing and Spoiler:** In this block the wing and spoiler surface areas and the relation between their chords are calculated. The wing surface is 14 m^2, and the wing aspect ratio is 7.14.

3. **Assumptions:** The velocity and flying altitude in different phases of the flight varies. The velocity is assumed to change linearly in both takeoff and landing and to be constant in the cruising period. The role of this block is to compute the vehicle velocity and altitude at each specific time. Fig 7.2 displays the assumed velocity profile for the takeoff and landing in 50 m runway.

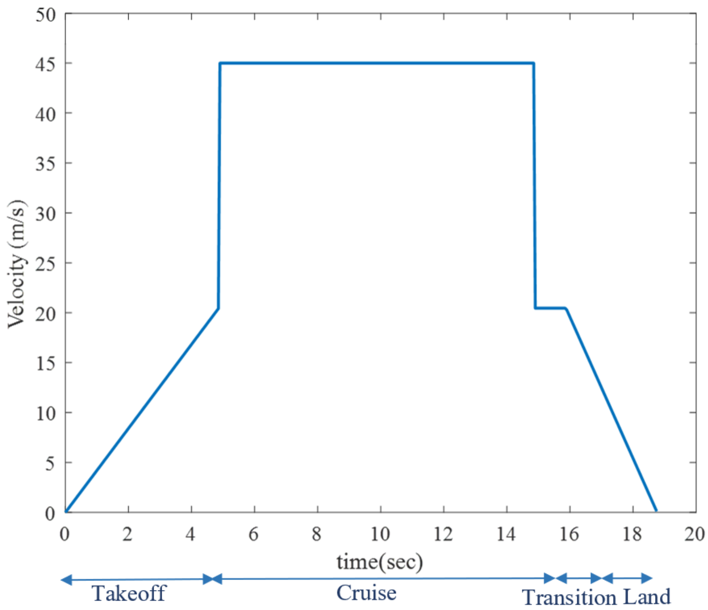

FIGURE 7.2: Airplane's assumed velocity profile for 50m takeoff and landing distances

4. **Standard Atmosphere Model:** By changing the altitude, the air density is changing meaning that the air density at takeoff and landing is different from the air density during the cruising. However, the variation is not drastic as the airplane is flying at low altitude. Based on the altitude assumption from the third block, the air density is estimated through section 4.1 and Eq 4.2 and Eq 4.4.

5. **Drag and Lift Coefficients:** Based on the chosen spoiler and airfoil, the total drag and lift coefficients at each flying phase are determined by using equations from the chapter 4 (Eq refTotalLiftCoeff and Eq 4.22) and look up tables for various airfoils. Table 6.5 and 6.6 show the final lift and drag coefficients in each flight section for the simulated aircraft.

6. **Lift and Drag Forces:** By having the wing area from block 2, aircraft velocity from block 3, lift and drag coefficients from block 5, and the air density from block 4, the lift and drag forces can be calculated using Eq 5.1 and Eq 5.2.

7. **Thrust and Power Calculations:** The required thrust and consequently required power for each phase of flight based on airplanes specifications are computed by applying relations and equations reviewed in chapter 5 (Eq 5.5 and Eq 5.6 for steady level flight, Eq 5.23 for takeoff and Eq 5.26, Eq 5.28 and Eq 5.29 for landing). Other essential parameters for calculation are taken from previous blocks such as airplane velocity, lift and drag forces, etc. As an example, the required thrust for taking off and landing by 50m and cruising for 10 sec with the speed of 45 m/s is provided in Fig 7.3. The required power can be effortlessly calculated by multiplying the velocity to the thrust.

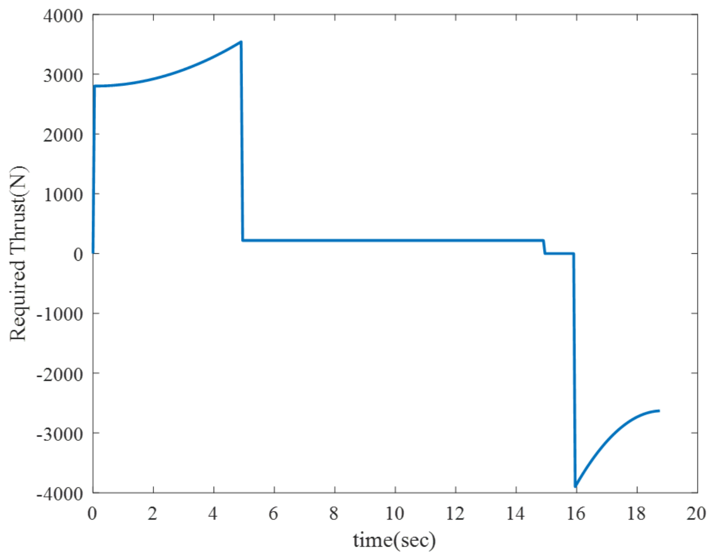

Figure 7.3: Required thrust for taking off and landing by 50m and cruising with the speed of 45m/s

7.1.2 Propeller and Electric Motor Operating Points

By using the previous model, the required power for the corresponding speed in flight segments are determined. The block diagram from the motor input power to the airplane output power is shown in Fig 7.4.

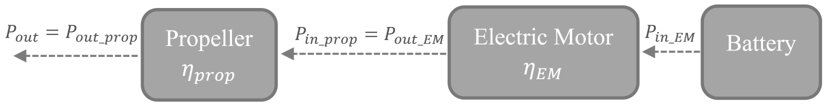

FIGURE 7.4: Block diagram of the input power to the output power

The calculated output power to the airplane should be divided by the propeller efficiency in order to find the output power of the electric motor. Next, to obtain the required input power to the electric motor power from the battery, the propeller input power ,which is equal to the output power of the electric motor, should be divided by the motor efficiency which is considered as a constant value in this study. However the propeller efficiency and power coefficient vary with the propeller rotational speed and the aircraft velocity. According to the Eq 6.2, With a constant propeller speed, as the aircraft velocity increases, the propeller advance ratio raises as well. Increasing the advance ratio means increasing the propeller power coefficient and efficiency. Consequently, higher power coefficient and propeller efficiency lead to a decrement in the propeller speed for delivering the same essential power (based on Eq 6.5). Hence, there is a tradeoff between the propeller rotational speed, the propeller efficiency, and the power coefficient.
The process which is used in this thesis to find the proper propeller speed is a numerical approach. In the following, the whole method is described for the takeoff phase. The same manner is applied for cruising and landing segments.

In takeoff, the airplane velocity is changing from zero to the lift-off velocity linearly. The velocity profile is discretized with a sampling time of 0.05 sec. For the velocity at each time step, the propeller speed is varied from zero to the maximum allowable speed (in this case from zero to 250 rps). Then the advance ratio, efficiency, and lift coefficient are found for each point. The resulting advance ratio is presented in Fig 7.5.

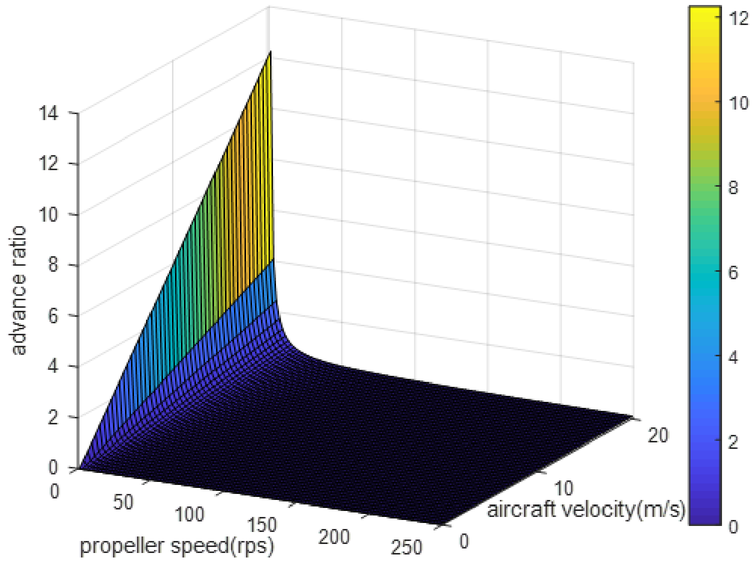

FIGURE 7.5: Propeller advance ratio based on airplane's velocity and propeller rotational speed

From Fig 7.5 it can be noted that the advance ratio for some points is too high, which is not acceptable for any type of propeller. Based on the chosen propeller in section 6.1.1, the maximum allowable advance ration is 1.1. Accordingly, any point that has the advance ratio above 1.1 gives zero power coefficient and efficiency. If a propeller with higher blade angles is being used, the operating range becomes wider. By removing points that are above the maximum allowable advance ratio, the advance ratio, and thrust coefficient changes to Fig 7.6 , and Fig 7.7.

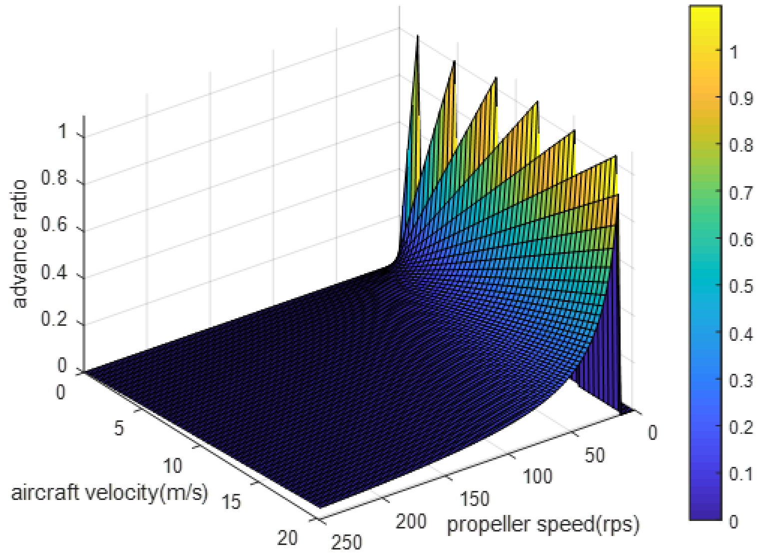

FIGURE 7.6: Adjusted propeller advance ratio based on airplane velocity and propeller rotational speed

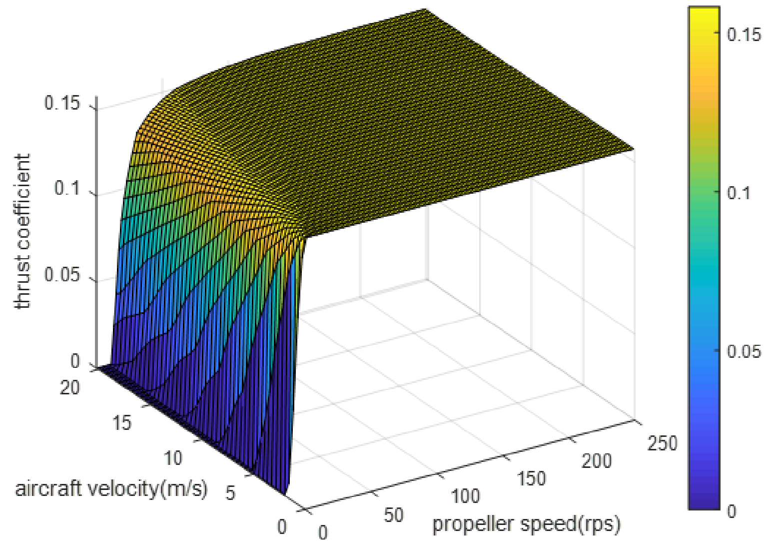

FIGURE 7.7: Adjusted propeller thrust coefficient based on airplane velocity and propeller rotational speed

On the next step, the propeller thrust is calculated from Eq 6.4. The thrust produced by the propeller is illustrated in Fig 7.8 based on propeller speed and airplane speed.

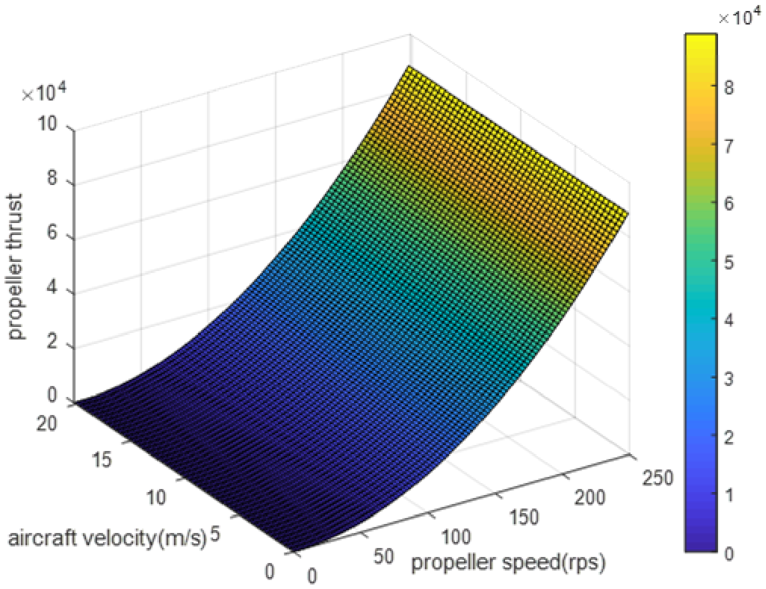

FIGURE 7.8: Propeller produced thrust based on airplane velocity and propeller rotational speed

The required thrust during takeoff from a 50m runway is calculated and shown in Fig 7.9. We can observe that the propeller is capable of delivering more thrust than demanded thrust in some areas.

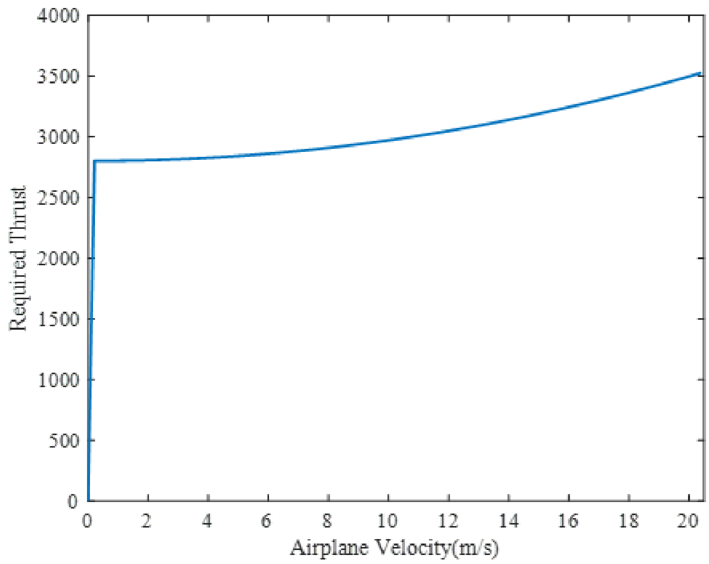

Figure 7.9: Required thrust during taking off of 50m runway

On the next step, the proper propeller speed, which is equal to the electric motor speed, is determined based on thrust requirement. The operating points which the propeller can produce slightly more thrust than the required amount are found. For those points that the propeller is not capable of providing adequate thrust, the maximum available thrust is chosen. Fig 7.10 illustrates the propeller command speed.

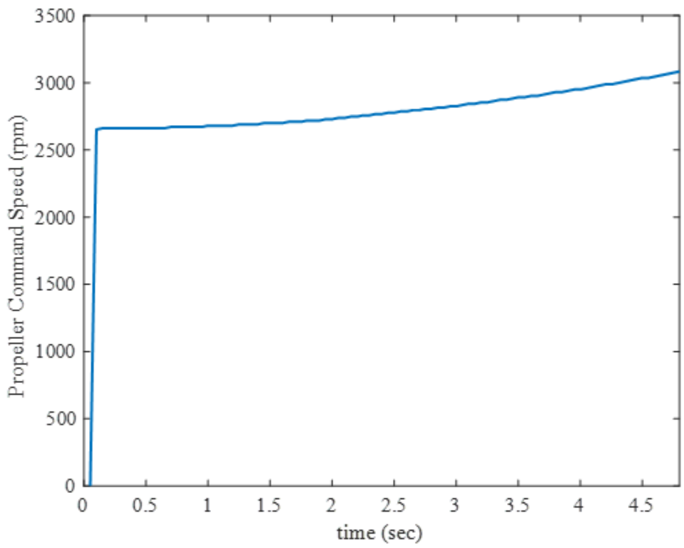

Figure 7.10: Propeller command speed during taking off of 50m runway

The output power by considering electric motor and propeller efficiency is presented in the Eq 6.1. As mentioned, the η_{prop} comes from the propeller block, and a constant 90% is assumed as the electric motor efficiency. Because the propulsion system is a direct drive without any gear, the electric motor's rotational speed is the same as the propeller. By having the electric motor power and speed, the electric motor torque can be computed.

The electric motor command speed, power-speed and torque-speed profiles for the whole mission are given in Fig 7.11 and Fig 7.12 respectively.

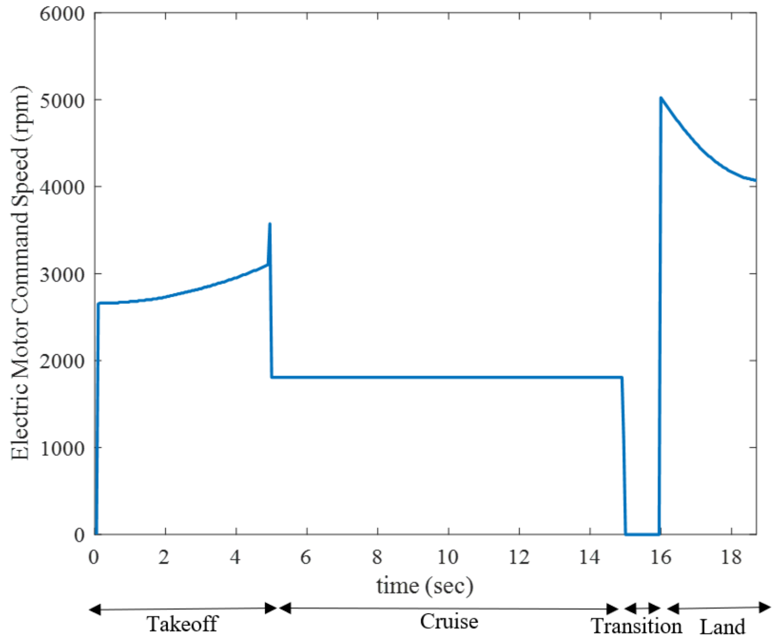

FIGURE 7.11: Electric motor command speed during the whole mission- 50m taking off and landing distance and 45m/s cruising speed

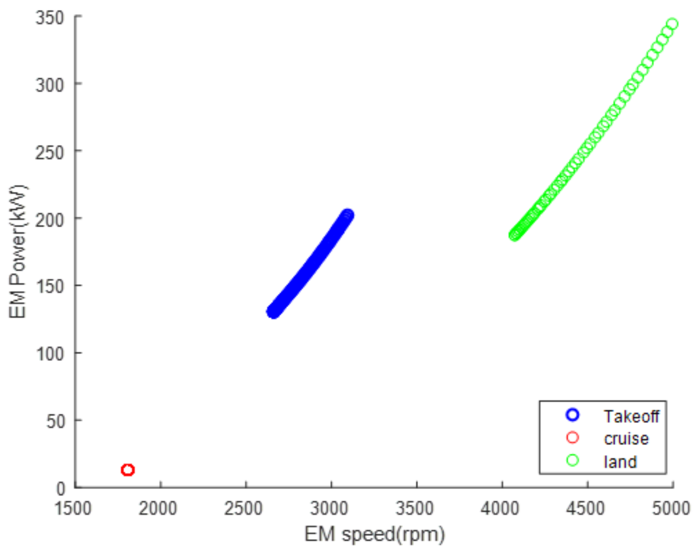

(A) Power-Speed

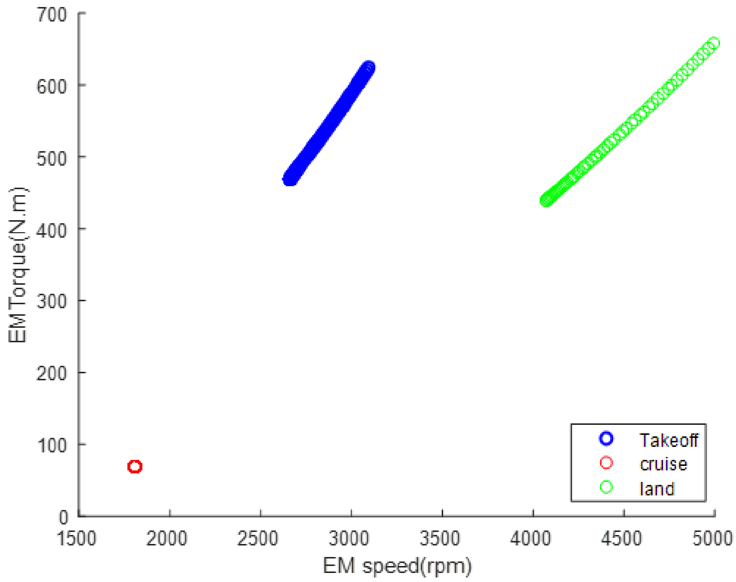

(B) Torque-Speed

FIGURE 7.12: Electric motor power-speed and torque-speed profile for takeoff and landing distance of 50m and cruising speed of 45m/s

7.1.3 Validation Model

A new airplane model is developed using MATLAB Simulink. The difference between the validation model and the first model is presented in Fig 7.13. This model has three extra blocks. The command propeller speed, which is calculated offline by the numerical model is the input to the validation model. Based on the input speed, the output thrust and power are obtained and fed to the other two blocks, which are *aircraft velocity calculator* and *aircraft altitude calculator*. These two blocks contain all the dynamic motion of the airplane. The airplane velocity is calculated in *body reference frame* and the airplane altitude is computed in *earth reference frame*. The x-axis in the body reference frame is along the airplane's flight direction, the Y-axis points to the right wing, and the Z-axis points down the airplane's plane. The x-axis in the earth reference frame is directed towards the North, the Y-axis is East, and the Z-axis is pointing down towards the center of earth [82]. It should be noted that for computing lift and drag, the calculated aircraft velocity is being used and not the assumed velocity. Moreover, the calculated aircraft velocity is an input to the propeller block, meaning the aircraft velocity is used for calculating propeller's advance ratio and consequently propeller efficiency. In the first model however, the assumed velocity has been used.

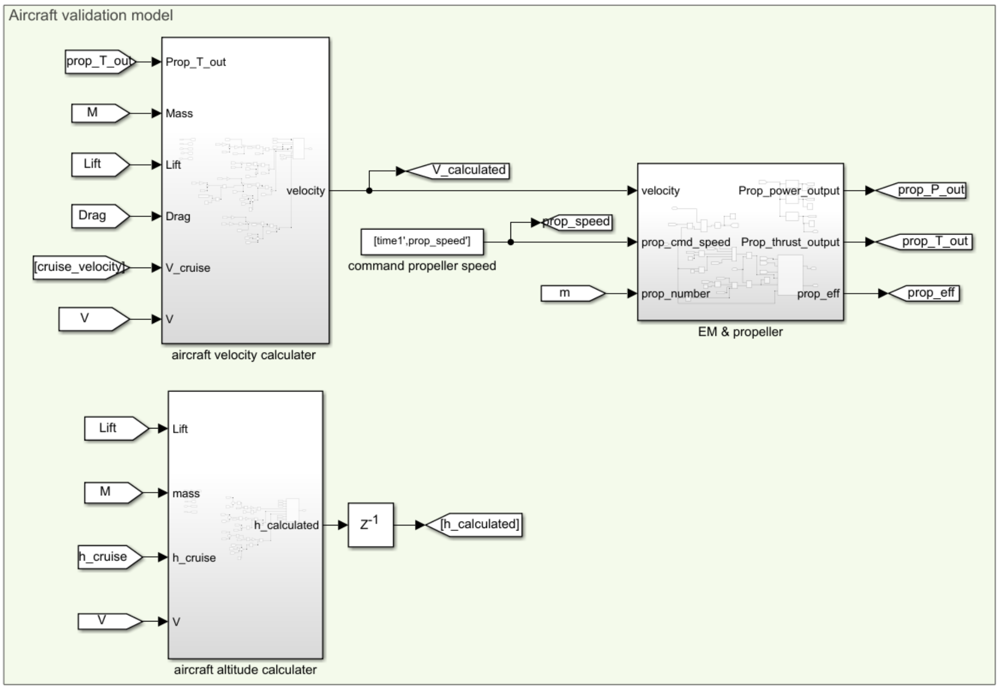

FIGURE 7.13: Extra blocks added to the aircraft model for validation

The comparison between the assumed velocity from the first model and the airplane's actual velocity is given in Fig 7.14. It can be observed that the airplane's velocity is following the assumed velocity trajectory. The same comparison between assumed altitude and airplanes altitude is presented at Fig 7.15.

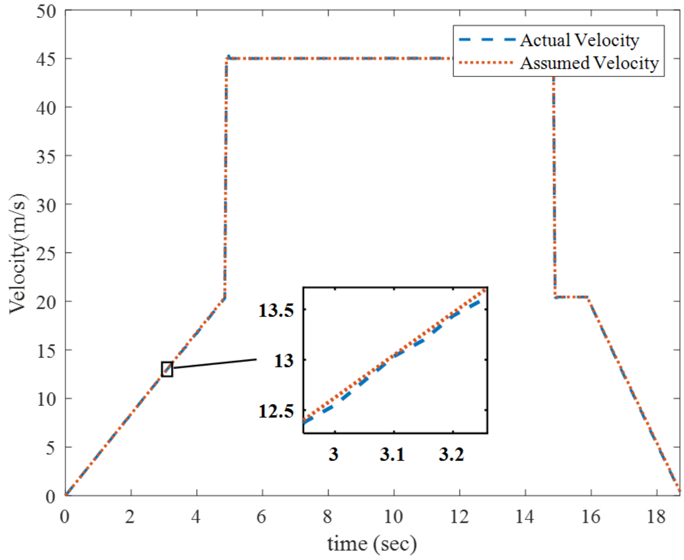

FIGURE 7.14: Assumed airplane's velocity versus the actual airplane's velocity

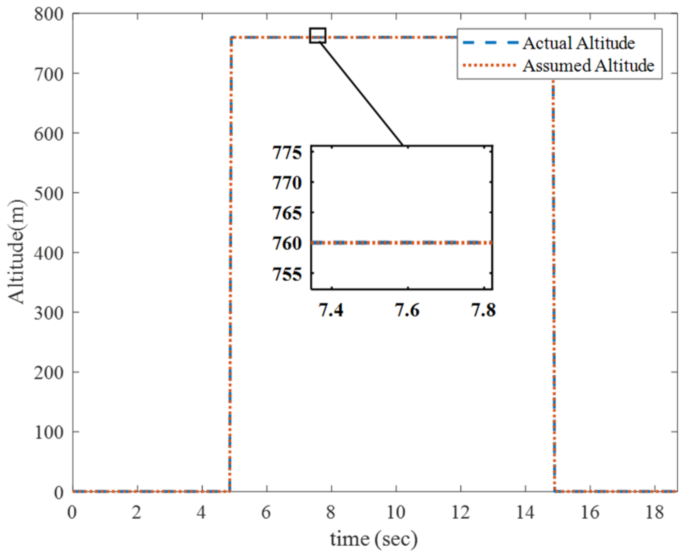

FIGURE 7.15: Assumed airplane's altitudes versus the actual airplane's altitude

7.2 Model Evaluation

In order to be able to rely on the results of the whole approach, the model's results should be compared to a baseline. To do so, specifications of a real electric airplane are applied to the model and the obtained electric motor maximum power from the model is compared to the actual airplane's electric motor power. This airplane does not use the electric motor in the landing; therefore, only take off and cruise mode are studied. The baseline airplane is from Pipistrel company named *Alpha Electro*, which is a light 2-seater sport aircraft. The specifications of this aircraft are provided in Table 7.2.

TABLE 7.2: Alpha Electro Specifications[64]

Number of Seats	2	Wing Chord	0.9 m
MTOW	550 kg	Wingspan	10.5 m
Spoiler	No Spoiler	Wing Height	2.05 m
Battery Weight	126 kg	Number of Motors	1
Cruise Velocity	43.6 m/s	Propeller Diameter	1.8 m
Takeoff Distance	149 m	Landing Distance (over 50ft obstacle)	460 m

According to the airplane's datasheet, the maximum power for take-off is 60kW, and the typical take-off motor speed is 2400 rpm [64]. Fig 7.16 shows the calculated power-speed profile by the model. It is apparent from the figure that the calculated EM power and speed are matching with the manufacturer data. The slight difference in results might be because of the propeller type and the wing airfoil selection.

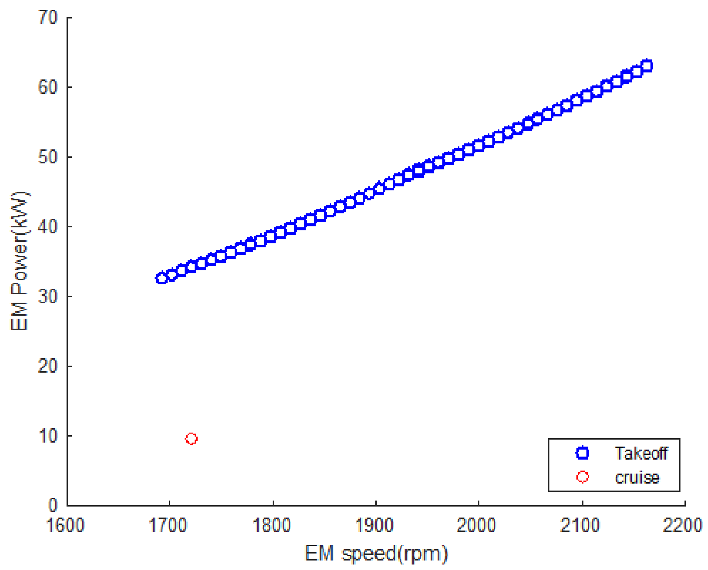

FIGURE 7.16: Required power calculated by the model for Alpha Electro's taking off and cruising modes

7.3 Results and Discussion

The defined airplane from the Table 7.1 is modeled, and several features are analyzed. The various aspects of this study are given as follow:

- The effect of takeoff and landing runway length on the electric motor power-speed and torque-speed profile.
- The effect of cruising speed on the electric motor power-speed and torque-speed profile.
- The effect of wheel brake strength on the landing distance.
- The effect of airplane weight on the landing distance.

7.3.1 Take-off and Landing Distances Effect On Electric Motor's Specification

The touchdown speed of the modeled aircraft is around 20 m/s and one second is considered for the pilot to enable all the braking systems as soon as the airplane wheels touch the ground. Therefore, the minimum landing distance is slightly more than 20m. Another point which should mention is that the airplane can stop in 100.07m by applying only full wheel brakes and spoiler. The airplane velocity profile is displayed in Fig 7.17, and the area under the curve is equal to the landing distance, which is 100.07 m. This implies that in real-life condition, it is not practical to use thrust reverser for any landing distance of more than 120.11m. In other words, it is not recommended to decelerate the airplane linearly.

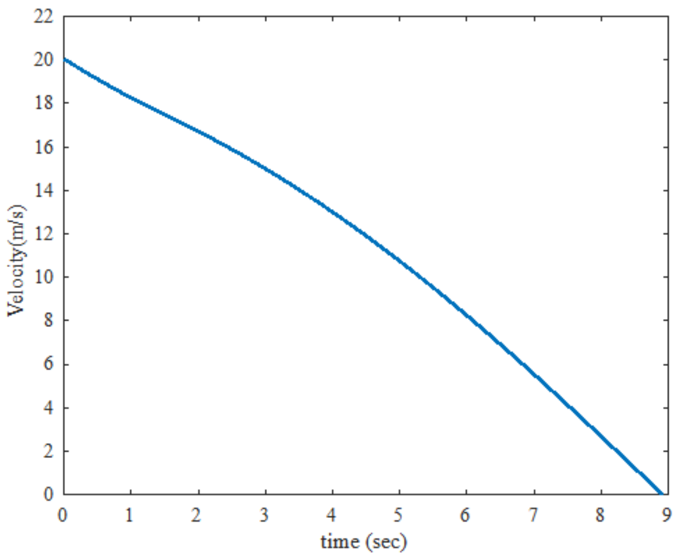

FIGURE 7.17: Airplane's velocity by applying full wheel brakes and spoiler

However, in this thesis a linear deceleration is considered for all landing distances meaning that for landing distances less than 100 m the full brakes are applied and the thrust reverser is always running but for any landing distances of more than 100 m, the thrust reverser is on at the beginning while the full brakes are applied and then the thrust reverser is off, and the wheel brakes coefficient (k in Eq 5.26) is adjusted to follow the airplane assumed velocity trajectory. As an example, Fig 7.18 demonstrates the braking coefficient for landing distance of 140m. From the figure, we can note that the full brake is utilized for 2.3 seconds while the thrust reverser is on and after that, there is no need for thrust reverser usage and the wheel brake coefficient is decreased.

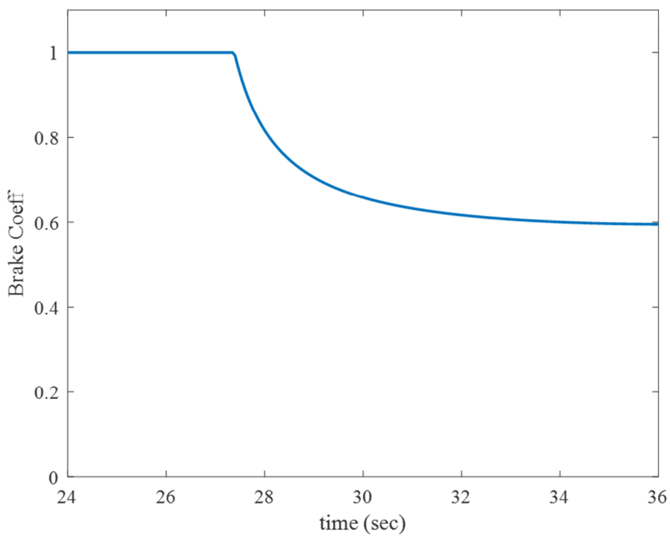

FIGURE 7.18: Brake Coefficient for 140 m landing distance

The effect of takeoff and landing distance on electric motor power, speed, and torque is analyzed. The takeoff and landing distance is changed from 40m to 300m. The required power-speed and torque-speed profiles are given in Appendix A. The maximum torque, power, and speed based on takeoff runway distance are given in Fig 7.19. It is clear that if the airplane takes off in a shorter runway, it needs a more powerful electric motor, which can deliver higher power at a higher speed. On the other hand, shorter runway implies quicker takeoff, meaning that the electric motor is running at the high power for a shorter time. As discussed in section 2.3.4, an electric motor can provide higher torque and power that its continuous torque and power for a short time interval. This ability can help the airplane to take off from a shorter runway.

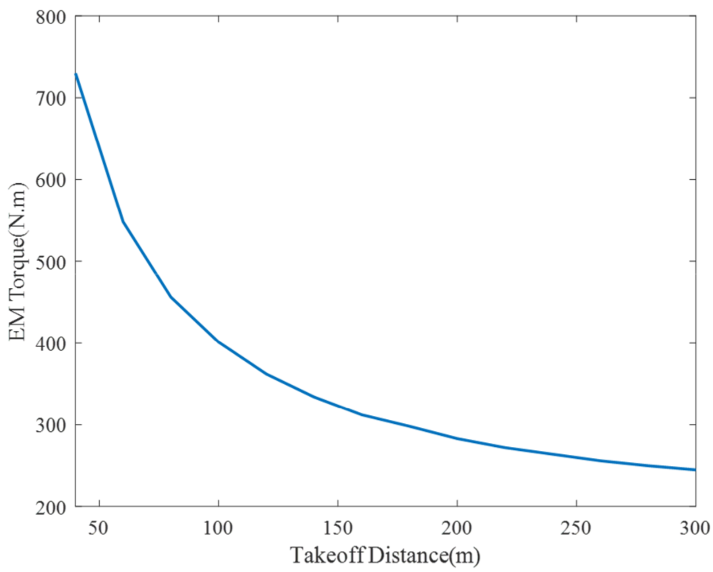

(A) EM Torque Vs Takeoff runway length

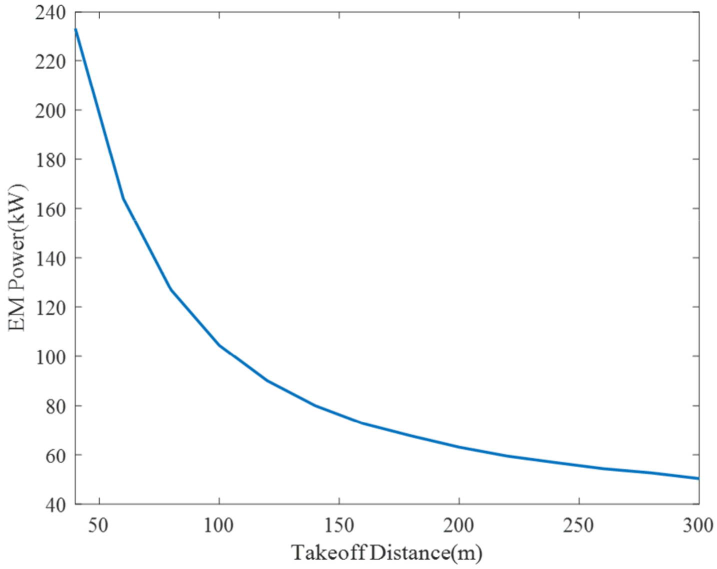

(b) EM Power Vs Takeoff runway length

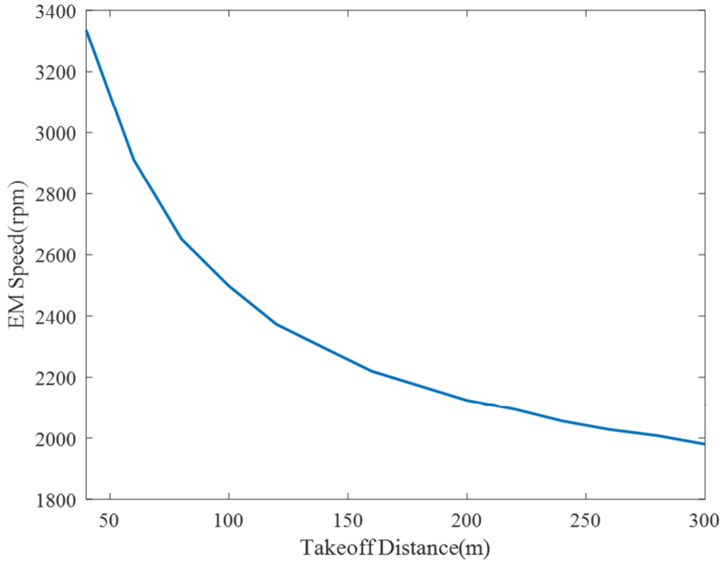

(c) EM Speed Vs Takeoff runway length

Figure 7.19: Electric motor specifications Vs Runway Length during Takeoff

The same study has been conducted for the landing phase. The electric motor specifications, including torque, power, and speed versus different landing distances are illustrated in Fig 7.20. It is observable that after a certain landing runway length (around 250 m), the thrust reverser is off. Because the propeller is producing 40% of the forward thrust while it is working as the thrust reverser, the required power and torque are fairly higher compared to the takeoff stage. The solution could be using an electric motor with the maximum continuous power obtained from the takeoff stage requirements and using its ability to provide higher torque/power in a short time in the landing phase.

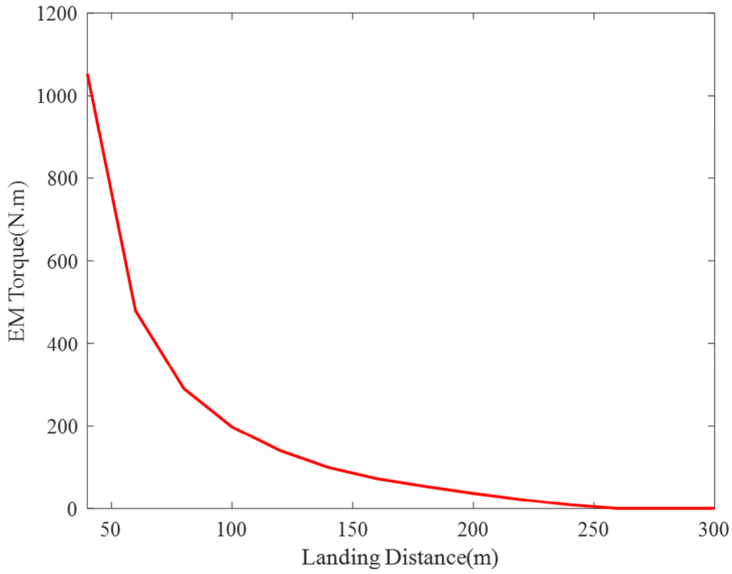

(A) EM Torque Vs Landing runway length

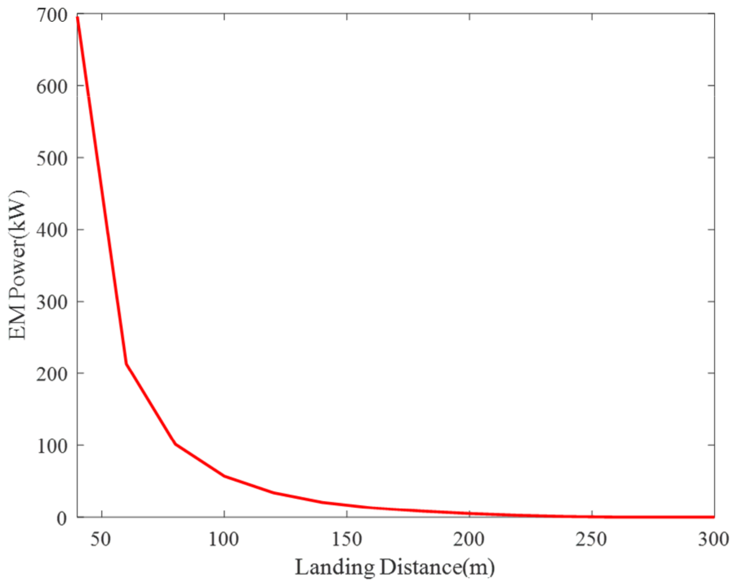

(B) EM Power Vs Landing runway length

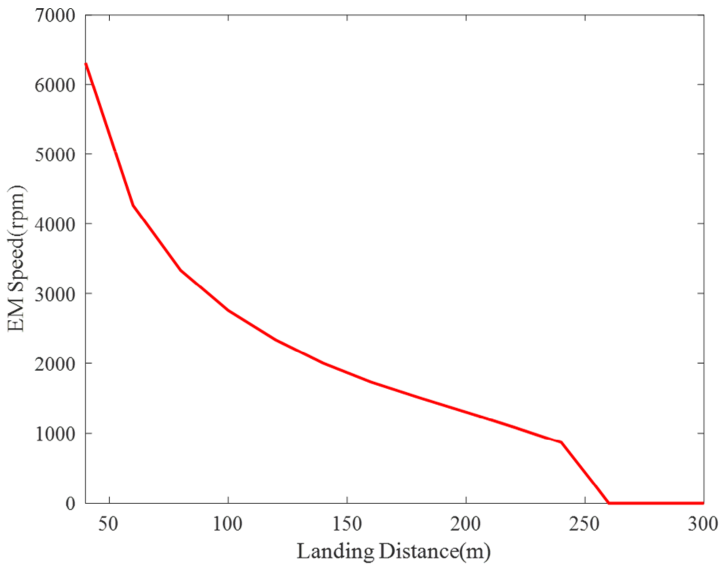

(C) EM Speed Vs Landing runway length

FIGURE 7.20: Electric motor specifications Vs Runway Length during Landing

Fig 7.21 highlights the electric motor specifications versus takeoff and landing distance for all three phases of flight, including takeoff, cruise, and landing stage. It is presented that the motor specifications for cruising are considerably lower than the requirements needed in short takeoff and landing runways. The low motor requirements in cruising imply the benefit associated with wing usage. The exact results values for takeoff and landing phases are given in Table 7.3. Achieving a power density of more than 6 kW/kg is not feasible with state-of-art motor technology. Having said that, manufacturing an electric motor with the power density of 23.2 kW/kg is impossible; however, it is predicted that a power-to-weight ratio of up to 10 kW/kg is achievable in the next decade [79].

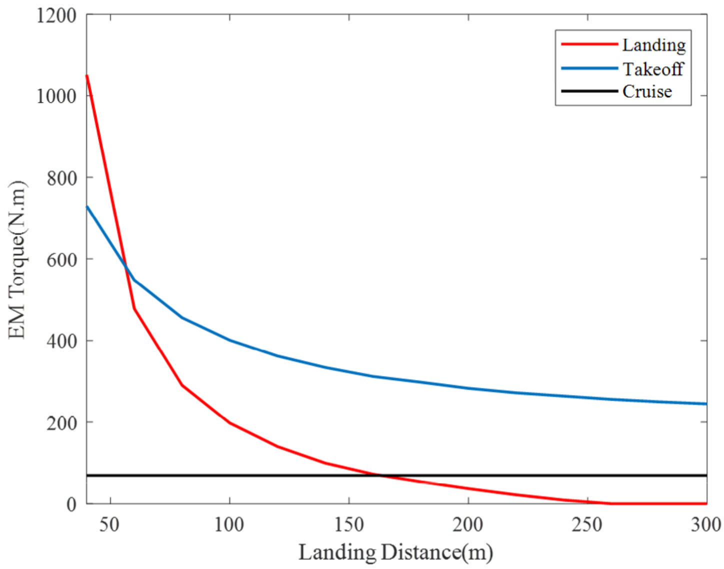

(A) EM Torque Vs Runway Length

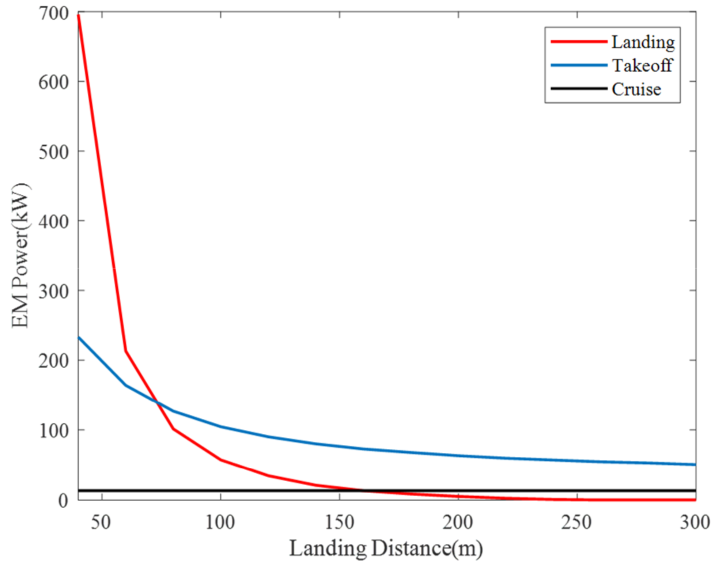

(B) EM Power Vs Runway Length

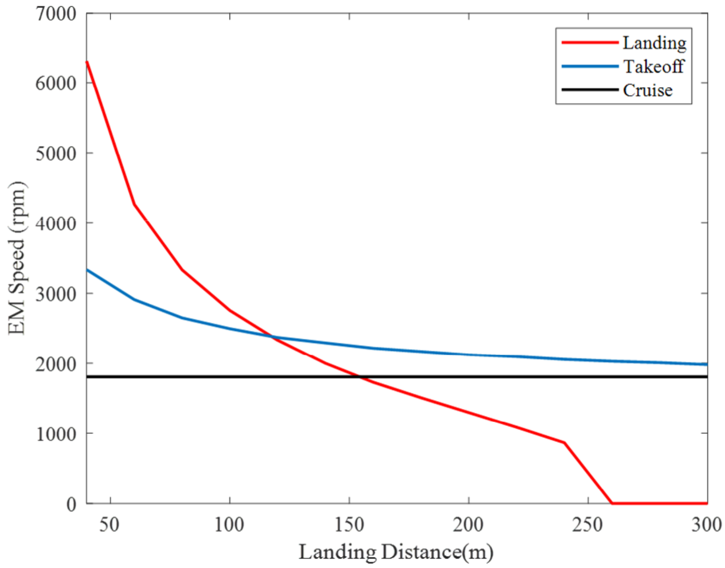

(C) EM Speed Vs Runway Length

FIGURE 7.21: Electric motor specifications Vs Runway Length during taking off, cruising and landing

Another important point from the Table 7.3 is the acceleration and deceleration value. It is mentioned in the Table 5.3 that a proper value of a/g is from 0.3 to

0.35 for a light aircraft with a simple baking system. This condition is feasible only for runways longer than 80m.

TABLE 7.3: Electric motor specifications during takeoff and landing

Runway Length(m)	T_TO (N.m)	P_TO (kW)	W_TO (rpm)	PD_TO (kW/kg)	a_TO/g	T_L (N.m)	P_L (kW)	W_L (rpm)	PD_L (kW/kg)	a_L/g
40	730	233	3336	7.76	0.53	1053	696	6309	23.2	1.08
60	548	164	2911	5.46	0.35	478	213	4264	7.1	0.53
80	456	126.8	2652	4.22	0.26	290.5	101.4	3333	3.38	0.35
100	401	104.5	2498	3.46	0.21	197.7	57.1	2757	1.9	0.26
120	362	90.1	2373	3	0.17	140	34.2	2335	1.14	0.21
140	334	80	2296	2.66	0.15	99.49	20.8	1999	0.69	0.17
160	312	72.7	2220	2.42	0.13	72.45	13.13	1730	0.43	0.15
180	298	67.7	2172	2.25	0.11	53.8	8.51	1509	0.28	0.13
200	283	63.7	2124	2.12	0.10	36.9	5.02	1298	0.16	0.11
220	272	59.5	2095	1.98	0.09	21.7	2.47	1087	0.08	0.10
240	264	56.9	2056	1.89	0.08	8.9	0.8	866	0.02	0.09
260	256	54.4	2028	1.81	0.08	0	0	0	0	0.08
280	250	52.7	2008	1.75	0.07	0	0	0	0	0.08
300	245	50.4	1980	1.68	0.07	0	0	0	0	0.07

Fig 7.22 shows the electric motor's running time based on runway length. It can be infers that the motor is not running for a long time in takeoff and in landing meaning that the motor's continues power can be much less than its short-time peak power and the peak power can be applied in takeoff an landing stages.It means that the motor specifications can be chosen based on other flight requirements such as climbing or cruising and the electric motor peak power can be used in the takeoff and landing. It should be mentioned that the required power for takeoff

and landing can be up to 18 times more than required power for the cruising flight mode based on the takeoff and landing distances and cruising speed. Even though the electric motor peak power can provide the high amount of required power for takeoff and landing, the battery may be damaged by the high rate of current drawn from it. It means that for some mission profiles, it is possible that there is no need to use a bigger, powerfull motor, but it might be needed to use a bigger battery with higher C-rate. 1

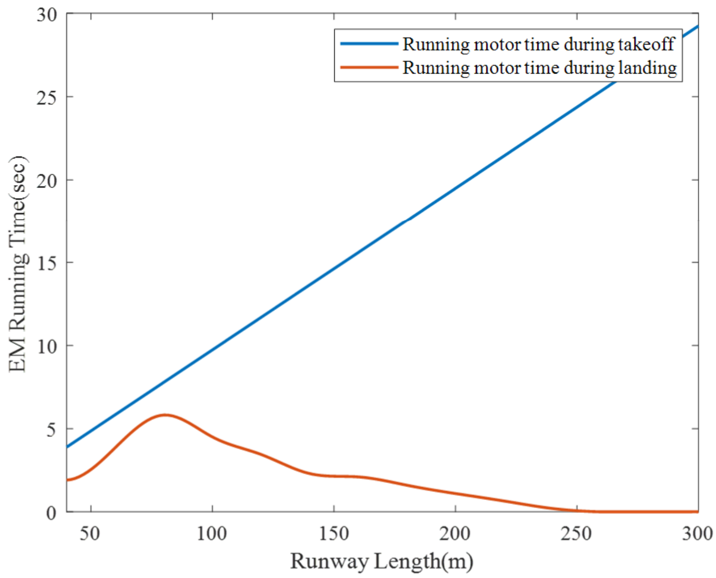

FIGURE 7.22: Electric motor's running time during takeoff and landing

7.3.2 Cruising Speed Effect on Electric Motor's Specification

The minimum flying speed (stall speed) is around 20m/s. Accordingly, the effect of cruising speed from 35m/s to 75m/s, which is equal to 126km/h to 270km/h on electric motor specifications is investigated. The required motor specification based on cruising velocity is given in Fig 7.23. Fig 7.23 shows there is not a significant difference in motor power, torque or speed by changing the airplane cruising velocity. In other words, by using the same EM which is used in takeoff and landing, the airplane velocity in cruising mode can be increased without any need for modifying EM size due to the considerable gap between takeoff and landing requirements and cruising.

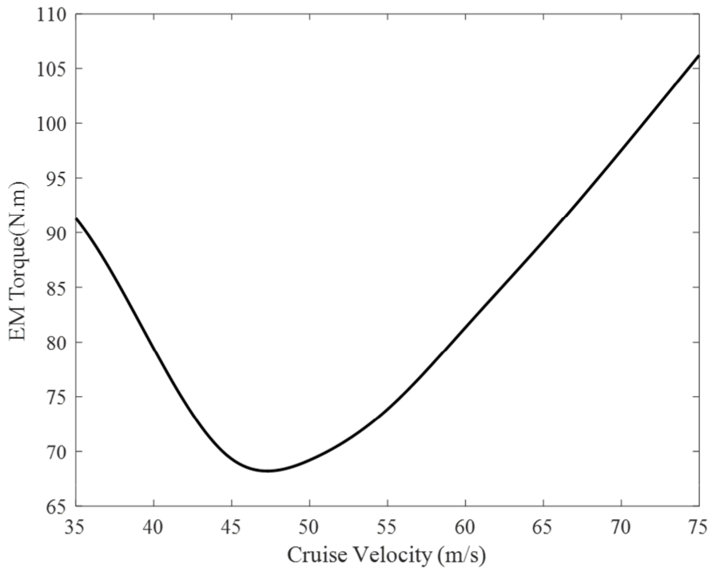

(A) EM Torque Vs Cruise Velocity

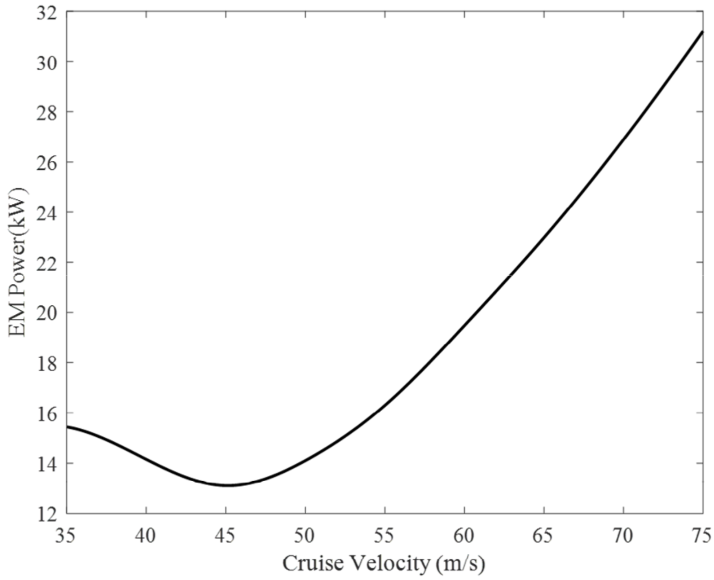

(B) EM Power Vs Cruise Velocity

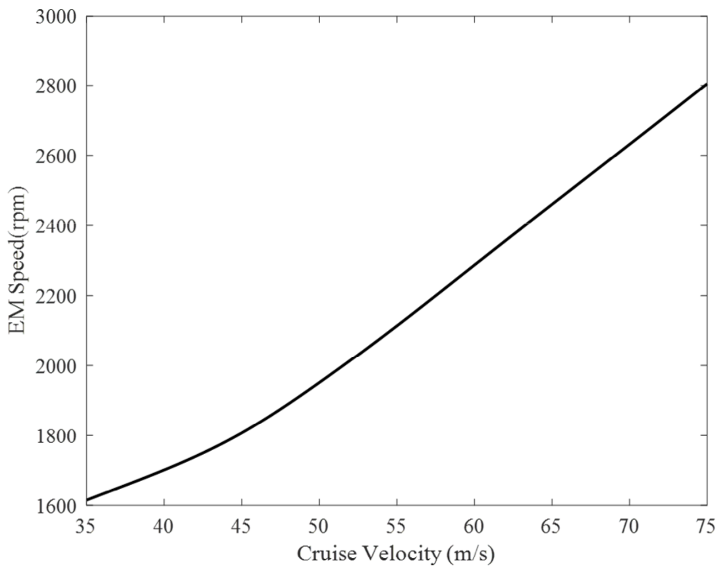

(c) EM Speed Vs Cruise Velocity

FIGURE 7.23: Electric motor specifications Vs cruising speed

7.3.3 Wheel Brake Coefficient Effect on the Landing Distance

The braking coefficient in the Eq 5.26 can vary from 0.25 to 0.4 and above. The value of the braking coefficient from a poor one to a good one is presented in Table 7.4 [76].A medium value of 0.3 is chosen for the modeling in previous sections, but the impact of braking coefficient on the landing distance is examined. It can be seen from the Fig 7.24 that a slight improvement in braking system can lead to a shorter landing distance. A braking coefficient of more than 0.4 is obtainable, which is not considered in the analysis.

TABLE 7.4: Braking Coefficients

Braking Action	**Braking Coefficient**
Good	0.4 and above
Medium/Good	0.36-0.39
Medium	0.30-0.35
Medium/Poor	0.26-0.29
Poor	0.25 and below

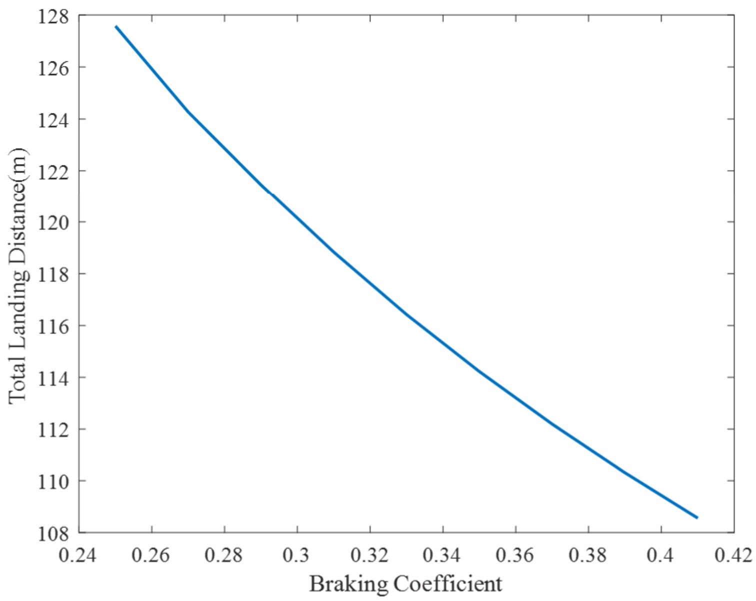

FIGURE 7.24: Total landing distance including the transition and ground roll distance Vs braking coefficient

7.3.4 Maximum Takeoff Weight Effect on the Landing Distance

V_{stall} which is the minimum required velocity for the airplane to fly is as follows:

$$V_{Stall} = \sqrt{\frac{2mg}{\rho S C_{Lmax}}} \tag{7.1}$$

According to the Eq 7.1, by decreasing the MTOW of the airplane the stall velocity drops which is desirable for having shorter landing distance because of two reasons. First, the distance travelled in transition stage is decreased and second it is easier to slow down the airplane to entirely stop becasue the touchdown velocity is lower. The touch down velocity based on the airplane maximum takeoff weight is illustrated in Fig 7.25.

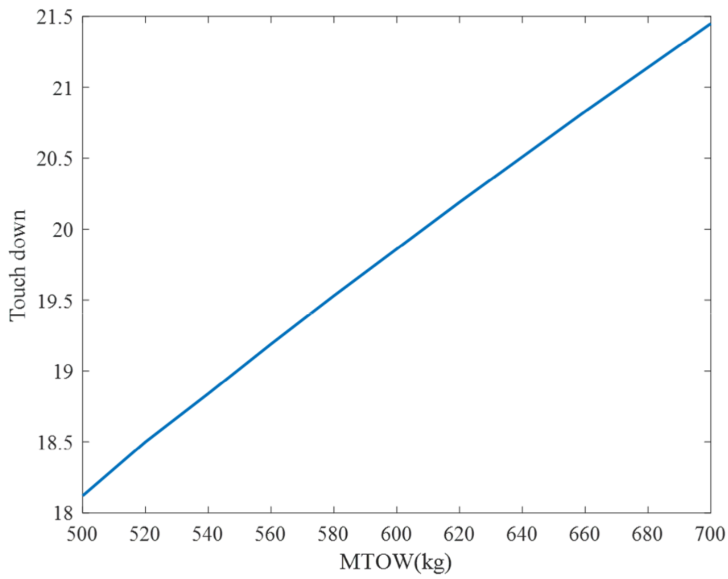

Figure 7.25: Airplane's touch down velocity Vs MTOW

The effect of MTOW on the landing distance with full medium brakes is analyzed and depicted in Fig 7.26. The total landing distance consists of the freeroll or transition distance and the ground roll distance.

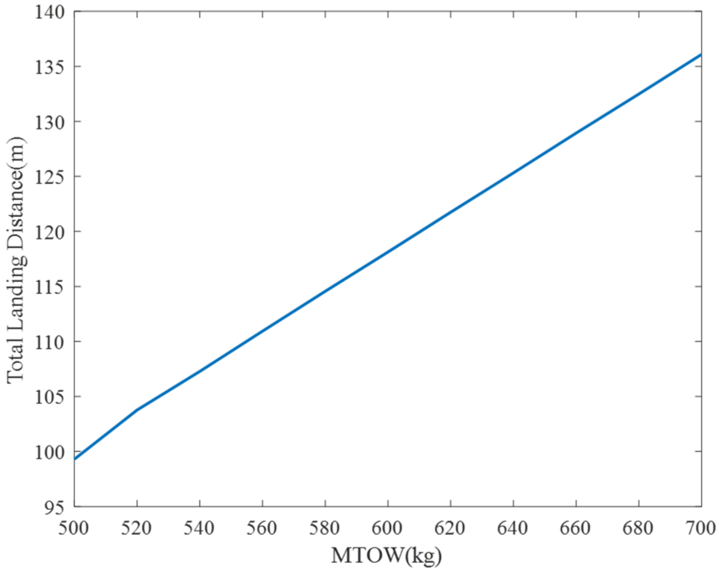

FIGURE 7.26: Airplane's total landing distance Vs MTOW

Chapter 8

Conclusion and Future Work

The modes of daily transporting are changing, and the next two decades more passengers will travel by the means of air transportation within populated cities. However, the general public and policymakers envison the following issues arise with the use of urban aerial vehicles: noise pollution, safety concerns, society acceptance, certification issues, fuel depletion, and the most critical one, which is global emission. The electric propulsion system can be an excellent candidate for the propulsion system of any new transportation system, as it is not suffering from some of the issues associated with the conventional propulsion system including fuel depletion, noise pollution and emissions. The necessity of using electric propulsion system for the future air transportation is explained in the chapter 2. Furthermore, any aerial transportation system intended to be used in populated cities should take off and land from the smallest field as possible. The reasons why an ESTOL vehicle is a fitting choice for the urban air vehicle are given in chapter 3. Moreover, modifying a CTOL airplane to ESTOL airplane can solve the problem of airport capacity shortage, as is described in section 1.1.1. In conclusion, an electric ESTOL aircraft can be a potential solution to the airports capacity shortage, travel delays and can be a suitable candidate as an urban aerial vehicle.

This thesis has investigated the effect of runway length on the electric motor specifications, including electric motor power, torque, and speed. A specific airplane is modeled in Simulink MATLAB for three phases of takeoff, cruise, and landing. The model is flexible to changes of several features meaning the model can be used for any direct drive propeller fixed-wing airplane.

The finding of this study supports the idea of using electric motors as the propulsion system for lightweight ESTOL airplanes. Even when the airfoil, wing and propeller structure of the modeled airplane are not optimized, the results from the takeoff phase indicate a reduced takeoff runway by using electric motors.

Another significant finding of this research is that the required power for takeoff is incredibly higher than cruising mode. Depending on the takeoff runway length and cruising speed, the required power for takeoff for the modeled airplane can be up to 18 times than the required power for the cruising. Another valuable finding is that it takes only a few seconds for an airplane to take off and electric motors can provide higher power than their continuous power for a short period. It means there is no need to use an incredibly high power electric motor to convert a CTOL airplane to an ESTOL airplane.

The evidence from this study suggests that using thrust reverser for a small airplane is not efficient as enormously high power and torque are demanded to stop the airplane in an extremely short runway. The required power for landing in an extremely short runway, 40m, is up to three times than the required power for taking off from the same runway length. However, if the runway length increases,

the difference between required power for takeoff and landing decreases and for runways more than 70 m the same electric motor can be used for taking off and landing as the amount of required power for landing becomes less than takeoff required power. Improvement of the airplane's braking system (section 7.3.3) and using lighten components and materials such as carbon fiber to make the aircraft lighter (section 7.3.4), leads to a shorter runway. Additionally, designing and utilizing the proper spoiler and high lift device for the airplane helps to reduce the landing distance. All the above suggestions are more practical than using electric motor and thrust reverser for a small airplane which takes off and lands in an extremely short runway (less than 50m). However, it is worth mentioning that using of thrust reverser can be beneficial for airplanes with the propellers which are designed to have high efficiency in takeoff and landing.
Future research in this area can address the following topics:

- Using an optimized propeller for takeoff and landing instead of a normal one designed for cruising mode to have higher efficiency on the takeoff and landing stages. By doing so, the required power from the electric motor decreases in both takeoff and landing phases, and would be more feasible to use the thrust reverser in the landing phase.
- Using an optimized spoiler and high lift device based on the performance requirement instead of using a typical one.
- Increasing the number of electric motors and propeller and placing them all over the wing (i.e. distributed propulsion systems).
- Doing study on the potential solutions for regenerative power in flying. As

an example, for an airplane with more than one electric motor as the propulsion system (distributed propulsion system architecture), in cruising mode, some of EMs can rotate towards the air stream and can be used as turbines to produce electricity and charge the batteries.

- Using electric motors attached to the wheels as an auxiliary force in takeoff and landing stages.
- Using ducted fans instead of propellers.
- Analyzing the required electric motor specification for the climbing phase

Appendix A

Results: Torque-Speed and Power-Speed Profiles

The effect of runway length on the electric motor's torque-speed and power-speed profile for the chosen airplane is illustrated in Table A1.1 and Table A1.2 respectively. The results indicate that for any runway more than 250 m there is absolutely no need for thrust reverser.

TABLE A1.1: Torque-Speed profiles for different take-off and landing distances

<table>
<tr><th>Runway(m)</th><th>Torque-Speed</th></tr>
<tr><td>40</td><td>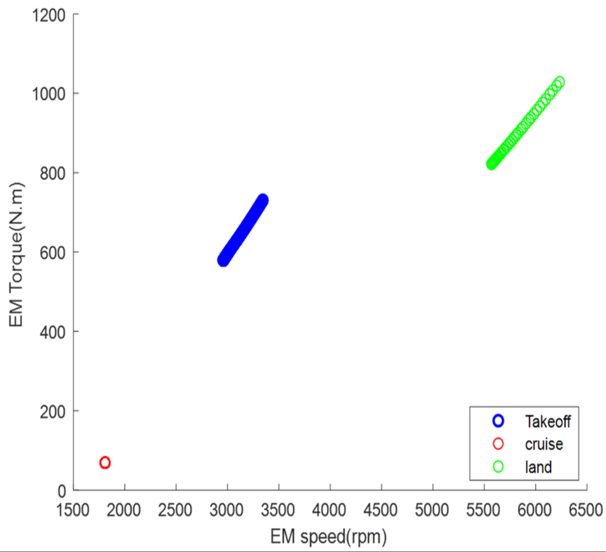
</td></tr>
<tr><td>60</td><td>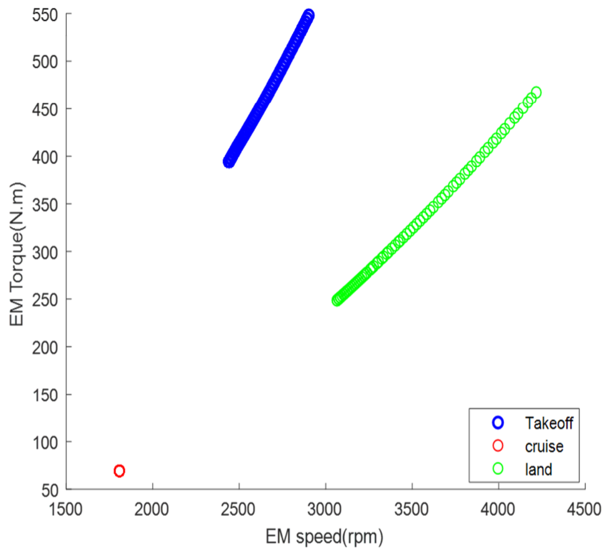
</td></tr>
</table>

80

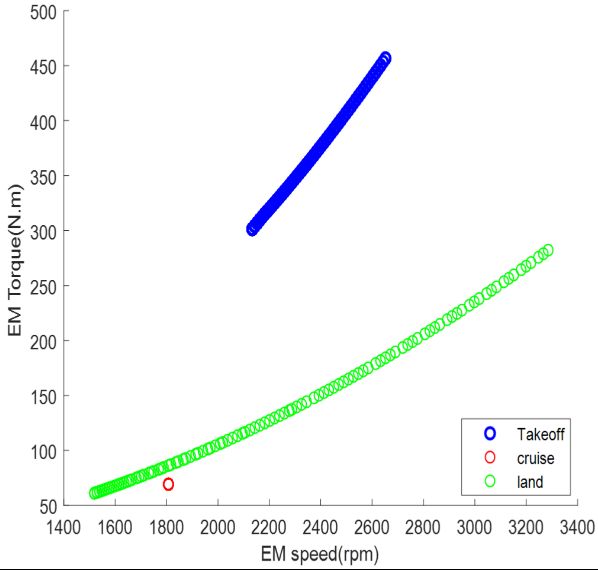
EM Torque(N.m)
EM speed(rpm)
Takeoff
cruise
land
500
450
400
350
300
250
200
150
100
50
1400
1600
1800
2000
2200
2400
2600
2800
3000
3200
3400

100

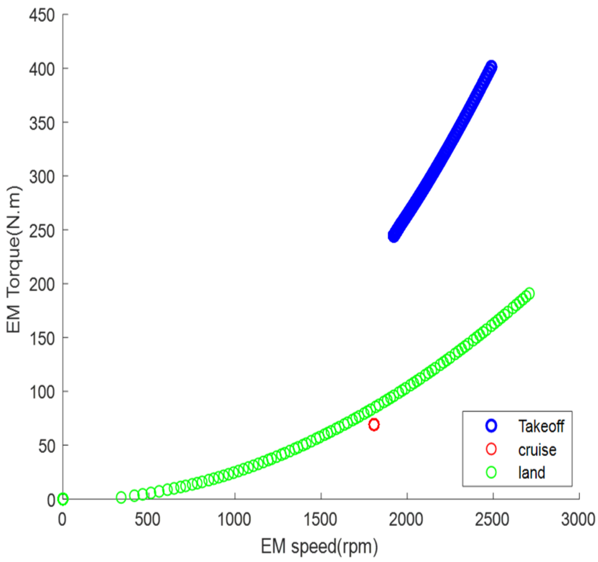
EM Torque(N.m)
EM speed(rpm)
Takeoff
cruise
land
450
400
350
300
250
200
150
100
50
0
0
500
1000
1500
2000
2500
3000

120	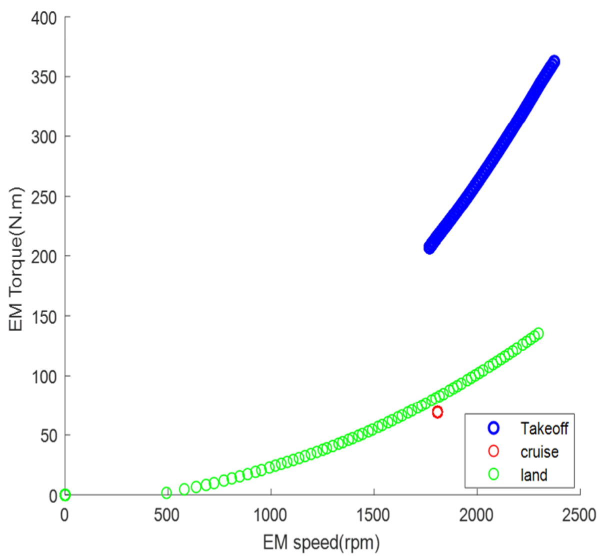
140	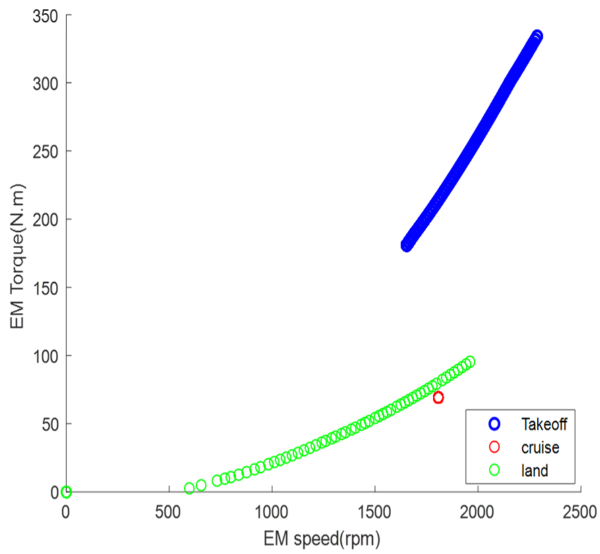

EM Torque(N.m)
EM speed(rpm)
Takeoff
cruise
land
0
50
100
150
200
250
300
350
400
500
1000
1500
2000
2500

EM Torque(N.m)
EM speed(rpm)
Takeoff
cruise
land
0
50
100
150
200
250
300
350
500
1000
1500
2000
2500

160	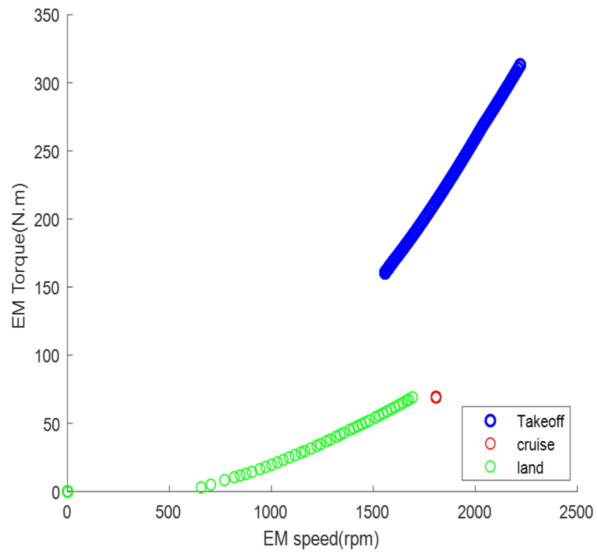EM Torque(N.m) EM speed(rpm) Takeoff cruise land
180	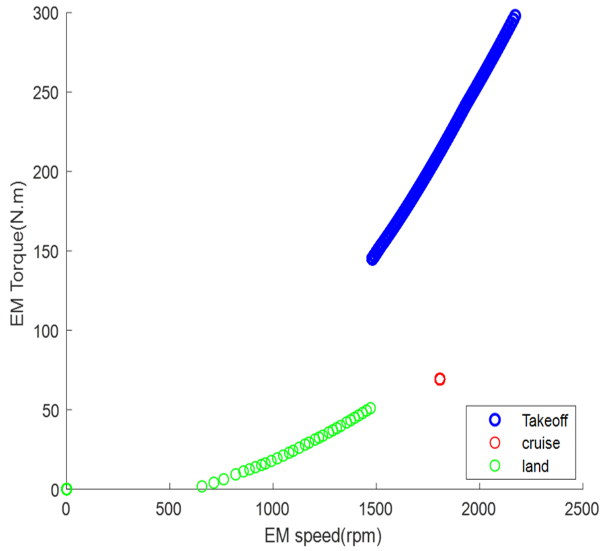EM Torque(N.m) EM speed(rpm) Takeoff cruise land

200	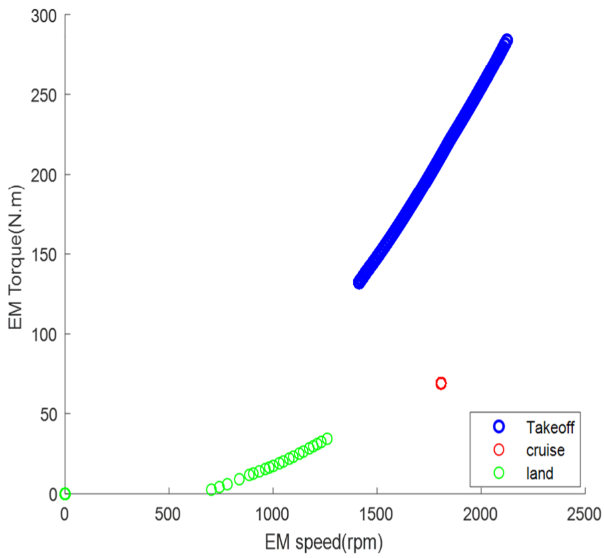
220	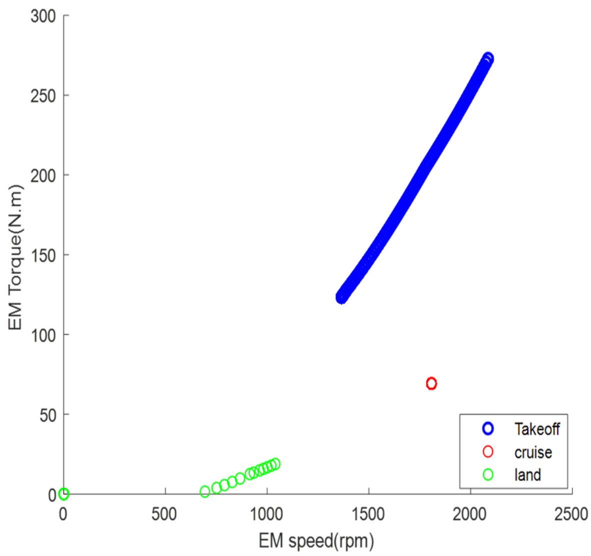

240	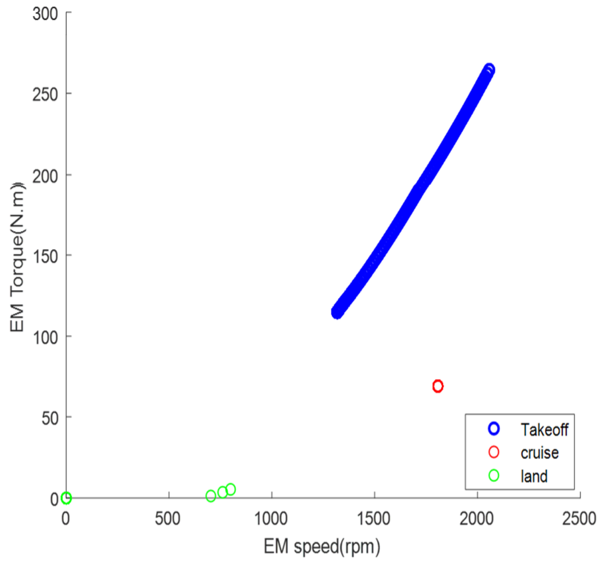 EM Torque(N.m) EM speed(rpm) Takeoff cruise land 0 50 100 150 200 250 300 0 500 1000 1500 2000 2500
260	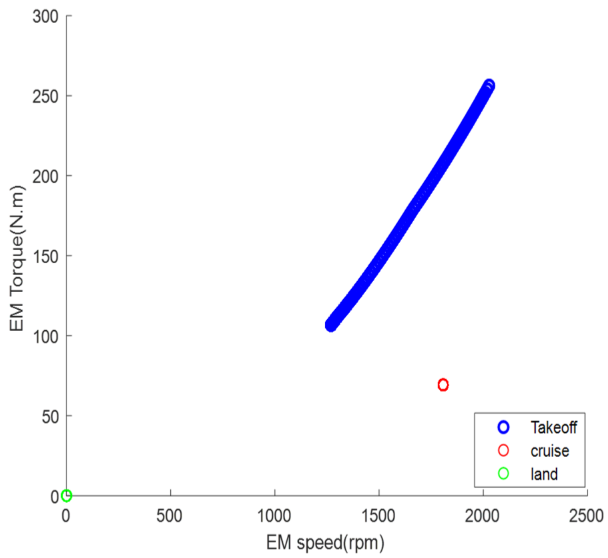 EM Torque(N.m) EM speed(rpm) Takeoff cruise land 0 50 100 150 200 250 300 0 500 1000 1500 2000 2500

280	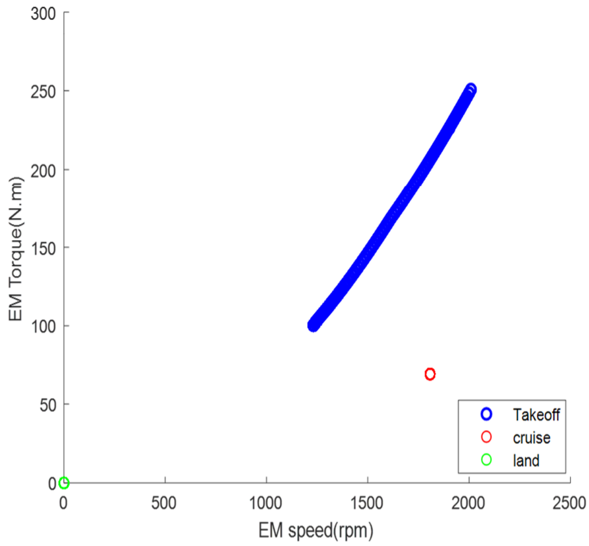 EM Torque(N.m) EM speed(rpm) Takeoff cruise land 0 50 100 150 200 250 300 0 500 1000 1500 2000 2500
300	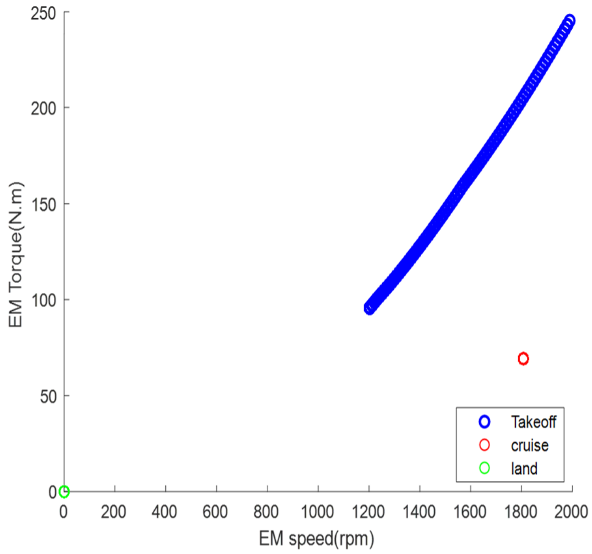 EM Torque(N.m) EM speed(rpm) Takeoff cruise land 0 50 100 150 200 250 0 200 400 600 800 1000 1200 1400 1600 1800 2000

TABLE A1.2: Power-Speed profiles for different take-off and landing distances

<table>
<tr><th>Runway(m)</th><th>Power-Speed</th></tr>
<tr><td>40</td><td>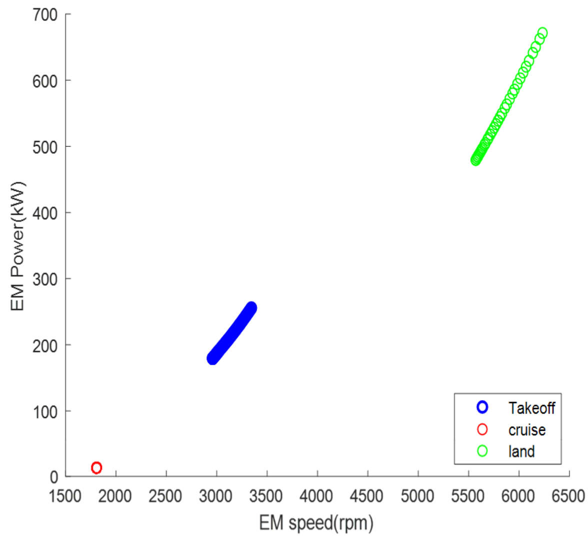
</td></tr>
<tr><td>60</td><td>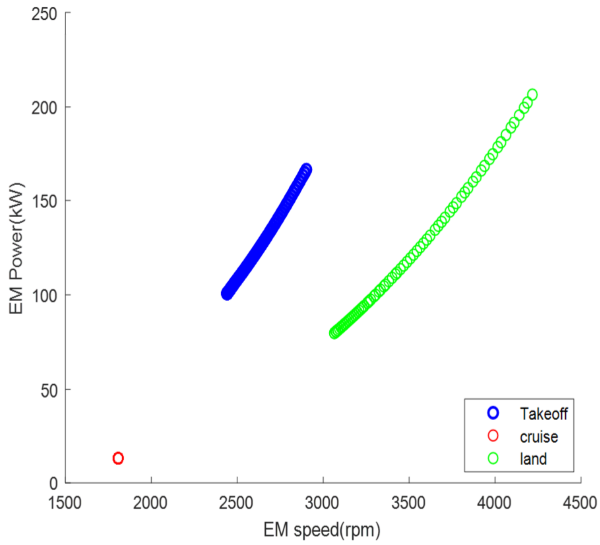
</td></tr>
</table>

80	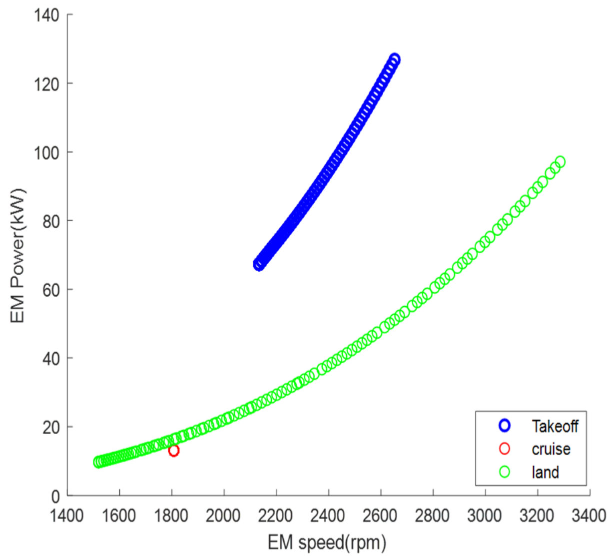 EM Power(kW) EM speed(rpm) Takeoff cruise land
100	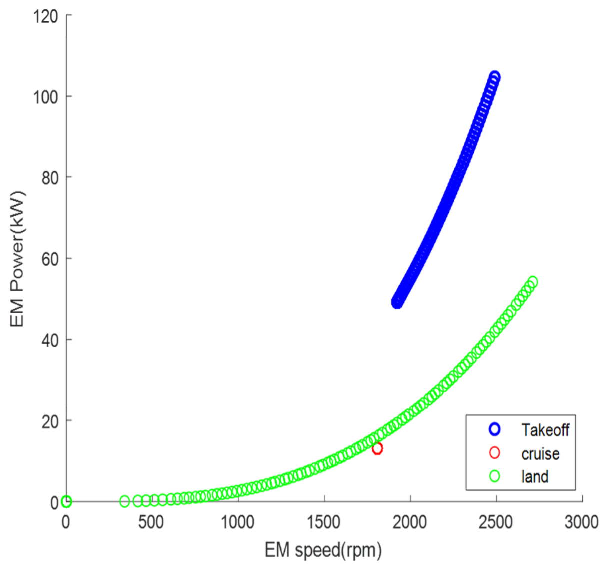 EM Power(kW) EM speed(rpm) Takeoff cruise land

120	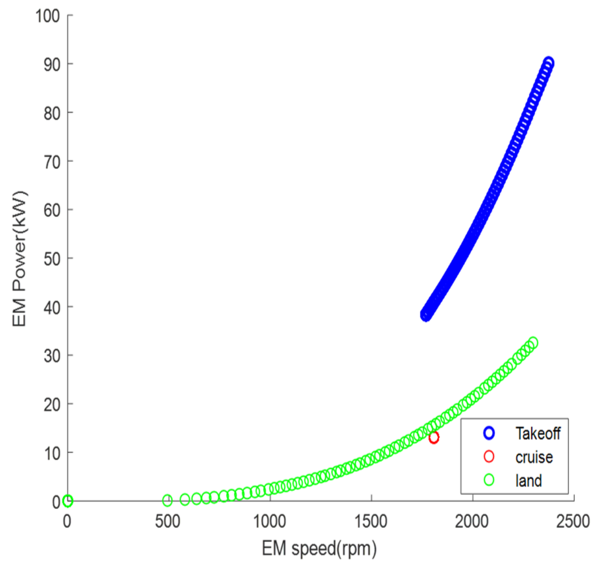 EM Power(kW) EM speed(rpm) 0 10 20 30 40 50 60 70 80 90 100 500 1000 1500 2000 2500 Takeoff cruise land
140	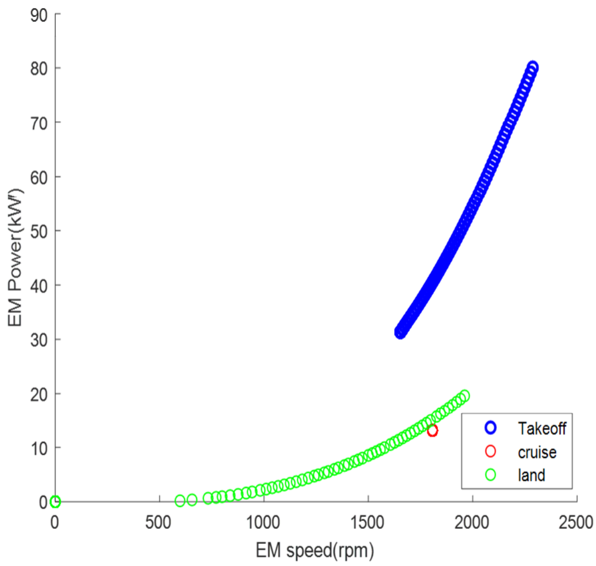 EM Power(kW) EM speed(rpm) 0 10 20 30 40 50 60 70 80 90 500 1000 1500 2000 2500 Takeoff cruise land

160	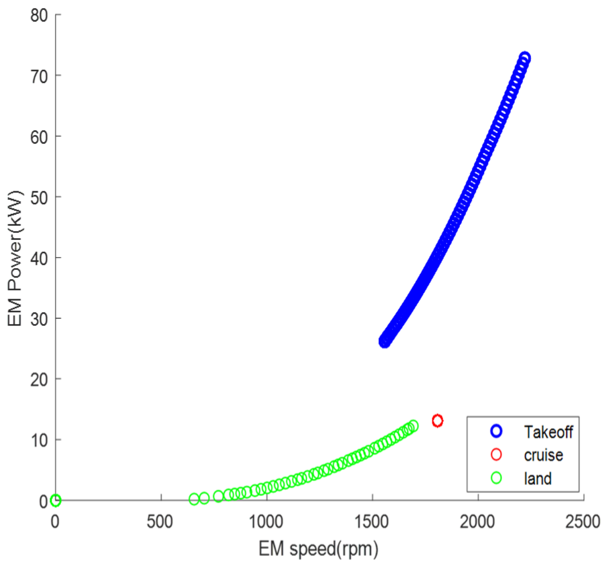 EM Power(kW) EM speed(rpm) Takeoff cruise land
180	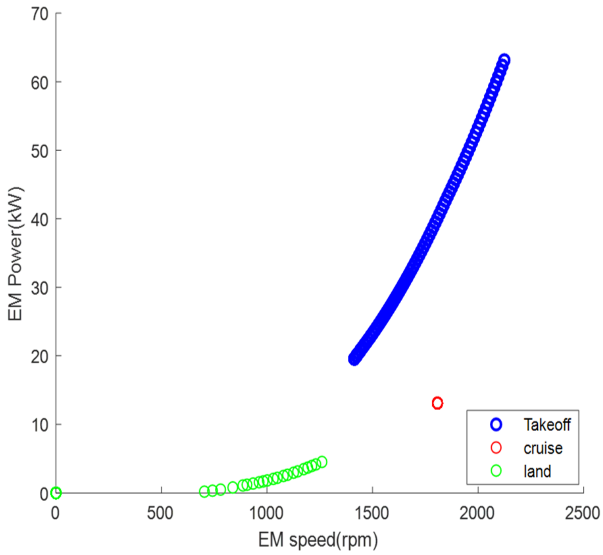 EM Power(kW) EM speed(rpm) Takeoff cruise land

200

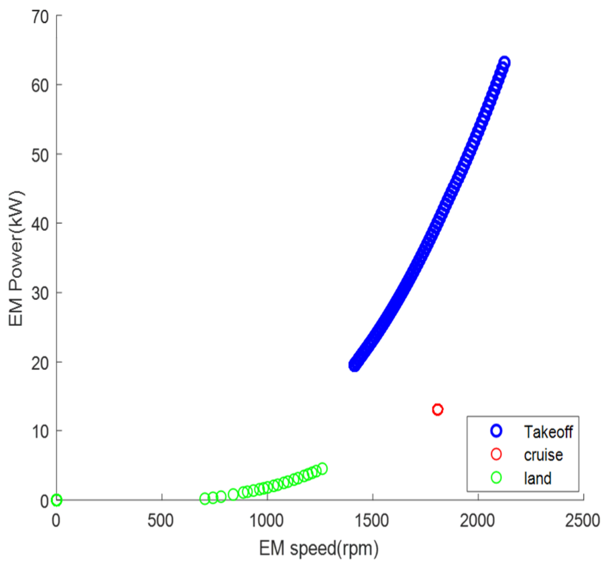
EM Power(kW)
EM speed(rpm)
Takeoff
cruise
land

220

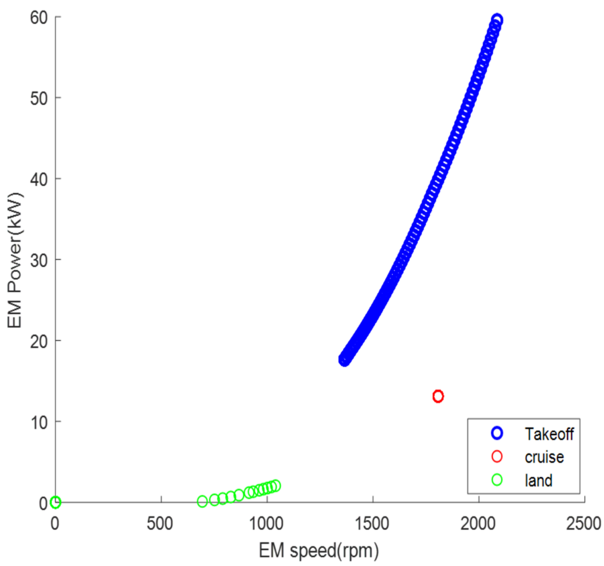
EM Power(kW)
EM speed(rpm)
Takeoff
cruise
land

240	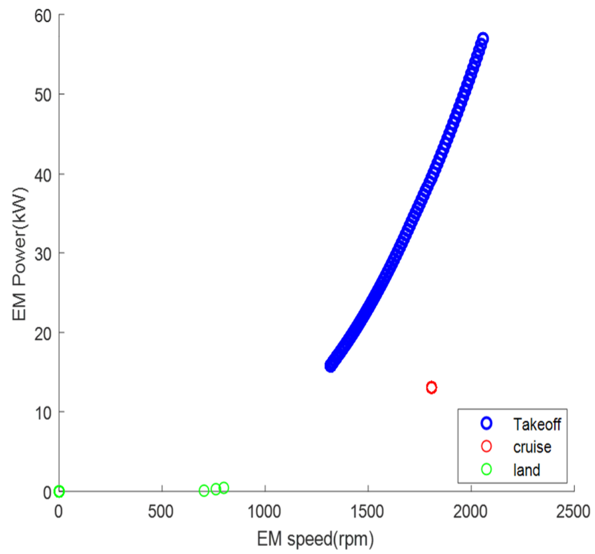EM Power(kW) EM speed(rpm) Takeoff cruise land
260	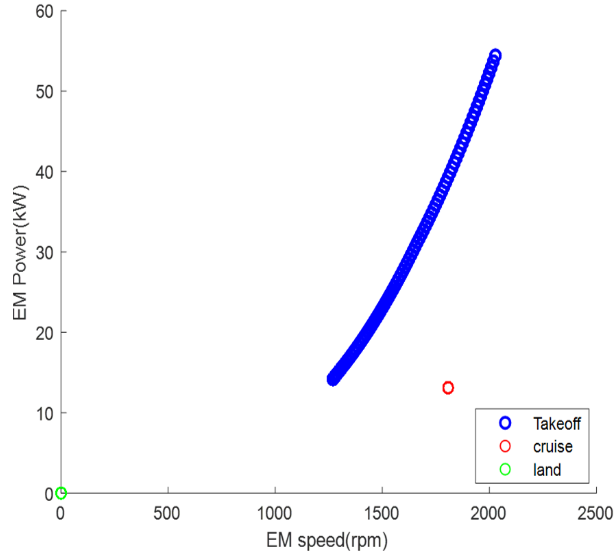EM Power(kW) EM speed(rpm) Takeoff cruise land

280	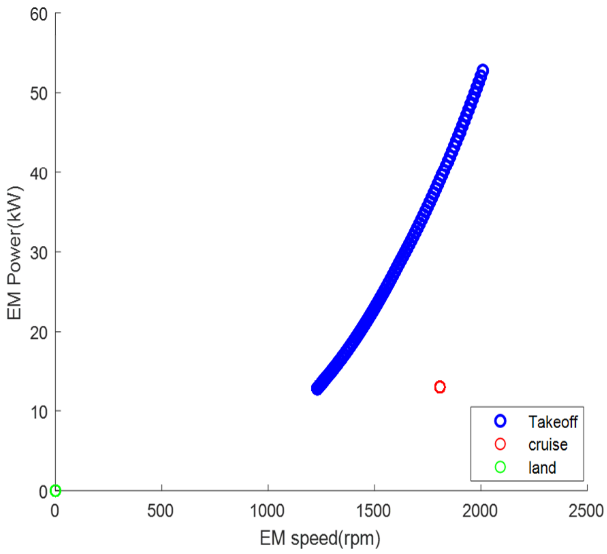 EM Power(kW) EM speed(rpm) Takeoff cruise land
300	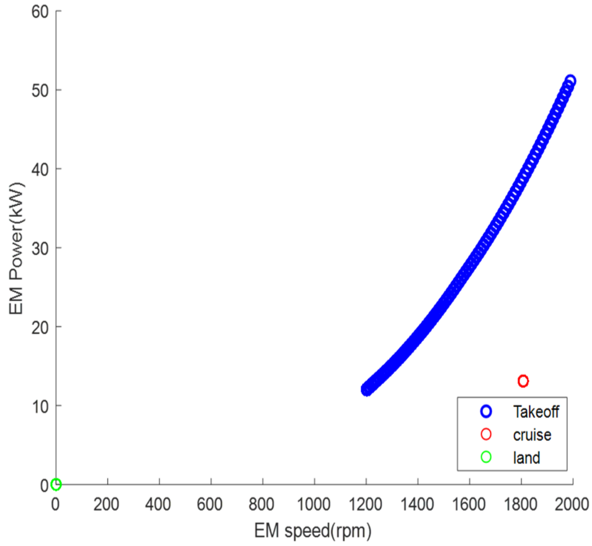 EM Power(kW) EM speed(rpm) Takeoff cruise land

References

[1] https://fedotov.co/wp-content/uploads/2018/03/Future-of-Vertical-Mobility.pdf.

[2] https://avinor.no/contentassets/c29b7a7ec1164e5d8f7500f8fef810cc/introduction-of-electric-aircraft-in-norway.pdf.

[3] https://www.aviationpros.com/article/12397085/airbus-on-the-way-to-the-electric-future.

[4] https://www.airbus.com/newsroom/news/en/2017/05/Electric-flight.html.

[5] https://www.telegraph.co.uk/finance/newsbysector/industry/engineering/11729838/Airbus-E-Fan-2.0-set-to-recreate-aviation-history-with-cross-Channel-flight-only-this-time-its-electric.html.

[6] https://www.sonexaircraft.com/e-flight_archive-032410/.

[7] https://newatlas.com/eads-acs-green-cri-electric-aerobatic-airplane/15621/.

[8] https://www.aopa.org/news-and-media/all-news/2011/january/01/big-fun-in-a-small-package.

[9] http://www.kreiselelectric.com/en/blog/electric-aeroplane-elektra-one-kreisel-battery-technology/.

[10] https://www.avweb.com/air-shows-events/sun-flyer-promises-three-hour-flight-time/.

[11] https://www.avweb.com/avwebflash/news/Siemens-Electric-Motor-Will-Power-Sun-Flyer-2-230896-1.html.

[12] https://www.pipistrel.si/news/wattsup-the-new-2seat-electric-trainer-took-its-maiden-fligh.

[13] https://www.pipistrel.si/plane/alpha-electro/technical-data.

[14] https://www.panthera-aircraft.com/technical-data.

[15] https://www.pipistrel.si/plane/panthera/overview.

[16] https://www.siemens.com/press/pool/de/events/2016/corporate/2016-12-innovation/inno2016-aerobatic-airplane-e.pdf.

[17] https://www.aerospace-technology.com/projects/extra-330le-electric-aircraft/.

[18] https://arstechnica.com/cars/2016/12/this-extra-330-is-the-fastest-climbing-electric-powered-airplane-ever/.

[19] https://www.hightechzentrum.ch/files/154/Energiesysteme/248/Claus-Mueller.pdf.

[20] https://www.aerospace-technology.com/projects/magnus-efusion-light-sport-aircraft/.

[21] http://www.ifb.uni-stuttgart.de/egenius.

[22] http://www.ifb.uni-stuttgart.de/egenius/page_Aircraft/.

[23] https://www.pipistrel-aircraft.com/aircraft/electric-flight/taurus-electro/#tab-id-3.

[24] https://www.pipistrel-usa.com/electric-propulsion/.

[25] http://www.electraflyer.com/electraflyer-uls.php.

[26] http://www.alisport.com/?product=silent-2-electro-2.

[27] https://www.schempp-hirth.com/en/sailplanes/arcus/arcus-e.html.

[28] https://www.lange-aviation.com/en/produkte/antares-20e/.

[29] https://www.aviationpros.com/article/12397085/airbus-on-the-way-to-the-electric-future.

[30] https://www.verticalmag.com/news/cityairbus-evtol-urban-air-mobility-program-presses-ahead/.

[31] https://www.ie-net.be/sites/default/files/Siemens%20eAircraft%20-%20Disrupting%20Aircraft%20Propulsion%20-%2000%20JH%20THO%20-%2020180427.cleaned.pdf.

[32] http://europe.autonews.com/article/20180606/ANE/180609838/airbus-flying-taxi-could-be-in-cities-by-2025.

[33] http://www.e-flight-journal.com/e-flight-journal-aero-special-2018-small.pdf.

[34] http://evtol.news/aircraft/ehang/.

[35] https://www.aerospace-technology.com/projects/ehang-184-autonomous-aerial-vehicle-aav/.

[36] http://www.ehang.com/ehang184/specs/.

[37] https://www.dronethusiast.com/ehang-184-is-a-manned-uav-you-will-never-get-to-fly/.

[38] http://evtol.news/wp-content/uploads/2018/08/EAA_Forum_The-Electric-VTOL-Revolution_VFS_20180725.pdf.

[39] https://www.volocopter.com/en/product/.

[40] https://bts.gov.

[41] https://www.volocopter.com/en/.

[42] https://www.ehang.com/.

[43] http://evtol.news/aircraft/zee-aero/.

[44] https://vahana.aero/.

[45] http://evtol.news/aircraft/a3-by-airbus/.

[46] https://terrafugia.com.

[47] https://lilium.com/the-jet.

[48] https://moller.com/moller_skycar400.html.

[49] https://www.autocar.co.uk/car-news/new-cars/new-terrafugia-tf-x-flying-car-revealed.

[50] https://www.dailymail.co.uk/sciencetech/article-1088843/What-way-fly-Avoid-traffic-Skycar.html.

[51] https://www.dronethusiast.com/ehang-184-is-a-manned-uav-you-will-never-get-to-fly/.

[52] https://www.aeromobil.com/aeromobil-4_0-stol/.

[53] https://www.flyskyrunner.com/.

[54] https://mavericklsa.com/specifications.html.

[55] https://www.pal-v.com/en/explore-pal-v.

[56] https://terrafugia.com/transition/.

[57] https://www.cbsnews.com/news/flying-car-gets-big-break-from-faa/.

[58] http://airfoiltools.com/polar/details?polar=xf-naca1412-il-1000000.

[59] http://www.windward-performance.com/.

[60] https://www.ainonline.com/aviation-news/general-aviation/2017-07-26/electric-sun-flyer-plans-fall-first-flight.

[61] 6E. S.v. "STOL aircraft." In: *McGraw-Hill Dictionary of Scientific Technical Terms*. 2003.

[62] Hashim H Abada. Turboelectric Distributed Propulsion System for NASA Next Generation Aircraft (2017).

[63] United States. Federal Aviation Administration. *Pilot's handbook of aeronautical knowledge [electronic resource*. U.S. Dept. of Transportation, Federal Aviation Administration, 2008.

[64] *Aircraft Information: Pipistrel Alpha Electro*. Pipistrel. Apr. 2016.

[65] J.D. Anderson. *Introduction to Flight*. McGraw-Hill series in aeronautical and aerospace engineering. McGraw-Hill Higher Education, 2005.

[66] C.F. Ansley and Columbia University. *The Columbia Encyclopedia*. Columbia University Press, 1935.

[67] Arthur Brown and Wesley Harris. A vehicle design and optimization model for on-demand aviation. In: *2018 AIAA/ASCE/AHS/ASC Structures, Structural Dynamics, and Materials Conference*. 2018, 0105.

[68] Aurélien Cabarbaye et al. VTOL aircraft concept, suitable for unmanned applications, with equivalent performance compared to conventional aeroplane. In: *2016 International Conference on Unmanned Aircraft Systems (ICUAS)*. IEEE. 2016, 219–226.

[69] Sean Clarke et al. X-57 power and command system design. In: *2017 IEEE Transportation Electrification Conference and Expo (ITEC)*. IEEE. 2017, 393–400.

[70] DP Coiro et al. Design of a Low-Cost Easy-to-Fly STOL Ultralight Aircraft in Composite Material. *Acta Polytechnica* 45(4) (2005).

[71] Lori Anne Costello. State of the Art of Piloted Electric Airplanes, NASA's Centennial Challenge Data and Fundamental Design Implications (2011).

[72] Christopher Courtin et al. Feasibility Study of Short Takeoff and Landing Urban Air Mobility Vehicles using Geometric Programming. In: *2018 Aviation Technology, Integration, and Operations Conference*. 2018, 4151.

[73] *Design specifications Volocopter 2X*. Volocopter. Apr. 2017.

[74] João Gonçalo Magriço Ferro. *New Aircraft Concepts for Improved Environmental and Energetic Efficiency*. M.Sc. 2014.

[75] *FES Battery Pack GEN2 Manual with integrates BMS(Battery Managemnet System)*. LZ Design. Oct. 2017.

[76] J Gerthoffert et al. Modelling of aircraft braking coefficient from IMAG friction measurements. *Airports in Urban Networks* 33 (2014).

[77] Richard Glassock et al. Hybrid electric aircraft propulsion case study for skydiving mission. *Aerospace* 4(3) (2017), 45.

[78] William E Gortney. Dictionary of Military and Associated Terms (2012).

[79] Martin Hepperle. Electric flight-potential and limitations (2012).

[80] Jeff Holden and Nikhil Goel. Fast-forwarding to a future of on-demand urban air transportation. *San Francisco, CA* (2016).

[81] Hyun Kim, Jeffrey Berton, and Scott Jones. Low noise cruise efficient short take-off and landing transport vehicle study. In: *6th AIAA aviation technology, integration and operations conference (ATIO)*. 2006, 7738.

[82] Steven Cornelius Kriel. A comparison of control systems for the flight transition of vtol unmanned aerial vehicles. PhD thesis. Stellenbosch: University of Stellenbosch, 2008.

[83] R Lineberger et al. *Elevating the future of mobility Passenger drones and flying cars*. 2018.

[84] Martin D Maisel, Demo J Giulianetti, and Daniel C Dugan. The history of the XV-15 tilt rotor research aircraft: from concept to flight (2000).

[85] B.W. McCormick. *Aerodynamics, Aeronautics, and Flight Mechanics*. Wiley, 1994. ISBN: 9780471575061.

[86] Julianna de la Montanya and David Marshall. Circulation control and its application to extreme short take-off and landing vehicles. In: *45th AIAA Aerospace Sciences Meeting and Exhibit*. 2007, 1404.

[87] Mark Moore. The Joby S2 VTOL concept: exploring the new degrees of design freedom of distributed electric propulsion. *Verti-flite* 60(6) (2014).

[88] Engineering National Academies of Sciences, Medicine, et al. *Commercial aircraft propulsion and energy systems research: reducing global carbon emissions*. National Academies Press, 2016.

[89] José A Posada. Advances, Challenges and Future of All-Electric Aircraft (2015).

[90] Q. Quan. *Introduction to Multicopter Design and Control*. Springer Singapore, 2017. ISBN: 9789811033827.

[91] Arvindhakshan Rajagopalan Srilatha. Design of a 4-Seat, General Aviation, Electric Aircraft (2012).

[92] Kaushik Rajashekara, Qingchun Wang, and Kouki Matsuse. Flying cars: Challenges and propulsion strategies. *IEEE Electrification Magazine* 4(1) (2016), 46–57.

[93] D.P. Raymer, American Institute of Aeronautics, and Astronautics. *Aircraft design: a conceptual approach*. Educ Series. American Institute of Aeronautics and Astronautics, 1989. ISBN: 9780930403515.

[94] J. Roskam and C.T.E. Lan. *Airplane Aerodynamics and Performance*. Airplane design and analysis. DARcorporation, 1997.

[95] Paul M Rothhaar et al. NASA Langley Distributed Propulsion VTOL TiltWing Aircraft Testing, Modeling, Simulation, Control, and Flight Test Development. In: *14th AIAA aviation technology, integration, and operations conference*. 2014, 2999.

[96] Mohamad Sadraey. *Spoiler design.*

[97] Thomas Schilling, Thomas Rötger, and Kai Wicke. Assessment of the Impact of Radically Climate-Friendly Aviation Technologies. *Greener Aviation* (2016), 11–13.

[98] Oliver Schneider, Stefan Kreth, and Lothar Bertsch. Towards a quiet short take-off and landing transportation system: Concept evaluation and ATM integration. In: *International powered lift conference*. American Helicopter Society, Inc, 2010, 481–492.

[99] Dieter Scholz. *Short Course Aircraft Design.* Chap. 5.

[100] Alex M Stoll et al. Conceptual design of the Joby S2 electric VTOL PAV. In: *14th AIAA Aviation Technology, Integration, and Operations Conference*. 2014, 2407.

[101] Wei-Chien Sun et al. Promissing Future Aircraft Concepts-ESTOL. In: *26th Congress of the international council of the aeronautical sciences*. 2008, 14–19.

[102] J Thinesen. at the Wayback Machine photo archive (28 August 2009).

[103] R Thomson et al. Aircraft electrical propulsion the next chapter of aviation. *Roland Berger* (2017), 17.

[104] Egbert Torenbeek. *Synthesis of subsonic airplane design: an introduction to the preliminary design of subsonic general aviation and transport aircraft, with emphasis on layout, aerodynamic design, propulsion and performance.* Springer Science & Business Media, 2013.

[105] Michele Travierso. Five electric planes to watch [News]. *IEEE Spectrum* 50(8) (2013), 9–11.

[106] S Tsach et al. *ESTOL (Extremely Short Take-Off and Landing)*. 2011.

[107] Muntwyler Urs and Andrea Vezzini. Electric flight–history–state of the art and first applications. In: *EVS28 International Electric Vehicle Symposium and Exhibition*. 2015.

[108] Douglas Wells. NASA green flight challenge: conceptual design approaches and technologies to enable 200 passenger miles per gallon. In: *11th AIAA Aviation Technology, Integration, and Operations (ATIO) Conference, including the AIAA Balloon Systems Conference and 19th AIAA Lighter-Than*. 2016, 7021.

[109] Richard Whittle. Air mobility bonanza beckons electric VTOL developers. *Verti-flite* (2017).

[110] Jeffrey A Yetter. Why do airlines want and use thrust reversers? A compilation of airline industry responses to a survey regarding the use of thrust reversers on commercial transport airplanes (1995).

[111] James Richard Young and David W Hall. Executive Summary of Cal Poly/NASA Extreme Short Takeoff and Landing (ESTOL) Work. *SAE transactions* (2005), 781–792.